Discrete Morse Theory for Random Complexes

by

Anton Nikitenko

A thesis presented to the Graduate School of the Institute of Science and Technology Austria in partial fulfillment of the requirements for the degree of Doctor of Philosophy.

Klosterneuburg, Austria.

October, 2017.

Abstract

The main objects considered in the present work are simplicial and CW-complexes with vertices forming a random point cloud. In particular, we consider a Poisson point process in $\mathbb{R}^n$ and study Delaunay and Voronoi complexes of the first and higher orders and weighted Delaunay complexes obtained as sections of Delaunay complexes, as well as the Čech complex. Further, we examine the Delaunay complex of a Poisson point process on the sphere $\mathbb{S}^n$, as well as of a uniform point cloud, which is equivalent to the convex hull, providing a connection to the theory of random polytopes.

Each of the complexes in question can be endowed with a *radius function*, which maps its cells to the radii of appropriately chosen *circumspheres*, called the *radius* of the cell. Applying and developing discrete Morse theory for these functions, joining it together with probabilistic and sometimes analytic machinery, and developing several integral geometric tools, we aim at getting the distributions of circumradii of typical cells. For all considered complexes, we are able to generalize and obtain up to constants the distribution of radii of typical *intervals* of all types. In low dimensions the constants can be computed explicitly, thus providing the explicit expressions for the expected numbers of cells. In particular, it allows to find the expected density of simplices of every dimension for a Poisson point process in $\mathbb{R}^4$, whereas the result for $\mathbb{R}^3$ was known already in 1970's.

Acknowledgments

I wish to say thank you to those people who made it possible for this work to happen, listed in order of appearance in my life:

my parents, Natalia and Valentin, and all my grandparents for your support throughout my life,
Oleg Musin, for your presence at random moments and being my diploma advisor,
Natalia Andreevna, for preparing me for Austria,
Igor Zilberbord, for being the first really pushing me into math,
Mikhail Zhitomirsky, for being an awesome high school teacher,
Nikita Necvetaev and Mikhail Lifshits, for the geometry and probability in my head,
all my colleagues from Chebyshev Lab in St. Petersburg (especially you, Shoorick), for being awesome and creating the mathematical atmosphere around me,
my PhD advisor Herbert Edelsbrunner, for all your help and advice,
Robert Adler, László Erdős and Uli Wagner, for being on my committee and for your help,
Harald, Gaspar and Juliane, for all the weird things I did with you instead of working,
and Matthias Reitzner, for your valuable input to the thesis and joining the committee.

Additionally, special thanks go to all those people who visited me during these four years in Vienna (especially to Zhenya, who did it three times!). Thank you, it would be much sadder without you. Special thanks also go to all the people from my group, for maintaining the working environment at the institute. And, last but not least, to Slip for all the stupid talks we had.

List of publications

The main part of the thesis is or will be published in the following articles: [31, 29, 30, 28].

Edelsbrunner, H., Nikitenko, A., and Reitzner, M. (2017). Expected sizes of Poisson– Delaunay mosaics and their discrete Morse functions. First published in Adv. Appl. Probab., 49. Copyright (c) Applied Probability Trust [2017].

Edelsbrunner, H. and Nikitenko, A. (2017). Random inscribed polytopes have similar radius functions as Poisson–Delaunay mosaics.
arXiv:1705.02870 [math.PR].

Edelsbrunner, H. and Nikitenko, A. (2017). Weighted Poisson–Delaunay mosaics.
arXiv:1705.08735 [math.PR].

Edelsbrunner, H. and Nikitenko, A. (2017). Poisson–Delaunay mosaics of order k.
arXiv:1709.09380 [math.PR].

Contents

List of Tables

List of Figures

1. Introduction

The work is focused on studying different random complexes. In this introduction, we define the concepts, introduce the notation and summarize the tools used to produce the results. Sections 1.1 – 1.4 are devoted to geometric complexes, associated to a point cloud in a metric space, that are widely used in shape reconstruction and topological data analysis. Section 1.5 contains a short introduction to the discrete Morse theory. Sections 1.6 and 1.7 introduce the random setup we are working in, mainly focusing on Euclidean space, while Section 1.8 focuses on spheres. Section 1.9 introduces the integral geometric tools used in the proofs of the main results.

1.1 Čech complex

Recall that an *abstract simplicial complex* is defined as a set $S \subseteq 2^V$ of *simplices* closed under taking subsets: $\sigma \in S$ and $\tau \subseteq \sigma$ imply $\tau \in S$. The empty set is conventionally excluded from S. All elements of the simplices in S form the *vertex set*: $V = \bigcup_{\sigma \in S} \sigma$. Every vertex is identified with the one-element simplex containing this vertex. The *dimension* of a simplex τ is defined as $\dim \tau = |\tau| - 1$, and the dimension of the complex is the maximal dimension of its simplices. An abstract simplicial complex can be geometrically realized in $\mathbb{R}^{|V|+1}$ as a subset of the standard simplex by mapping distinct vertices in V to distinct vertices of the standard simplex. In general, a *geometric simplicial complex* C is a collection of simplices in $\mathbb{R}^n$ closed under taking faces, with an additional property that for any two simplices of C their intersection is either empty or a face of both. For every geometric simplicial complex one gets an abstract simplicial complex by considering the vertex sets of geometric simplices and dropping all geometric information. It can be easily shown that all geometric realizations of the same abstract simplicial complex are homeomorphic. In particular, the *homotopy type of an abstract simplicial complex* is well-defined. For a more detailed introduction into simplicial complexes see [26, Section III.1].

One motivation for the work reported in this thesis is the desire to reconstruct surfaces from point sets; see [21] and in particular the Wrap algorithm described in [25]. While the points usually describe a distinctive shape and are therefore not random, they are affected by noise and display random features locally. To effectively cope with local noise is a necessary component of every high quality surface reconstruction software. Another motivation derives from the work in topological data analysis; see [17]. Let X be a point set in a metric space. We assume that the space is $\mathbb{R}^n$ for the sake of simplicity of exposition, but it can be substituted with any other metric space, like a sphere $\mathbb{S}^n$. This set X may be considered as sampled from some n-dimensional shape, and the Čech complex

is used to define a way to possibly reconstruct the shape. Fix a radius r and consider a set $X_r \subseteq \mathbb{R}^n$ which is obtained as a union of closed balls of radius r centered at points of X:

$$X_r = \bigcup_{x \in X} B(x, r).$$

This set can be considered as an approximation of the shape. By definition, X_r is covered by a family of balls $\mathcal{B} = \{B(x, r) \colon x \in X\}$, and the Nerve theorem can be applied to obtain a simplicial complex that is homotopy equivalent to X_r. For a collection of sets $\mathcal{U}$, the *nerve* $\operatorname{Nrv}\mathcal{U}$ is defined as an abstract simplicial complex with $V = \mathcal{U}$ and every $\sigma \subseteq \mathcal{U}$ is a simplex of $\operatorname{Nrv}\mathcal{U}$ if $\bigcap_{U \in \sigma} U \neq \emptyset$. In simple terms, a vertex gets assigned to every set, and a set of vertices forms a simplex, if the corresponding sets have a non-empty common intersection. We are now ready to state the simplest version of the Nerve theorem [51, 26, 41]:

Theorem (Nerve theorem)**.** *Let $\mathcal{U}$ be a finite collection of closed, convex sets in Euclidean space. Then the nerve of $\mathcal{U}$ and the union of the sets in $\mathcal{U}$ have the same homotopy type.*

The Nerve theorem shows thus that $X_r = \bigcup_{B \in \mathcal{B}}$ is homotopy equivalent to $\operatorname{Nrv}\mathcal{B}$, and the latter is called the *Čech complex* of X for radius r and denoted $\check{\operatorname{C}}\operatorname{ech}_r X$. It is an abstract simplicial complex, which is generically not embeddable in $\mathbb{R}^n$. Its vertices correspond to the balls around every point of X, so we identify the vertices with points of X. An example is shown in Figure 1.1. The complexes for different values of r are nested. It means that

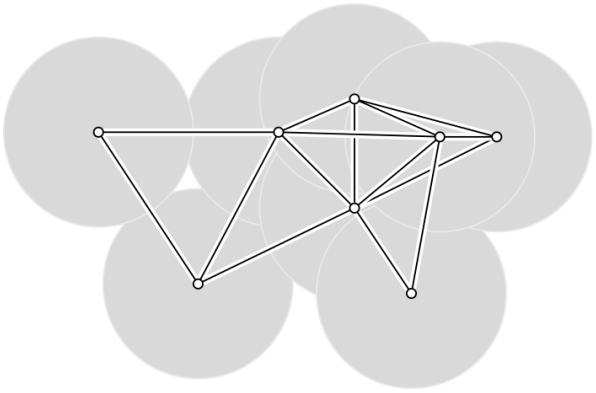

Figure 1.1: Čech complex

for every $r_1 \leq r_2$ complex $\check{\operatorname{C}}\operatorname{ech}_{r_1} X$ is a subcomplex of $\check{\operatorname{C}}\operatorname{ech}_{r_2} X$, with $\check{\operatorname{C}}\operatorname{ech}_0 X = X$ and $\check{\operatorname{C}}\operatorname{ech}_\infty X = 2^X$, implying that every subset of X enters the Čech complex at some value of radius.

With this in mind, the Čech complex can be alternatively described using *enclosing balls*. For a set $\sigma \subseteq X$ define the smallest enclosing ball (or the *Čech ball*) of σ to be the unique smallest closed ball that contains σ. Let $\mathcal{R}_{\check{\mathcal{C}}} \colon 2^X \to \mathbb{R}$ be the function, called the *Čech radius function*, that maps every σ to the radius of such ball, called the *Čech radius* of σ. Then $\sigma \in \check{\operatorname{C}}\operatorname{ech}_r X$ iff $r \geq \mathcal{R}_{\check{\mathcal{C}}}(\sigma)$. Indeed, the balls $B(x, r)$ for $x \in \sigma$ have a common intersection iff there is a point, which has distance not more than r to all points of σ, see also [26].

The Čech complex, though being relevant in the way that it encodes the topology of X_r, has several drawbacks, mainly coming from the fact that it is exponential in size and is hard

to compute. One simplification is the *Vietoris–Rips* complex, which relaxes the conditions of the nerve. More precisely, a simplex σ belongs to the Vietoris–Rips complex for radius r if every two closed balls of radius r centered at vertices of σ intersect. The edges of this complex are thus the same as in the Čech complex, but it might have more simplices of higher dimensions. Although easier to compute, it is still exponential in size, and does not preserve the topology of X_r. Nevertheless, it is still used in applications for approximating the Čech complex. Another advantage of the Vietoris–Rips complex is that it considers only pairwise distances between points, hence not depending on the ambient space.

1.2 Voronoi and Delaunay complexes

Another way of representing the topology of the union of balls is provided by the Delaunay complex. In contrast to the Čech complex, it is easier to compute, has size polynomial (and, often, linear) in the number of points, and generically has a canonical geometric realization. To define the concept, we start with introducing Voronoi diagrams. Recall that X is a point set in a metric space, which is assumed to be $\mathbb{R}^n$. The *Voronoi domain* of a point $x \in X$ consists of all points for which x minimizes the Euclidean distance: $\mathrm{dom}(x) = \{a \in \mathbb{R}^n \colon \|a - x\| \leq \|a - y\|, \text{ for all } y \in X\}$. Every Voronoi domain is a possibly unbounded convex polyhedron. The *Voronoi diagram* or the *Voronoi tessellation* is the collection of Voronoi domains, see Figure 1.2. The *Delaunay mosaic* or *Delaunay triangulation* $\mathrm{Del}X$ is isomorphic to the nerve of the Voronoi domains. Specifically, the Delaunay mosaic is the collection of subsets $Q \subseteq X$ whose corresponding Voronoi domains have a non-empty common intersection: $\mathrm{Vor}(Q) = \bigcap_{x \in Q} \mathrm{dom}(x)$. Adopting the convention from the discussion of abstract simplicial complexes, we call Q a *simplex*, and, as common in combinatorial topology, identify it with the convex hull of Q when it is convenient. The Delaunay mosaic is an n-dimensional simplicial complex iff the Voronoi diagram is *primitive* (the notion used in discrete geometry) or *normal* (the notion used in stochastic geometry), that is: the intersection of any $0 \leq k + 1 \leq n + 2$ Voronoi domains is either empty or $(n - k)$-dimensional. In particular, the intersection of any $n + 2$ domains is necessarily empty. In this case the Delaunay mosaic can be canonically embedded into $\mathbb{R}^n$ with vertex set X by mapping every Voronoi domain to the point of X it is defined by, and it is the dual of the Voronoi diagram [20]. The primitivity of the Voronoi diagram is guaranteed if X is

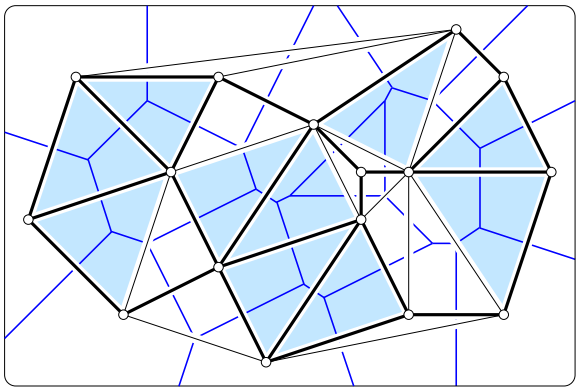

Figure 1.2: Voronoi diagram and corresponding Delaunay mosaic. Blue triangles and bold edges are *critical* in the sense of Section 1.5.

in general position, that stands for the following conditions, that are a bit stronger than the ones required in [20], throughout this work: for every $0 \leq k < n$,

1. no $k+2$ points belong to a common k-plane,
2. no $k+3$ points belong to a common k-sphere,
3. considering the unique k-sphere that passes through $k+2$ points, no $k+1$ of these points belong to a k-plane that passes through the center of the k-sphere, and the radii of all such spheres are different.

It is also possible to describe the Delaunay mosaic using the way similar to describing Čech complexes using smallest enclosing balls. By construction, every point $z \in \mathrm{Vor}(Q)$ is equally far from all points in Q and at least as far from all points in $X \setminus Q$. We call a sphere with center z and radius $\|z-x\|$, $x \in Q$, an *empty circumscribed sphere* of Q because all points of Q lie on the sphere, and all points of X lie on or outside the sphere. The unique smallest empty circumscribed sphere is called the *Delaunay sphere* (sometimes just *circumsphere*, [31]), and its radius and center are called the *Delaunay radius* and the *Delaunay center* of Q. Note that only Delaunay simplices have a Delaunay sphere. Indeed, if a simplex Q has an empty circumscribed sphere with center z, then $z \in \mathrm{Vor}(Q)$, implying that $\mathrm{Vor}(Q) \neq \emptyset$. The *Delaunay radius function*, $\mathcal{R}_D \colon \mathrm{Del}X \to \mathbb{R}$, maps every simplex to its Delaunay radius. Observe that the function is increasing: for $P \leq Q$, meaning that P is a face of Q, we clearly have $\mathcal{R}_D(P) \leq \mathcal{R}_D(Q)$. Fixing an $r \geq 0$ and taking all simplices from $\mathrm{Del}X$ that have Delaunay radius not greater than r we thus obtain a subcomplex of $\mathrm{Del}X$, the *Alpha* or *Delaunay complex* for radius r, $\mathrm{Del}_r X$. In contrast to $\mathrm{Del}X$, its simplices do not cover the entire convex hull of X and can therefore form cycles and other topological features, and it is indeed homotopy equivalent to the union of balls, X_r; see [23]. It can even be showed that $\check{\mathrm{C}}\mathrm{ech}_r X$, which is also homotopy equivalent to X_r, *collapses* onto $\mathrm{Del}_r X$; see [8].

There is another way to get the Delaunay complex without the radius function. For this, we decompose $X_r = \bigcup_{x \in X} B(x,r)$ as $X_r = \bigcup_{x \in X} (B(x,r) \cap \mathrm{dom}(x))$. It is easy to see that it is indeed a cover of X_r: if a point a belongs to some ball $B(x_1,r)$, but to $\mathrm{dom}(x_2)$, then $\|a-x_2\| \leq \|a-x_1\| \leq r$, so $a \in B(x_2,r) \cap \mathrm{dom}(x_2)$. Then the Delaunay complex for radius r is isomorphic to the nerve of this cover. By the Nerve theorem, it follows that X_r is homotopy equivalent to $\mathrm{Del}_r X$.

It is also worth mentioning that there is a way to define the Delaunay mosaic, that is embedded in $\mathbb{R}^n$ even if the points are not in general position, by requiring only *geometric duality*. We want to assign to every j-dimensional Voronoi polyhedron an $(n-j)$-dimensional Delaunay cell preserving incidences: if two Voronoi polyhedra are incident (i.e., share a common face), then their duals must belong to the dual of the common face. This procedure is similar to taking the dual graph in two-dimensional case, and a simple formal way to show its consistency in higher dimensions is the *lifting* to paraboloid. More precisely, embed $\mathbb{R}^n$ into $\mathbb{R}^{n+1}$ as a plane $x_{n+1} = 0$ and lift every point x of X to $(x, \|x\|^2)$. Then it can be shown, that the orthogonal projection of the lower convex hull of the lifted points onto $\mathbb{R}^n$ satisfies these properties; see [24]. Moreover, for points in general position the construction gives the same Delaunay mosaic as before; but in the other case it produces a cell complex, embedded in $\mathbb{R}^n$, which is not necessarily simplicial.

1.3 Weighted Voronoi and Delaunay complexes

The first generalization of the Voronoi diagrams and Delaunay mosaics considered in this work assigns weights to the points; see Figure 1.3. This extra degree of freedom permits

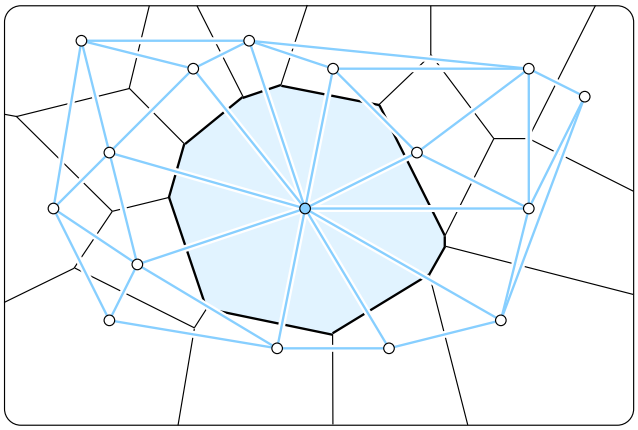

Figure 1.3: Weighted Voronoi tessellation in $\mathbb{R}^2$ with superimposed weighted Delaunay mosaic. All points have zero weight except the point with the shaded domain, which has positive weight.

better approximations of observed tilings, such as cell cultures in plants [62] and microstructures of materials [16]. Let Y be a point set in $\mathbb{R}^k$, and define for a point $y \in Y$ with weight $w(y) \in \mathbb{R}$ the *power distance* of any point $a \in \mathbb{R}^k$ to be $\|a - y\|^2 - w(y)$. If $w(y)$ is 0, then the power distance is the squared Euclidean distance, but it can be negative if the weights are positive. As before, the *weighted Voronoi domain* of y is defined as the set of points, whose power distance to x is not greater than to the other points of Y. The *weighted Voronoi diagram* or *power diagram* [4] or *Laguerre tessellation* [49] is the collection of all weighted Voronoi domains. The *weighted Delaunay mosaic* $\mathrm{WDel}Y$, sometimes called *Laguerre triangulation* [59] or *regular triangulation* [38], is again isomorphic to its nerve. Assuming general position, which now requires an additional assumption on weights (see [26, page 68]), it can be geometrically realized in $\mathbb{R}^k$ with vertices being a subset of Y. We note that some points of X might have an empty weighted Voronoi domain, thus not belonging to weighted Delaunay mosaic. As in the remark on Delaunay mosaics, one can also cope with points not in general position using the *weighted lifting*. The procedure is similar with the only difference that one now lifts y to $(y, \|y\|^2 - w(y))$ in $\mathbb{R}^{k+1}$.

A simple intuition can be given for the concept when the weight is negative: assume $\mathbb{R}^k$ is embedded into $\mathbb{R}^n$ and consider the point $\hat{y}$ which lies at the distance $\sqrt{-w(y)}$ to y in the space orthogonal to $\mathbb{R}^k$. Then the power distance of any point $a \in \mathbb{R}^k$ to x is exactly the squared Euclidean distance to $\hat{y}$, which gives a way to construct a weighted Voronoi diagram by taking a *slice* of an (unweighted) Voronoi diagram in $\mathbb{R}^n$; see [6, 69]. Specifically, if X is a discrete set of points in $\mathbb{R}^n$ and $\mathbb{R}^k \hookrightarrow \mathbb{R}^n$ is spanned by the first $k \leq n$ coordinate axes, then the Voronoi tessellation of X in $\mathbb{R}^n$ intersects $\mathbb{R}^k$ in a k-dimensional weighted Voronoi tessellation. The points in $\mathbb{R}^k$ that generate the weighted tessellation are the orthogonal projections y_x of the points $x \in X$, and their weights are $w_x = -\|x - y_x\|^2$. While all weights in this construction are non-positive, this is not a restriction of generality because the tessellation remains unchanged when all weights are increased by the same amount. Indeed, every finite weighted Voronoi tessellation can be obtained as a slice of an

unweighted Voronoi tessellation. If X is in general position (see below) in $\mathbb{R}^n$, then this slice is a normal tessellation in $\mathbb{R}^k$, guaranteeing that the dual weighted Delaunay mosaic can be canonically embedded in $\mathbb{R}^k$. There is also an intriguing connection between the volumes of skeleta of unweighted Voronoi tessellations and the number of simplices in weighted Delaunay mosaics through the Crofton formula, which is worth exploring. We will state this result in Section 1.9 after introducing the necessary notation.

This work focuses on weighted Delaunay mosaics that are obtained as duals of slices of random unweighted Voronoi diagrams. In this case, the radius function can be naturally defined. Before doing this, however, we need to slightly adjust the notion of *general position* for points in $\mathbb{R}^n$. Specifically, we add the following two requirements to the definition on page 4: for every $0 \leq j < n$,

4. considering the unique j-plane that passes through $j+1$ points, this plane is neither orthogonal nor parallel to $\mathbb{R}^k$,

5. no two points have identical distance to $\mathbb{R}^k$.

For $j = 0$, property 4 means that no point belongs to $\mathbb{R}^k$. This additional properties assert that $\mathbb{R}^k$ is a "generic plane" in $\mathbb{R}^n$. Now we are ready to define the radius function. Given a point set X in general position in $\mathbb{R}^n$, denote its projection onto $\mathbb{R}^k$ by X'. The *radius function*, $\mathcal{R}_{WD}\colon \mathrm{WDel}X' \to \mathbb{R}$, maps every simplex Q of $\mathrm{WDel}X'$ to the radius of the smallest $(n-1)$-sphere that satisfies the following properties:

- it passes through all preimages of the vertices of the simplex,
- it does not contain any points of X inside,
- its center lies in $\mathbb{R}^k$.

In other words, this is the smallest empty circumscribed sphere of the preimage of Q that has its center in $\mathbb{R}^k$. Indeed, simplex Q belongs to the weighted Delaunay mosaic iff the Voronoi domains of the preimages of vertices of Q have a common intersection with $\mathbb{R}^k$, and a point belongs to this intersection iff it is a center of such sphere. We call this sphere the *weighted Delaunay sphere* of Q or the *anchored Delaunay sphere* of the preimage of Q. Also, its center is called the *anchor* of Q or of its preimage. Note that $\mathcal{R}_{WD} = \mathcal{R}_D$ if $k = n$.

1.4 Voronoi and Delaunay complexes of higher order

Another generalization of Voronoi diagram partitions the space not according to the closest point, but to the closest k points. As usual, we start with a discrete set $X \subseteq \mathbb{R}^n$, and for k points $x_1, \ldots, x_k$ of X we define the *order-k Voronoi domain* $\mathrm{dom}_k(x_1, \ldots, x_k)$, generated by these points, to consist of points $a \in \mathbb{R}^n$, such that $x_1, \ldots, x_k$ are the k closest to a points of X. An *order-k Voronoi diagram* $\mathrm{Vor}^{(k)}(X)$ [68, 35] is defined as the collection of order-k Voronoi domains, spanned by k-point subsets of X. An example is presented in Figure 1.4. The order-1 Voronoi diagram is thus the usual Voronoi diagram. Note that for $k > 1$ the diagram may not be normal even generically, i.e., for some t domains their intersection can be not $(n-t+1)$-dimensional. For example, if X consists of four points in general position in $\mathbb{R}^3$, then the six order-2 Voronoi domains intersect in a common point,

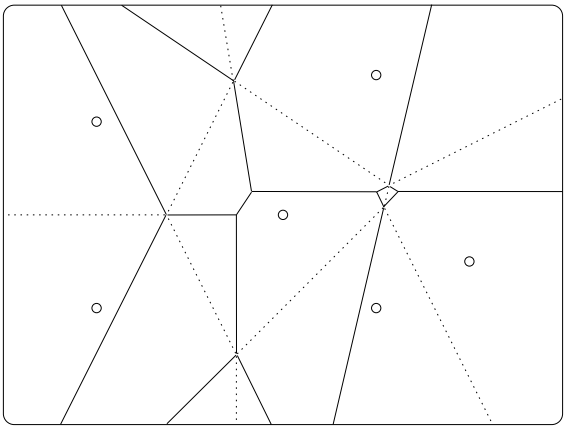

Figure 1.4: The dotted edges decompose the plane into the order-1 Voronoi domains, while the solid edges decompose it into order-2 Voronoi domains. The two tessellations share some of their vertices but not all.

the circumcenter of the tetrahedron. It is not completely straightforward therefore, how to generalize the Voronoi–Delaunay duality for order-k diagrams. We cannot take the shortcut with the nerve, because the inconvenient case when the nerve can not be embedded in $\mathbb{R}^n$ is typical now, so we have to construct a geometrically dual tessellation with a bit more care. As in the note on geometrical duality in Section 1.2, we would like to have a dual diagram in a sense that every j-dimensional polyhedron of the order-k Voronoi diagram corresponds to an $(n-j)$-dimensional polytope in the order-k Delaunay triangulation, and the incidence is preserved: if two order-k Voronoi polyhedra share a common face, then their duals must be the faces of the dual of the common face. It can be shown [5] that it is possible to construct such dual tessellation in the following way. Assign to each non-empty order-k Voronoi domain, generated by k points of X, the center of mass of these points. These will be the duals of order-k Voronoi domains. Then the *order-k Delaunay mosaic* of X, denoted by $\mathrm{Del}^{(k)}X$, is obtained by connecting every two points with a segment if the corresponding order-k Voronoi domains share a common face of dimension $n-1$. The polytopes of higher dimensional skeleta are then defined as above, i.e., if a face of the order-k Voronoi diagram is the intersection of several order-k Voronoi domains, then the

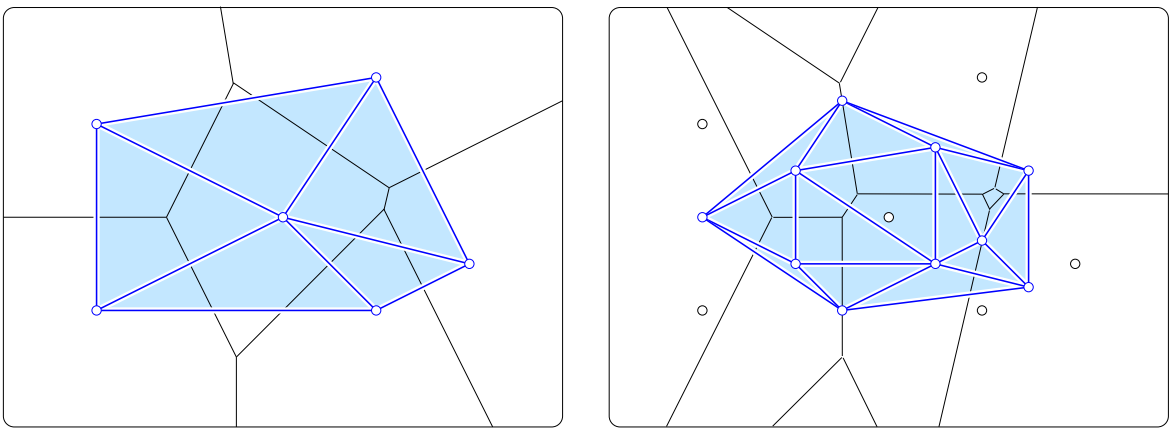

Figure 1.5: The order-1 Delaunay mosaic on the *left* and the order-2 Delaunay mosaic on the *right*, both superimposed on their corresponding Voronoi tessellations.

polytope in the dual is the convex hull of the vertices dual to these domains. An example is presented in Figure 1.5. To prove that this construction is consistent, we can describe it as a projection of a special lower convex hull of points in $\mathbb{R}^{n+1}$. More precisely, we can consider the order-k Voronoi diagram as a (non-generic) weighted Voronoi diagram with appropriately chosen weights; see [5, 27]. Another way to construct the order-k Delaunay mosaic is iterative, where one can obtain the order-k diagram from the order $k-1$ [50, 5]. Clearly, when the order-k Voronoi diagram is not normal, the corresponding dual is not a triangulation. Throughout the text we will refer to the cells of the order-k Voronoi tessellations as order-k Voronoi polyhedra.

After defining the Delaunay mosaic of order k, we aim at generalizing the radius function to this case. Unfortunately, the discrete Morse theory for order-k diagrams seems to not have been developed yet, and the idea of the radius function originates from it. So we do not have any reference, and we defer the definition until Chapter 6. As we are going to see, the order-1 and order-k cases are not significantly different from the probabilistic point of view, so the discrete Morse theory will be the main topic of that chapter.

1.5 Discrete Morse theory

1.5.1 Main definitions

In this section we summarize the concepts of the discrete Morse theory introduced in [36], generalized in [37], and applied to Delaunay complexes in [8]. The motivation comes from the classical Morse theory, which studies smooth manifolds by analyzing functions on them; see [57]. The generalization to the discrete case is not straightforward, see [26] for a discussion, and there are some further differences in notation. In our case we stick to the following. Let Σ be a simplicial complex, and consider a function $f : \Sigma \to \mathbb{R}$. For us this function is a *generalized discrete Morse function* if it is *increasing*, meaning that if a simplex $P \in \Sigma$ is a face of $Q \in \Sigma$ then $f(P) \leq f(Q)$, and provides an interval structure on Σ. To explain the latter concept, for two simplices $L, U \in \Sigma$ with L being a face of U we define an *interval* $[L, U] = \{P \in \Sigma \colon L \subseteq P \subseteq U\}$ to contain all faces of U that have L as their face. L is called the *lower bound* and U the *upper bound* of the interval. If P is a face of Q and $f(P) = f(Q)$, then all simplices of $[P, Q]$ also have the same function value. A simple definition of the *interval structure* would just require that every *level set* $f^{-1}(r) \subseteq \Sigma$ is an interval. However, it would prohibit that all vertices have the same function value, which is often the case in our considerations. So, not aiming at the full generality, for the purposes of this work we require that $f(P) \geq 0$ for all simplices, and $f(P) = 0$ can only hold if P is a single vertex. So, for every $r > 0$ we require that $f^{-1}(r)$ is an interval and $f^{-1}(0)$ contains only vertices. The interval structure on Σ is the decomposition of Σ into maximal intervals sharing the function value. If an interval $[L, U]$ in this decomposition contains a single simplex, i.e., if $L = U$, then this simplex is called *critical* and the interval *singular*. All simplices which are not critical are called *regular*. In particular, all vertices with function value 0 are required to be critical. Function values on critical (corr. regular) simplices are called *critical* (corr. *regular*) values.

This terminology mimics the classical Morse theory, and, indeed, critical simplices are of topological significance. The following theorem [36, 37] is an analogue of the classical theorem on retractability of sublevel sets of classical Morse functions:

Theorem. *Let Σ be a simplicial complex and f a generalized discrete Morse function on it. Write Σ_r for the* sublevel set*: $\Sigma_r = f^{-1}([0,r])$. If a real half-segment $(r_1, r_2] \subseteq \mathbb{R}$ does not contain critical values, then $\Sigma_{r_2} \searrow \Sigma_{r_1}$.*

Here by $\searrow$ we mean *collapsability* [73], which is a simplicial analogue of deformation retraction. What is important is that it implies that Σ_{r_2} and Σ_{r_1} are homotopy equivalent. A stronger statement holds: there exists a CW-complex, which has one cell of the corresponding dimension for every critical simplex of Σ and is homotopy equivalent to Σ. It is called the *Morse complex*. Writing n_j for the number of j-dimensional simplices in Σ, c_j for the number of j-dimensional critical simplices, we can thus obtain the *discrete Morse relations*:

$$\begin{aligned} \chi(\Sigma) = \sum (-1)^j \beta_j(\Sigma) &= \sum (-1)^j n_j = \sum (-1)^j c_j, \\ \beta_j(\Sigma) &\leq c_j, \\ \sum_{q=0}^{j} (-1)^{j-q} \beta_q(\Sigma) &\leq \sum_{q=0}^{j} (-1)^{j-q} c_q(\Sigma). \end{aligned}$$

Here $\chi(\Sigma)$ is the Euler characteristic, defined by the first equality, and $\beta_j(\Sigma)$ is the j-th Betti number of Σ, i.e., the rank of the j-th homology group (say, modulo $\mathbb{Z}/2\mathbb{Z}$). See [41, 26] for an introduction to these concepts. The last two expressions are called *discrete Morse inequalities*.

Before we continue, we want to make a remark on the number of simplices in an interval. Let $[L, U]$ be an interval with $\dim L = \ell$ and $\dim U = m$. Then we call (ℓ, m) the *type* of the interval, and the interval itself an (ℓ, m)*-interval*. Most of the time we will count the intervals in random mosaics, and to get the number of simplices out of the number of intervals we note that an (ℓ, m)-interval has $\binom{m-\ell}{j-\ell}$ simplices of dimension j. This simple fact can be used to prove the Euler relation above: for every non-singular interval the alternating sum of numbers of simplices in it is thus $\sum (-1)^j \binom{m-\ell}{j-\ell} = (1-1)^{m-\ell} = 0$. To get the number j-simplices in a complex knowing its interval structure we have the following lemma.

Lemma 1.5.1 (Simplices and intervals)**.** *Let Σ be a simplicial complex with a generalized discrete Morse function and write $c_{\ell m}$ for the number of (ℓ, m)-intervals and d_j for the number of j-simplices in Σ. Then*

$$d_j = \sum_{\ell=0}^{j} \sum_{m=j}^{\infty} \binom{m-\ell}{m-j} c_{\ell m}.$$

This equation will be used every time we compute densities of j-dimensional simplices in a random simplicial complex.

1.5.2 Delaunay and other mosaics

In [8] it was shown that $\mathcal{R}_D$ and $\mathcal{R}_{\check{C}}$ are generalized discrete Morse functions on the Delaunay and Čech complexes if the underlying point set is in general position. The main idea is that if two simplices share a common Delaunay sphere (or a common smallest enclosing ball), then their intersection and union do so, implying that a set of simplices sharing

a Delaunay sphere (or a smallest enclosing ball) is always an interval. An identical claim holds for anchored Delaunay spheres of the weighted Delaunay mosaics, so $\mathcal{R}_{WD}$ is also a generalized discrete Morse function. An important fact is that the intervals imposed by these functions have nice intrinsic characterizations. The crucial role plays the number of points inside the smallest sphere, circumscribed around the simplex, and the visibility of facets. We turn to this in more details right away.

Delaunay radius function intervals. By general position assumption and by definition, the intervals of the Delaunay mosaic are the simplices that share the Delaunay sphere. Recall that the Delaunay sphere $S(Q)$ of a Delaunay simplex $Q \in \mathrm{Del}X$ is the smallest sphere that has no points of X inside and passes through all vertices of Q. We follow [8] to describe the interval containing Q. Define $U = S(Q) \cap X$. Clearly, $U \supseteq Q$ is the upper bound of the interval. Indeed, $S(Q)$ is the smallest empty sphere that passes through vertices of U, otherwise we would find a smaller empty sphere that passes through vertices of Q. To determine the lower bound, we need the notion of *visibility*. Consider a d-dimensional simplex σ in $\mathbb{R}^n$ and consider its affine hull, a d-dimensional space $\alpha \cong \mathbb{R}^d$. A facet, i.e., a $(d-1)$-dimensional face of σ is called *visible from point* $p \in \alpha$, if the $(d-1)$-plane it lies within separates the opposite vertex from p. Every ray, originating from p and passing through a facet, enters the simplex at a visible and leaves at an invisible facet, explaining the choice of the term; see Figure 1.6. If p is the center of the unique circumscribed sphere of σ in α, we omit the "from" part and just call the facet *visible*. We refer to [8] for the proof

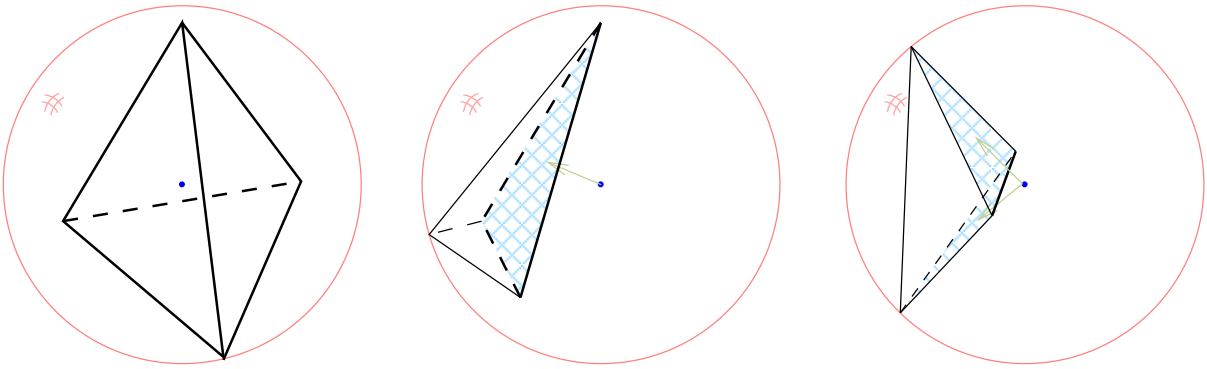

Figure 1.6: Visible facets of different tetrahedra. The intersection of all visible facets is in bold. If there are no visible facets, the intersection is the whole tetrahedron.

that the lower bound L of the interval containing Q is the intersection of all visible facets of U. Similar results will be proven in Lemmas 1.8.1 and 6.3.1. We summarize this in the lemma:

Lemma 1.5.2 (Delaunay complex interval structure)**.** *Letting $X \subseteq \mathbb{R}^n$ be in general position, a pair $L \subseteq U$ of subsets of X, considered as simplices, defines an interval of the radius function $\mathcal{R}_D \colon \mathrm{Del}X \to \mathbb{R}$ iff the smallest circumscribed sphere of U is empty and L is the largest face of U common to all visible facets, i.e., $L = U \cap \bigcap_{F \in \mathrm{vis}(U)} F$, where $\mathrm{vis}(U)$ denotes the set of visible facets of U. The smallest circumscribed sphere of U is the common Delaunay sphere of all simplices in this interval.*

Recall the special case of a critical simplex, $L = U$, which is characterized by containing the center of its Delaunay sphere inside. In this case, the closed ball bounded by the Delaunay sphere is also the smallest enclosing ball of U (see page 2).

Čech radius function intervals. An even simpler intrinsic characterization can be provided for the Čech complex. Again, by general position assumption the simplices that belong to a common interval are the simplices sharing the smallest enclosing ball. Take a simplex $Q \subseteq X$ and write $B(Q)$ for its (closed) smallest enclosing ball. Let $L = X \cap \operatorname{bd} B(Q)$ and $U = X \cap B(Q)$. Clearly, $\operatorname{bd} B(Q)$ is the smallest sphere passing through vertices of L, and trivially $L \subseteq Q$, because otherwise a smaller enclosing ball would exist. Further, $B(Q)$ is by definition the smallest enclosing ball of U. The interval of $\mathcal{R}_{\check{\mathcal{C}}}$ containing Q is thus $[L, U]$; more details can be found in [8]. Note that the smallest enclosing ball of L passes through all vertices of L iff the smallest circumscribed sphere of L has its center in $\operatorname{conv} L$, or, equivalently, L has no visible facets. The statement about the interval structure for Čech complex follows:

Lemma 1.5.3 (Čech complex interval structure)**.** *Letting $X \subseteq \mathbb{R}^n$ be in general position, a pair $L \subseteq U$ of subsets of X, considered as simplices, defines an interval of $\mathcal{R}_{\check{\mathcal{C}}} \colon \check{\mathrm{C}}\mathrm{ech}\, X \to \mathbb{R}$ iff L has no visible facets and, writing $B(L)$ for the closed ball bounded by the smallest $(n-1)$-sphere passing through vertices of L, $U = B(L) \cap X$. The smallest circumscribed sphere of L bounds the common smallest enclosing ball of all simplices of this interval.*

Note that critical simplices of Čech and Delaunay complexes are the same.

Weighted Delaunay radius function intervals. The weighted case is a simple extension of the Delaunay characterization. Without going into details, we state that they are identical modulo anchoring:

Lemma 1.5.4 (Weighted Delaunay complex interval structure)**.** *Let $X \subseteq \mathbb{R}^n$ be in general position and X' its projection onto $\mathbb{R}^k$. Projections L' and U' of a pair $L \subseteq U$ of subsets of X, considered as simplices, define an interval $[L', U']$ of $\mathcal{R}_{WD} \colon \mathrm{WDel}\, X' \to \mathbb{R}$ iff the smallest anchored circumscribed sphere of U is empty and L' is the largest face of U' common to all facets of U' visible from its center, i.e., $L' = U' \cap \bigcap_{F \in \mathrm{vis}(U')} F$. The smallest anchored circumscribed sphere of U is the common* anchored *Delaunay sphere of all simplices of this interval.*

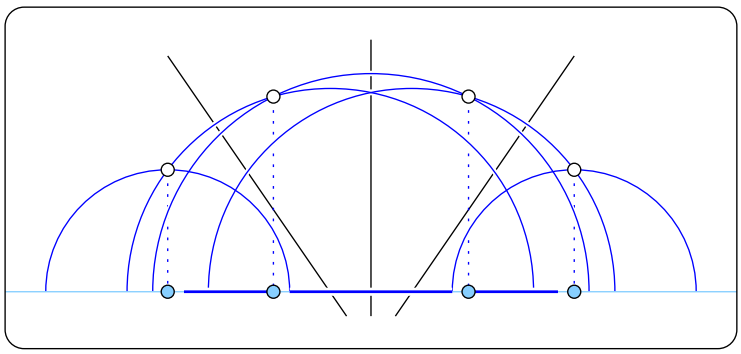

Figure 1.7: From *left* to *right* on the horizontal line: a critical vertex, an edge-vertex pair, a critical edge, a vertex-edge pair, and another critical vertex.

The proof is also identical to [8] modulo anchoring, and details are left to the reader. See Figure 1.7 for a 1-dimensional example. A notable difference to the two previous complexes is that it is no longer true that all vertices are critical and have function value 0. That is why a rich interval structure appears already in low dimensions.

1.6 Poisson point process

We study properties of randomly generated discrete point sets in $\mathbb{R}^n$ using a *Poisson point process*. It is defined by an *intensity measure*, which is a Borel measure on $\mathbb{R}^n$, absolutely continuous with respect to the Lebesgue measure. As before, the space $\mathbb{R}^n$ is chosen to simplify the notation, any other measurable space can be used instead, and we will also use $\mathbb{S}^n$ later. The Poisson point process can be characterized by the following two properties:

1. The numbers of points within a finite collection of pairwise disjoint Borel sets are independent random variables;
2. The expected number of points within a Borel set is the intensity measure of the set.

The *intensity function* is the Radon–Nikodym derivative of the intensity measure, $\varsigma\colon \mathbb{R}^n \to [0, +\infty)$, i.e. the function, such that the intensity measure of any Borel set is the integral of this function with respect to the Lebesgue measure. Formally, a Poisson point process is thus a random counting measure on $\mathbb{R}^n$. We do not go into the measure-theoretic details however, and refer to [46] for a good introduction to Poisson point processes.

We will work with *stationary* or *homogeneous* Poisson point processes, which are defined by constant intensity functions: $\varsigma(x) = \rho$, and the constant can be called *density* in this case. All processes will be assumed stationary unless explicitly stated. We further do not distinguish the process as random variable and its realization, writing $X \subseteq \mathbb{R}^n$ for a random point set, which has the corresponding distribution.

Properties. First we note that for stationary processes we can express Condition 2 more succinctly as $\mathbb{E}[|X \cap B|] = \rho\|B\|$. Here $\|B\|$ stands for the Lebesgue measure of B. The two conditions imply that the number of points in a Borel set B has a Poisson distribution with parameter $\rho\|B\|$. In particular, the probability of having k points in B is $\mathbb{P}[|X \cap B| = k] = \frac{(\rho\|B\|)^k}{k!} e^{-\rho\|B\|}$, so the probability of having no point in B is $\mathbb{P}[X \cap B = \emptyset] = e^{-\rho\|B\|}$.

Another important property is the *Slivnyak–Mecke formula*, which is used to rewrite expectations of random variables, depending on all k-tuples of points of a Poisson point process. Write δ_x for a delta-measure at point $x \in \mathbb{R}^b$, i.e., the measure which is 1 for any Borel set containing x and 0 otherwise, and let $\mathbf{N}$ be the space of all counting measures, i.e., finite and countable sums of delta-measures. We again skip the measure-theoretic details about defining the natural measure on $\mathbf{N}$ and refer to [67, Chapter 3]. The formula, stated as Corollary 3.2.3 in [67], is the following:

Lemma 1.6.1 (Slivnyak–Mecke formula)**.** *Let X be a Poisson process in $\mathbb{R}^n$ with intensity function ς, let $k \in \mathbb{N}$, and let $f\colon \mathbf{N} \times (\mathbb{R}^n)^k \to \mathbb{R}$ be a nonnegative measurable function. Write $\mathbf{x}$ for a k-ple of points $(x_1, \ldots, x_k) \in (\mathbb{R}^n)^k$. Then*

$$\mathbb{E}[\sum_{\mathbf{x}\in X^k} f(X, \mathbf{x})] = \int\limits_{\mathbf{x}\in(\mathbb{R}^n)^k} \mathbb{E}[f\left(X + \sum_{i=1}^{k} \delta_{x_i},\, \mathbf{x}\right)]\varsigma(x_1)\ldots\varsigma(x_k)\,\mathrm{d}\mathbf{x}.$$

This formula will be used in many contexts throughout this text, and now we can use it to show that the Poisson point process is in general position according to the definitions in Sections 1.2 and 1.3 with probability 1. Indeed, every general position assumption concerns the fixed number of points of X, so setting $f(X, \mathbf{x})$ to 1 iff $\mathbf{x}$ violates one of the assumptions, we get on the left the probability of this event and on the right 0, because the Lebesgue measure of the corresponding set is 0. It shows that X is in general position with probability 1, and we will always assume that it is the case.

1.7 Random mosaics

The term "random mosaic" stands for a random tessellation of the space. A random tessellation can be obtained either directly by taking random hyperplanes in the space, or indirectly, by first choosing random points and then producing a random tessellation based on these points. Questions under consideration in this work correspond to mosaics related to the Poisson point process. More precisely, given a Poisson point process X in $\mathbb{R}^n$ and using the fact that it is in general position with probability 1, we can consider all tessellations defined in previous sections. We thus obtain *Poisson–Voronoi* and Poisson–Delaunay mosaics, as well as *weighted Poisson–Voronoi* and *weighted Poisson–Delaunay mosaics* and *Poisson–Voronoi* and *Poisson–Delaunay mosaics of order* k. We can also study the subcomplexes with the radius bound, which have holes and are thus not tessellations of the space, as well as *Poisson-Čech* complexes, which do not partition the space either. We consider all mentioned random objects as random simplicial or CW-complexes, and the focus of this work is to find the expected number of their cells and the distribution of radius. These particular questions on Poisson–Delaunay mosaics have been pioneered by Miles almost 50 years ago [54, 55]. Properties of random weighted Voronoi diagrams with given distributions of weights, like normal or uniform, were studied in [48, 49]. Weighted Poisson–Delaunay mosaics corresponding to slices of Poisson–Voronoi tessellations were briefly considered in [58]. Topological characteristics of Čech and Rips complexes over Poisson point processes have been investigated in work of Kahle [44, 45], Bobrowski and Weinberger [13], Bobrowski and Adler [11], and Decreusefond et al. [19]. A good survey on random mosaics and stochastic geometric background is [67]. Another survey is the chapter "Poisson Voronoi Diagrams" in [59, pp. 291–410]. There is also a connection to percolation theory. Namely, the Poisson–Delaunay complex for radius r has the same topology as the *Boolean* or *Gilbert disk model* [15]. Percolation on the Poisson–Voronoi mosaic itself is also interesting [10, 14]. We now summarize the relevant results for this work and then state our questions formally.

We start with mentioning that with probability 1 the Poisson–Voronoi mosaic is normal, because as noticed before the Poisson point process is in general position with probability 1. Further, since $\operatorname{conv} X = \mathbb{R}^n$ with probability 1, all Voronoi domains are bounded convex polyhedra, see [67]. The first relevant result concerns volumes and areas of the skeleta of Poisson–Voronoi mosaic [56, 58, 67].

Theorem 1 (Expected volume of Poisson–Voronoi skeleta)**.** *Fix $0 \leq \ell \leq n$, fix a Borel region $\Omega \subseteq \mathbb{R}^n$, and let X be a stationary Poisson point process with density ρ in $\mathbb{R}^n$. Then the expected ℓ-dimensional volume of the ℓ-dimensional skeleton of the Poisson–Voronoi mosaic intersected with Ω is*

$$\mathbb{E}[\eta_\ell] = \rho^{\frac{n-\ell}{n}} \|\Omega\| \frac{2^{n-\ell+1}\pi^{\frac{n-\ell}{2}}}{n(n-\ell+1)!} \frac{\Gamma\left(\frac{n^2-n\ell+\ell+1}{2}\right)\Gamma\left(1+\frac{n}{2}\right)^{n-\ell+\frac{\ell}{n}}\Gamma\left(n-\ell+\frac{\ell}{n}\right)}{\Gamma\left(\frac{n^2-n\ell+\ell}{2}\right)\Gamma\left(\frac{n+1}{2}\right)^{n-\ell}\Gamma\left(\frac{\ell+1}{2}\right)}.$$

Here Γ stands for the Gamma function, see Section 2.1. Setting $\ell = 0$ in this theorem, we get the number of Voronoi vertices, or, equivalently the number of Delaunay n-simplices. A simple observation that every point of the point process is a Delaunay vertex and that every Delaunay $(n-1)$-simplex belongs to two n-simplices gives the following relations [67], which are enough to establish the size of Poisson–Delaunay mosaics for $n \leq 3$:

Theorem 2. *Fix a Borel region $\Omega \subseteq \mathbb{R}^n$ and let X be a stationary Poisson point process with density ρ in $\mathbb{R}^n$. Write d_j^n for the expected number of j-dimensional Delaunay simplices in Ω. Then*

$$d_0^n = \rho\|\Omega\| \qquad d_n^n = \mathbb{E}[\eta_0]$$
$$d_{n-1}^n = \frac{n+1}{2} d_n^{(n)} \qquad \sum_{j=0}^{n} (-1)^j d_j^n = 0.$$

The last relation comes from the Euler formula. There are several subtleties hidden in this statement, the first one is the definition of the relation "simplex lies in the region". The usual way of defining this relation for random mosaics is to consider *centroids* of faces and to count the faces with centroid inside the region. One possible choice of the centroid is the center of mass of the face, but any other translationally invariant choice is acceptable and gives the same result, see [58] for details. In other words, for a random mosaic we construct a point process of centroids of j-dimensional faces and compute the expected number of points of this point process in the region. Another problem is that it is no longer true that every $(n-1)$-simplex belongs to two n-simplices when we restrict the mosaic to Ω, but this can be worked around [58, 67]. If instead we say that a simplex is inside Ω if its intersection with Ω is not empty, then under appropriate formalization the same result holds for regions with smooth boundary up to $o(\|\Omega\|)$ as $\|\Omega\| \to \infty$, compare with Lemma 5.3.2. We are not going to use this formalization of centroids, rather going for the characterization which takes into account the neighboring faces. Before turning to this, we would just like to mention the result about the weighted Poisson–Delaunay mosaics. Relations between volumes of skeleta of Voronoi tessellations and weighted Voronoi tessellations were studied in [58], and for the expected number of weighted Voronoi vertices, or, equivalently, the number of weighted Delaunay top-dimensional simplices, the following formula was obtained:

Theorem 3 (Expected sizes of weighted Poisson–Delaunay mosaics)**.** *Fix a Borel region $\Omega \subseteq \mathbb{R}^k \subseteq \mathbb{R}^n$ and let X be a stationary Poisson point process with density ρ in $\mathbb{R}^n$. Write $d_j^{k,n}$ for the expected number of j-dimensional weighted Delaunay simplices in Ω. Then*

$$d_k^{k,n} = \rho^{\frac{n-\ell}{n}} \|\Omega\| \frac{\sigma_1\sigma_{n+1}}{\sigma_{k+1}\sigma_{n-k+1}} \frac{2^{k+1}\pi^{k/2}}{n(k+1)!} \frac{\Gamma\left(\frac{kn+n-k+1}{2}\right)}{\Gamma\left(\frac{kn+n-k}{2}\right)} \frac{\Gamma\left(\frac{n+2}{2}\right)^{k+1-\frac{k}{n}}}{\Gamma\left(\frac{n+1}{2}\right)^{k}} \frac{\Gamma\left(k+1-\frac{k}{n}\right)}{\Gamma\left(\frac{n-k+1}{2}\right)}$$
$$d_{k-1}^{k,n} = \frac{k+1}{2} d_k^{k,n},$$

where σ_i stands for the $(i-1)$-dimensional area of the unit sphere in $\mathbb{R}^i$.

Subsets and subcomplexes. In this paragraph we emphasize the difference in the way we use to count simplices. Take for instance the Poisson–Delaunay mosaic. Assuming X is in general position, we use a Borel set Ω to specify three subsets of it.

- The subcomplex $K_0 = K_0(\Omega)$ of $\mathrm{Del}X$ consists of all simplices Q such that $\mathrm{Vor}(Q) \cap \Omega \neq \emptyset$; see Figure 1.8. Equivalently, K_0 consists of all simplices such that the intersection $\bigcap_{x\in Q}[\mathrm{dom}(x) \cap \Omega] \neq \emptyset$. If Ω is convex, the intersections $\mathrm{dom}(x) \cap \Omega$ are convex as well, and the Nerve Theorem applies and asserts that K_0 and Ω have the same homotopy type, and since a convex set is contractible, this implies $\chi(K_0) = 1$.

- The subset $K_1 = K_1(\Omega)$ of $\mathrm{Del}X$ consists of all simplices in K_0 whose Delaunay spheres (recall the definition of the Delaunay sphere in Section 1.2) have center in Ω. We can construct K_1 by removing one simplex at a time from K_0. Each removed simplex changes the Euler characteristic by 1, which gives

$$|\chi(K_1) - \chi(K_0)| \leq |K_0 \setminus K_1|.$$

- The subset $K_2 = K_2(\Omega)$ of $\mathrm{Del}X$ consists of all simplices in $\mathrm{Del}X$ whose center of mass lies in Ω.

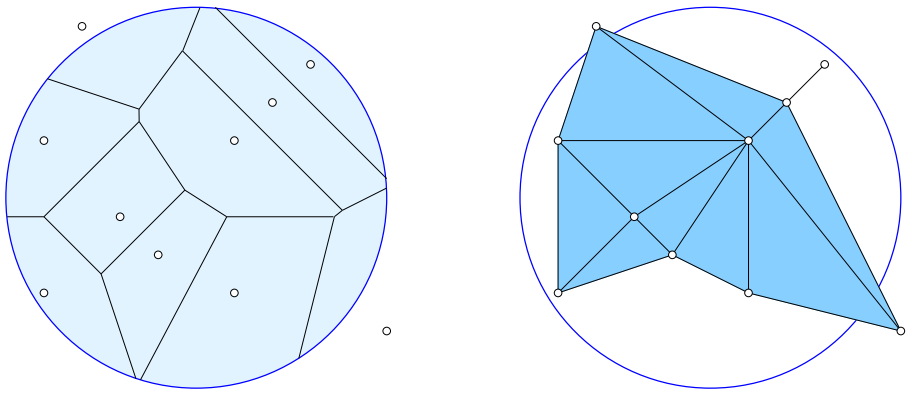

Figure 1.8: The Voronoi diagram restricted to a disk on the *left*, and the corresponding restricted Delaunay mosaic, K_0, on the *right*. In this case, the set K_1 consists of all simplices in K_0 except for the two vertices that lie outside Ω.

We will always work with K_1. So, we say that a Delaunay simplex lies in Ω if its Delaunay center lies in Ω. The Delaunay center of the simplex, as defined in Section 1.2 is not an internal characteristic of the face, it relies on the emptiness of some spheres, so this definition is not equivalent to choosing a centroid, which gives K_2. Nevertheless, this choice is still very "local": if Ω is a nice set, then the difference between the number of simplices in K_0 and K_1 is $o(\|\Omega\|)$; see Section 5.3. This is so because a simplex belongs to $K_0 \setminus K_1$ only if the common intersection of the corresponding Voronoi domains touches the boundary of Ω, and there are not many such simplices. The details are a bit lengthy and can be found in Section 5.3. It is also known (see [67]) that the difference between K_0 and K_2 is $o(\|\Omega\|)$, so the expected numbers of simplices in K_1 and K_2 differ at most by $o(\|\Omega\|)$, but we will get precise expressions without these small-order terms, implying that the expected numbers of simplices in K_1 and K_2 are the same, so Theorem 2 holds both for K_1 and K_2, and up to $o(\|\Omega\|)$ for K_0. Similar remarks hold for all other complexes in question.

1.8 Random inscribed polytopes and Fisher space

One more question targeted in this work is about the sizes of Poisson–Delaunay mosaics on the sphere. Our reason for comparing random sets in the Euclidean space and on the sphere is the Fisher information metric, which measures the dissimilarity between discrete probability distributions. Write $\mathbf{x} = (x_0, x_1, \ldots, x_n)$ and $\mathbf{y} = (y_0, y_1, \ldots, y_n)$ for two such distributions, with $\sum_{i=0}^{n} x_i = \sum_{i=0}^{n} y_i = 1$ and $x_i, y_i \geq 0$ for all i, and note that $\mathbf{x}$ and $\mathbf{y}$

are points of the n-dimensional standard simplex, Δ^n. Letting $\gamma\colon [0,1] \to \Delta^n$ be a smooth curve connecting $\mathbf{x} = \gamma(0)$ to $\mathbf{y} = \gamma(1)$, we define its *length* as

$$\text{Length}(\gamma) = \int_{t=0}^{1} \sqrt{\frac{1}{2}\sum_{i=0}^{n} \frac{\dot{\gamma}_i(t)^2}{\gamma_i(t)}}\, \mathrm{d}t,$$

in which $\gamma_i(t)$ and $\dot{\gamma}_i(t)$ are the i-th components of the curve and its velocity vector. The *Fisher information metric* assigns the length of the shortest connecting path to the pair $\mathbf{x}, \mathbf{y}$; see [2, Section 2.2] as well as [1, Section I.4], where this metric is referred to as the Shahshahani metric. This way of measuring distance is fundamental in information geometry and in population genetics.

To shed light on the Fisher information metric, we map every point $\mathbf{x} = (x_0, x_1, \ldots, x_n)$ of Δ^n to the point $\varphi(\mathbf{x}) = (u_0, u_1, \ldots, u_n)$ with $u_i = \sqrt{2x_i}$ for every i. The coordinates of $\varphi(\mathbf{x})$ are all non-negative and satisfy $\sum_{i=0}^{n} u_i^2 = 2$. In words, $\varphi(\mathbf{x})$ is a point of $\sqrt{2}\mathbb{S}^n_+$, which is our notation for the non-negative orthant of the sphere with radius $\sqrt{2}$ centered at the origin in $\mathbb{R}^{n+1}$; see Figure 1.9 on the right. As noticed already by [3], see also [1, page 39], this mapping is an isometry between Δ^n and $\sqrt{2}\mathbb{S}^n_+$. We can therefore understand Δ^n under the Fisher information metric by studying $\mathbb{S}^n_+$ under the geodesic distance. To get a handle on the difference between random sets in $\mathbb{R}^n$ and in Δ^n, we compare point sets selected from Poisson point processes in $\mathbb{R}^n$ and on $\mathbb{S}^n$, the latter being the topic of this section. Figure 1.9 illustrates the isometry by showing three level lines each for seven points in the standard triangle on the left and for the seven corresponding points in the positive orthant of the sphere on the right.

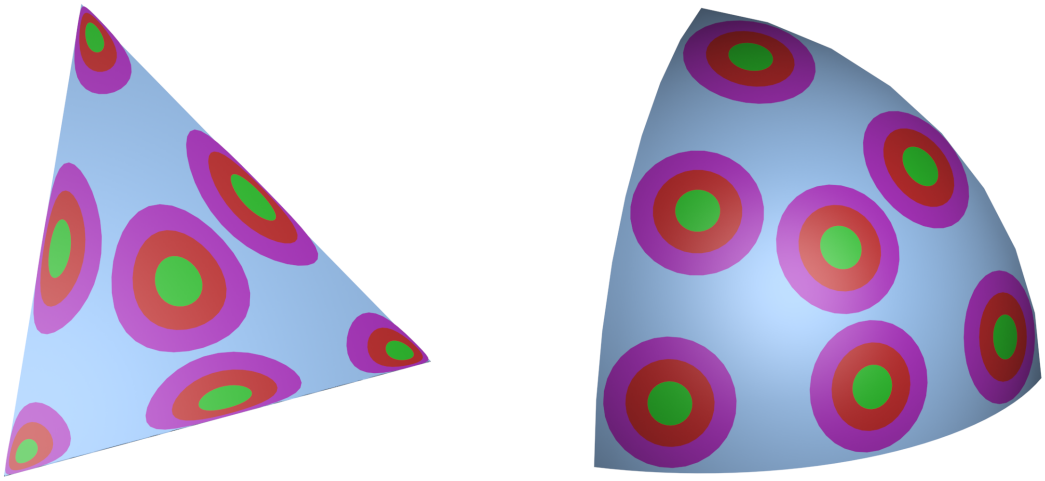

Figure 1.9: *Left:* disk neighborhoods under the Fisher information metric of seven points in the standard triangle. *Right:* the corresponding seven points and cap neighborhoods in the isometric non-negative octant of the 2-sphere. For aesthetic reasons, the octant is scaled to $1/\sqrt{2}$ times its actual size. Thanks to Hubert Wagner for providing the figure.

Consider the model in which a random polytope is generated by taking the convex hull of randomly chosen points on the unit sphere. The first paper with substantial results on this topic is [55]. The large body of work on the expected number of faces of random polytopes and their volume is summarized and surveyed in [7, 43, 63, 66, 67]. A survey of

recent results can be found in [70]. The more general setting in which the points are selected on the boundary of a convex body is addressed in [64], and the linear dependence of the expected number of faces on the number of vertices is proved. The connection to the present work becomes clear if we notice that the Delaunay mosaic for a point set on the sphere is essentially their convex hull.

Voronoi tessellations and Delaunay mosaics. We recall that the object under consideration is $\mathbb{S}^n \subseteq \mathbb{R}^{n+1}$ with the *geodesic distance*, $d\colon \mathbb{S}^n \times \mathbb{S}^n \to \mathbb{R}$, the metric inherited from the Euclidean metric on $\mathbb{R}^{n+1}$. The distance between any pair of points is defined to be the length of the shortest connecting path: $d(x,y) = 2 \arcsin \frac{\|x-y\|}{2}$. This shortest path is unique, unless $y = -x$, in which case there are infinitely many shortest paths of length π. Letting X be a finite set of points on $\mathbb{S}^n$, we follow [65] to define the *Voronoi domain* of $x \in X$ as the points for which x minimizes the geodesic distance, further constraining it to within the open hemisphere centered at x:

$$\mathrm{dom}(x) = \{w \in \mathbb{S}^n \mid d(w,x) \leq d(w,y) \text{ for all } y \in X \text{ and } d(w,x) < \tfrac{\pi}{2}\}.$$

Note that $d(w,x) \leq d(w,y)$ defines a closed hemisphere, namely all points $w \in \mathbb{S}^n$ that satisfy $\|w-x\| \leq \|w-y\|$ in $\mathbb{R}^{n+1}$. It follows that $\mathrm{dom}(x)$ is the intersection of a finite collection of hemispheres — a set we refer to as a *(convex) spherical polytope*. Any two of these spherical polytopes have disjoint interiors. The *Voronoi tessellation* of X is the collection of Voronoi domains, one for each point in X. It covers the entire n-sphere, except if X is contained in a closed hemisphere, in which case it covers $\mathbb{S}^n$ minus a possibly degenerate but non-empty spherical polytope; see Figure 1.10. Generically, the common

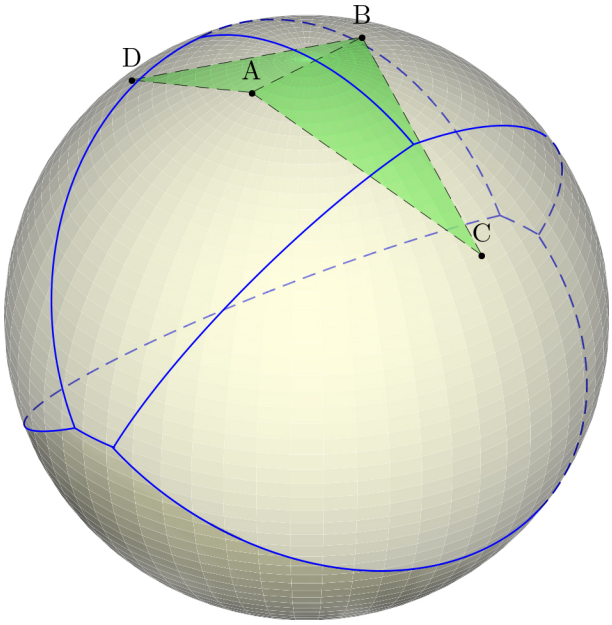

Figure 1.10: The Voronoi domains of four points on the 2-dimensional sphere. The darker region in the south does not belong to any of these domains because the four points all belong to the northern hemisphere. The dual Delaunay complex consists of two triangles glued along a shared edge.

intersection of $1 \leq k \leq n+1$ Voronoi domains is either empty or a shared face of dimension $n-k+1$, and the common intersection of $n+2$ or more Voronoi domains is empty.

The *Delaunay mosaic* of X is isomorphic to the nerve of the Voronoi tessellation:

$$\mathrm{Del}X = \{Q \subseteq X \mid \bigcap_{x\in Q} \mathrm{dom}(x) \neq \emptyset\}.$$

The Nerve Theorem implies that the Delaunay mosaic has the same homotopy type as the union of Voronoi domains. Assuming there is no closed hemisphere that contains all points, this is the homotopy type of $\mathbb{S}^n$.

Delaunay mosaics and inscribed polytopes. The Delaunay mosaic is an (abstract) simplicial complex. In the generic case, $\mathrm{Del}X$ can be geometrically realized in $\mathbb{R}^{n+1}$, namely by mapping every abstract simplex, Q, to the convex hull of its points. To make this precise, we compare $\mathrm{Del}X$ with the boundary complex of $\mathrm{conv}\, X$, which is a convex polytope inscribed in the n-sphere. Each $(n-1)$-sphere $S \subseteq \mathbb{S}^n$ defines two (closed) caps. If S is a great-sphere, these caps are hemispheres, else they have different volume and we call one the *small cap* and the other the *big cap*. Every facet of $\mathrm{conv}\, X$ defines such a pair of caps, namely the portions of $\mathbb{S}^n$ on the two sides of the n-plane spanned by the facet. One of these caps is *empty*, by which we mean that no point of X lies in its interior. If 0 is in the interior of $\mathrm{conv}\, X$, then all empty caps are small, but if $0 \notin \mathrm{conv}\, X$, then there is at least one empty big cap. For non-generic sets, 0 may lie on the boundary of $\mathrm{conv}\, X$, in which case there is at least one empty hemisphere cap. Parsing the definitions of Voronoi and Delaunay mosaics, we observe that a simplex $Q \subseteq X$ belongs to the Delaunay mosaic iff there is an $(n-1)$-sphere, S, that contains Q, which is not a great-sphere, and whose empty cap is small. In the generic case, these simplices Q are exactly the faces of the facets of $\mathrm{conv}\, X$ whose small caps are empty. In particular, it shows that if points are not contained in any hemisphere, then $\mathrm{Del}X$ is isomorphic to the boundary of $\mathrm{conv}\, X$, a random inscribed polytope.

Radius function. Consider growing a spherical cap from each point in X. To formalize this process, we write $\mathrm{Cap}_\eta(x) = \{w \in \mathbb{S}^n \mid d(w,x) \leq \eta\}$ for the cap with center $x \in X$ and geodesic radius η. Clipping the Voronoi domain to within the cap, for each point $x \in X$, we get a subcomplex of the Delaunay mosaic when we take the nerve:

$$\mathrm{Del}_\eta X = \{Q \subseteq X \mid \bigcap_{x\in Q} [\mathrm{dom}(x) \cap \mathrm{Cap}_\eta(x)] \neq \emptyset\}.$$

By construction, $\mathrm{Del}_\eta X$ is a simplicial complex, which we call the *spherical Delaunay complex*, and $\mathrm{Del}_\eta X \subseteq \mathrm{Del}_\zeta X$ whenever $\eta \leq \zeta$. For $\eta = \frac{\pi}{2}$, each restricting cap is a hemisphere and thus contains its corresponding Voronoi domain, which implies $\mathrm{Del}_{\pi/2} X = \mathrm{Del}X$. We are now ready to introduce the *spherical Delaunay radius function*, $\mathcal{R}_S \colon \mathrm{Del}X \to \mathbb{R}$, which maps every simplex to the smallest geodesic radius for which the simplex belongs to the subcomplex of the Delaunay mosaic:

$$\mathcal{R}_S(Q) = \min\{\eta \mid Q \in \mathrm{Del}_\eta X\}.$$

In other words, $\mathcal{R}_S{}^{-1}[0,\eta] = \mathrm{Del}_\eta X$. We will prove shortly that for generic X, the radius function on the Delaunay mosaic is a generalized discrete Morse function. Formally, we say a finite set $X \subseteq \mathbb{S}^n$ is in *general position* if $|X| > n+1$ and for every $0 \leq k < n$

1. no $k+3$ points of X belong to a common k-sphere on $\mathbb{S}^n$,
2. considering the unique $(k+1)$-sphere that passes through $k+3$ points of X, no $k+2$ of these points belong to a common k-sphere that shares its center with the $(k+1)$-sphere.

Condition 2 implies that no $n+1$ points of X lie on a great-sphere of $\mathbb{S}^n$. We need a few additional concepts. Assume X is in general position and $Q \subseteq X$ is a k-simplex with $0 \leq k \leq n$. A cap *circumscribes* Q if the bounding $(n-1)$-sphere passes through all points of Q. Since X is generic, Q has a unique *smallest circumscribed cap*, which we denote $\mathrm{cap}(Q)$. If $Q \in \mathrm{Del}X$, Q also has a unique *smallest empty circumscribed cap*, which may or may not be the smallest circumscribed cap. We call it the *Delaunay cap* of Q and denote it as $\mathrm{cap}_\emptyset(Q)$. The *Euclidean center* of a cap is the center of the bounding $(n-1)$ sphere, which is a point in $\mathbb{R}^{n+1}$ but not on $\mathbb{S}^n$. Using this center, we use the notion of visibility within the affine hull of Q, which is a k-dimensional plane in $\mathbb{R}^{n+1}$. Recall that a facet of Q is *visible* from this center if the $(k-1)$-plane spanned by the facet separates the center from Q or, equivalently, if the center lies in one closed k-dimensional halfspace bounded by the $(k-1)$-plane and Q is contained in the other such halfspace. It is easy to see that the radius function maps every simplex to the geodesic radius of its Delaunay cap; compare with Section 1.2.

Lemma 1.8.1 (Spherical radius function)**.** *Let $X \subseteq \mathbb{S}^n$ be a finite set in general position. Then $\mathcal{R}_S \colon \mathrm{Del}X \to \mathbb{R}$ is a generalized discrete Morse function, and $[L,U]$ is an interval of $\mathcal{R}_S$ iff $\mathrm{cap}(U)$ is empty and L is the maximal common face of all facets of U that are visible from the Euclidean center of $\mathrm{cap}(U)$. Furthermore, for every $Q \in [L,U]$, we have $\mathrm{cap}_\emptyset(Q) = \mathrm{cap}(U)$.*

Proof. We prove that for each $Q \in \mathrm{Del}X$ there are unique Delaunay simplices $L \subseteq Q \subseteq U$ such that $\mathrm{cap}(U) = \mathrm{cap}_\emptyset(U)$, L is the intersection of all visible facts of U, and all simplices in $[L,U]$ share the Delaunay cap. Note that $\mathcal{R}_S(Q)$ is the geodesic radius of the Delaunay cap of Q. Letting $U \subseteq X$ be the set of all points on the $(n-1)$-sphere that bounds this Delaunay cap, we have $\mathrm{cap}_\emptyset(U) = \mathrm{cap}(U)$ for else we could find a smaller empty circumscribed cap. Let z be the center and η the geodesic radius of $\mathrm{cap}(U)$. By assumption of general position, $|U| \leq n+1$, so U is a Delaunay simplex. For every facet F of U, let z_F be the center and η_F the geodesic radius of $\mathrm{cap}(F)$, and let u_F be the unique vertex in $U \setminus F$. We move the center of this cap along the shortest path from z_F to z while adjusting the radius so that all points of F remain on the boundary of the cap. During this motion, the radius increases continuously, and when it reaches η, the boundary of the cap passes through u_F. If F is visible from z, then u_F is inside the cap at the beginning and on the boundary of the cap at the end of the motion. If F is not visible from the Euclidean center, then u_F changes from outside at the beginning to on the boundary of the cap at the end of the motion. In other words, $\mathrm{cap}(U)$ is the Delaunay cap of every visible facet of U, but every invisible facet has a smaller empty circumscribed cap. Since the intersection of two simplices with common Delaunay cap has the same Delaunay cap [8, Lemma 3.4], we can take L as the intersection of all visible facets of U and get $\mathrm{cap}_\emptyset(L) = \mathrm{cap}(U)$. On the other hand, any face of U that does not contain L is also a face of an invisible facet and therefore has a smaller empty circumscribed cap. This implies $L \subseteq Q$.

We note that the construction gives a partition of $\mathrm{Del}X$ into intervals. Indeed, any two Delaunay simplices sharing the Delaunay cap give rise to the same simplex U and therefore to the same interval $[L,U]$. This concludes the proof. □

REMARK. While the proof follows almost verbatim the proof in the Euclidean case [8], and actually the Euclidean Delaunay mosaic of the spherical point set is almost identical to the one we are talking about, there is a subtlety hidden in its definition. Indeed, because each Voronoi domain is restricted to within the open hemisphere centered at the generating point, the sets $\mathrm{dom}(x) \cap \mathrm{Cap}_\eta(x)$ form a system in which every common intersection

is either empty or contractible. The Nerve Theorem thus applies, proving that the subcomplex of the Delaunay mosaic has the same homotopy type as the union of caps of radius η. This property breaks down for the boundary complex of $\mathrm{conv}\, X$. This can be seen by considering the four points on $\mathbb{S}^2$ shown in Figure 1.10: $A, B = (\pm\varepsilon, 0, \sqrt{1-\varepsilon^2})$ and $C, D = (0, \pm 1/2, \sqrt{3}/2)$, in which ε is a sufficiently small positive real number. The great-circle arc shared by the Voronoi domains of C and D has length only slightly shorter than π and it intersects the union of four caps of geodesic radius η slightly larger than $\frac{\pi}{2}$ in two disconnected segments. The union of the four caps has the topology of a disk, while the nerve has the topology of a circle. Indeed, the latter consists of two triangles glued along a shared edge plus another edge connecting the two respective third vertices of the two triangles.

Poisson point process. We are interested in random sets $X \subseteq \mathbb{S}^n$, and we primarily consider Poisson point process on the sphere. Now we prove that the difference between the boundary complex of $\mathrm{conv}\, X$ and $\mathrm{Del} X$ is small if X is a Poisson point process. More precisely, the number of faces of $\mathrm{conv}\, X$ that are visible from 0 outside $\mathrm{conv}\, X$ vanishes rapidly as the density increases. This is consistent with the rapid decrease of the probability that $0 \notin \mathrm{conv}\, X$, as computed in [72] for the uniform distribution on $\mathbb{S}^n$.

Lemma 1.8.2 (Non-Delaunay faces)**.** *Let X be a Poisson point process with density $\rho > 0$ on $\mathbb{S}^n$. For every $0 \leq k \leq n$, the expected number of k-faces of $\mathrm{conv}\, X$ that do not belong to $\mathrm{Del} X$ goes to 0 as ρ goes to ∞.*

Proof. We may assume that $\mathrm{conv}\, X$ is simplicial and that no $n+1$ points lie on a great-sphere of $\mathbb{S}^n$. Let $Q \subseteq X$ be a set of $n+1$ points and consider its small and big caps. The big cap has volume larger than of the volume of the sphere, $\sigma_{n+1}/2$, and Q is a facet of $\mathrm{conv}\, X$ but not a simplex of $\mathrm{Del} X$ iff this big cap is empty. The probability of this event is less than $e^{-\rho\sigma_{n+1}/2}$. The expected number of such facets of $\mathrm{conv}\, X$ is therefore less than a constant times $\rho^{n+1} e^{-\rho\sigma_{n+1}/2}$, which goes to 0 as ρ goes to ∞. Here we used that $\mathbb{E}[|X|^{n+1}]$ is at most a constant times ρ^{n+1}. For $k < n$, every k-face of $\mathrm{conv}\, X$ that does not belong to $\mathrm{Del} X$ is a face of a facet with this property. The expected number of such k-faces thus also goes to 0 as ρ goes to ∞. □

We need one more concept to express the asymptotic behavior of the expected numbers, when their density goes to infinity. Assuming a Poisson point process with density $\rho > 0$ on $\mathbb{S}^n$, for a cap with geodesic radius η, we call $\bar{\eta} = \eta\rho^{1/n}$ the *normalized radius* of the cap. It is the geodesic radius of the cap after scaling the unit sphere to the sphere with area ρ times bigger.

Uniform distribution. Taking points on the sphere uniformly at random may seem to be more natural then considering a Poisson point process. For questions addressed in this work there is not much difference, though. This will be briefly discussed in Section 7.3. Curiously, we will need other related results for uniform distributions. In Section 1.9 and in Chapter 3 we will often face powers of the volume of a simplex under the integral over all possible inscribed simplices. These integrals will be further investigated in Chapter 4, and the starting point is formed by the following theorems.

The first, simpler, result gives the moments of the volumes of *cones* over facets of a uniformly random inscribed simplex. Let $\mathbf{u} = (u_0, u_1, u_2, \ldots, u_k)$ be a k-simplex with vertices on $\mathbb{S}^{n-1} \subseteq \mathbb{R}^n$. For each $0 \leq i \leq k$, let $\mathbf{u}_i$ be the k-simplex obtained by substituting 0 for

u_i and write $V_i = \mathrm{Vol}(\mathbf{u}_i)$ for its k-dimensional volume. We call this simplex a *cone* over the i-th facet. The next theorem is [53, Equation 2.11] and with a minor correction [55, Equation (23)], although known before.

Theorem 4 (Moments of cone volumes)**.** *Let $u_0, u_1, u_2, \ldots, u_k$ be independently and uniformly distributed on $\mathbb{S}^{n-1} \subseteq \mathbb{R}^n$. Then for any integer $a \geq 0$, the a-th moment of the volume of a cone over any facet, i.e., the expectation of V_i^a, is*

$$\mathrm{Mnt}_1(k, n; a) = \mathbb{E}[V_i^a] = \frac{1}{k!^a} \left[\tfrac{\Gamma(n/2)}{\Gamma((n+a)/2)}\right]^{k-1} \prod_{i=1}^{k-1} \tfrac{\Gamma((n-k+a+i)/2)}{\Gamma((n-k+i)/2)}. \tag{1.1}$$

With the exception of the proof of the next theorem, we will only need the case $k = n$. Besides these moments, we also need the mixed moments to get our results. In general, it seems to be a complicated problem, which can be reformulated in the language of random matrices, asking about the mixed moments of minors of Wishart matrices, the question considered e.g. in [22]. Indeed, there is a connection between uniform distribution on the sphere and the Gaussian distribution, it will be used in Section 2.1. It leads to an equivalent question for Gaussian random simplex, and a Gaussian random simplex can be represented as a random $n \times (n+1)$-matrix M with independent identically normally distributed elements. The cone volumes are the $n \times n$-minors of this matrix, or equivalently, the square roots of $n \times n$-minors of $M^T M$, the latter being known as *Wishart ensemble*. Not going further into this connection, we will compute the moments only for pairs of cones now.

Theorem 5 (Pairwise mixed moments of cone volumes)**.** *Let $\mathbf{u}$ be a sequence of $n+1$ independently and uniformly distributed points on $\mathbb{S}^{n-1}$. Then for any $0 \leq i < j \leq n$ and integers $a, b \geq 0$, the expectation of $V_i^a V_j^b$ is*

$$\mathrm{Mnt}_2(n; a, b) = \tfrac{\mathrm{Mnt}_1(n-1, n; a+b)}{n^{a+b}} \left[\tfrac{\Gamma(n/2)}{\Gamma(1/2)}\right]^2 \tfrac{\Gamma((a+1)/2)}{\Gamma((n+a)/2)} \tfrac{\Gamma((b+1)/2)}{\Gamma((n+b)/2)}. \tag{1.2}$$

Proof. Note that $V_i = \frac{1}{n} h_i A$ and $V_j = \frac{1}{n} h_j A$, in which A is the $(n-1)$-dimensional volume of the shared facet of $\mathbf{u}_i$ and $\mathbf{u}_j$, and h_i, h_j are the distances of the points u_i, u_j from the hyperplane spanned by the shared facet. For geometric reasons, it is clear that h_i, h_j, A are independent; see [53] for details. Hence, we get

$$\mathbb{E}[V_i^a V_j^b] = \tfrac{1}{n^{a+b}}\, \mathbb{E}[h_i^a]\, \mathbb{E}[h_j^b]\, \mathbb{E}[A^{a+b}],$$

with $\mathbb{E}[A^{a+b}] = \mathrm{Mnt}_1(n-1, n; a+b)$ with value given in (1.1). The value for $\mathbb{E}[h_i^a]$ given in [53], right before Formula (2.11), is $\Gamma(\frac{n}{2})/\Gamma(\frac{1}{2})$ times $\Gamma(\frac{a+1}{2})/\Gamma(\frac{n+a}{2})$. Substituting the analogous expression for $\mathbb{E}[h_j^b]$ gives the claimed relation. □

We illustrate Theorems 4 and 5 by computing Mnt_1 and Mnt_2 for a selected set of small values of k, n, a, b, chosen so the results will be useful in Section 4.4; see Table 1.1.

Another relevant result is about the moments of the total volume of a random inscribed simplex. It seems to be much more complicated then Theorem 4, and can actually be seen as a consequence of Theorem 21 proved in this work if we set $f \equiv 1$. Indeed, a very similar reasoning was used in [55] to get the following statement.

$\mathrm{Mnt}_1(k,n;a)$	$a=1$	$a=2$	$a=3$
$k=n=2$	$\frac{1}{\pi}$	$\frac{1}{8}$	$\frac{1}{6\pi}$
3	$\frac{\pi}{48}$	$\frac{1}{162}$	
4	$\frac{8}{81\pi^2}$		

$\mathrm{Mnt}_2(n;a,b)$	$a=1$ $b=1$	$a=2$ $b=1$	$a=2$ $b=2$
$n=2$	$\frac{1}{\pi^2}$	$\frac{1}{8\pi}$	
3	$\frac{1}{216}$		
4			

Table 1.1: Values of Mnt_1 for small values of k, n, a on the *left*, and values of Mnt_2 for small values of n, a, b on the *right*.

Theorem 6 (Moments of simplex volumes)**.** *Let $u_0, \dots, u_k$ be $k+1$ independent uniformly distributed random points on $\mathbb{S}^{n-1} \subseteq \mathbb{R}^n$, and write $\mathbf{u} = (u_0, \dots, u_k)$ for the k-simplex with these vertices. Then for any integer $a \geq 0$, the a-th moment of the volume of this simplex, is*

$$\mathbb{E}[\mathrm{Vol}(\mathbf{u})^a] = \frac{1}{k!^a}\left[\frac{\Gamma(n/2)}{\Gamma((n+a)/2)}\right]^k \frac{\Gamma\left(\frac{(k+1)(n+a)}{2} - k\right)}{\Gamma\left(\frac{(k+1)(n+a)-a}{2} - k\right)} \prod_{i=1}^{k-1} \frac{\Gamma((n-k+a+i)/2)}{\Gamma((n-k+i)/2)}.$$

1.9 Blaschke–Petkantschin formulas

Blaschke–Petkantschin formula is a classic result in integral geometry. It is used to change from integration over k points in $\mathbb{R}^n$ to the integration over the affine hull of these points. In this section we present the two well known variants of this formula and the necessary notation. Let $0 < k \leq n$ and write $\mathcal{L}_k^n$ for the Grassmannian consisting of all k-planes passing through the origin in $\mathbb{R}^n$. We recall that there is a standard measure on Grassmanian; see [39] and Section 2.1. The following theorem is the classic formula in the form [55, Equation (27)]:

Theorem 7 (Linear Blaschke–Petkantschin formula)**.** *Fix $0 \leq k \leq n$. Then for a measurable non-negative function $f\colon (\mathbb{R}^n)^{k+1} \to \mathbb{R}$*

$$\int_{\mathbf{x}\in(\mathbb{R}^n)^{k+1}} f(\mathbf{x})\,\mathrm{d}\mathbf{x} = \int_{L\in\mathcal{L}_k^n} \int_{h\in L^\perp} \int_{\mathbf{x}\in L^{k+1}} f(h+\mathbf{x})(k!\mathrm{Vol}(\mathbf{x}))^{n-k}\,\mathrm{d}\mathbf{x}\,\mathrm{d}h\,\mathrm{d}L,$$

in which $\mathbf{x} = (x_0, x_1, \dots, x_k)$, each x_i is a point in $\mathbb{R}^n$, $h + \mathbf{x}$ is $(h + x_0, h + x_1, \dots, h + x_k)$, and $\mathrm{Vol}(\mathbf{x})$ is the k-dimensional volume of the simplex spanned by $\mathbf{x}$.

Almost all $(n+1)$-tuples of points in $\mathbb{R}^n$ define a unique $(n-1)$-sphere that passes through all of them. In other words, the following formula [67, Theorem 7.3.1] integrates over circumscribed spheres of simplices in $\mathbb{R}^n$:

Theorem 8 (Top-dimensional spherical Blaschke–Petkantschin formula)**.** *Every measurable non-negative function $f\colon (\mathbb{R}^n)^{n+1} \to \mathbb{R}$ satisfies*

$$\int_{\mathbf{x}\in(\mathbb{R}^n)^{n+1}} f(\mathbf{x})\,\mathrm{d}\mathbf{x} = \int_{z\in\mathbb{R}^n} \int_{r\geq 0} \int_{\mathbf{u}\in(\mathbb{S}^{n-1})^{n+1}} f(z+r\mathbf{u})r^{n^2-1}n!\mathrm{Vol}(\mathbf{u})\,\mathrm{d}\mathbf{u}\,\mathrm{d}r\,\mathrm{d}z,$$

in which we use the standard spherical measure on $\mathbb{S}^{n-1}$.

Further formulas of these type were studied in [74, 64].

Not explicitly used in this work but relevant for the derivation of the number of vertices in a weighted Voronoi diagram is the *Crofton's formula*. Using (50) and (103) from Chapter 6 of [39] (see also [67, Theorem 9.4.7]), we can obtain the following formula for a convex set $A \subseteq \mathbb{R}^{n-k} \subseteq \mathbb{R}^n$:

$$\lambda_{n-k}(A) = \frac{\nu_1 \dots \nu_{k-1}}{\nu_{n-k} \dots \nu_{n-1}} \int\limits_{L \in \mathcal{L}_k^n} \int\limits_{x \perp L} \mathbf{1}_{x+L \cap A \neq \emptyset} \, \mathrm{d}x \, \mathrm{d}L, \tag{1.3}$$

where λ_{n-k} is the $(n-k)$-dimensional Lebesgue measure and ν_i is the volume of a unit ball in $\mathbb{R}^i$. The $\mathbf{1}$ is the indicator function, which is equal to 1 if $x + L \cap A \neq \emptyset$ and is zero otherwise. This formula clearly generalizes to the following:

Theorem (Crofton's formula)**.** *Let A be an $(n-k)$-dimensional set in $\mathbb{R}^n$ which can be decomposed as a countable union of convex sets. Then*

$$\lambda_{n-k}(A) = \frac{\nu_1 \dots \nu_{k-1}}{\nu_{n-k} \dots \nu_{n-1}} \int\limits_{L \in \mathcal{L}_k^n} \int\limits_{x \perp L} \#\{(x+L) \cap A\} \, \mathrm{d}x \, \mathrm{d}L,$$

where $\#$ is the (possibly infinite) number of points in the set.

Further generalizations are possible. For example, the convexity requirement can be replaced with appropriate smoothness, but we are not going into these details.

2. Results

In this chapter we collect new results of the work. Section 2.1 gives the background and notation for standard functions and measures needed to state the results, while the results themselves are summarized in the remaining sections, grouped by the random complex they are related to.

2.1 Standard notation and functions

Before stating the results, we summarize the notation and functions used in the text.

Gamma functions. We recall that the *lower incomplete Gamma function* takes two parameters, j and $t_0 \geq 0$, and is defined by

$$\gamma(j;\, t_0) = \int_{t=0}^{t_0} t^{j-1} e^{-t}\, \mathrm{d}t.$$

The corresponding complete *Gamma function* is $\Gamma(j) = \gamma(j;\, \infty)$. An important relation for Gamma functions is $\Gamma(j+1) = j\Gamma(j)$, which holds for any real j that is not a non-positive integer. We often use the ratio, $\gamma(j;\, t_0)/\Gamma(j)$, which is the density of a probability distribution and called the *Gamma distribution* with parameter j. We prove a technical lemma about incomplete Gamma functions, which will be repeatedly used in the following chapters.

Lemma 2.1.1 (Gamma function)**.** *Let $c, p, j, t_0 \in \mathbb{R}$ with $p \neq 0$ and $t_0 > 0$. Then*

$$\int_{t=0}^{t_0} t^{j-1} e^{-ct^p}\, \mathrm{d}t = \frac{\gamma\left(\frac{j}{p};\, ct_0^p\right)}{pc^{j/p}}.$$

Proof. We rewrite the numerator of the right-hand side of the claimed identity using the definition of the lower incomplete Gamma function and substituting $u = ct^p$ and $\mathrm{d}u = cpt^{p-1}\, \mathrm{d}t$:

$$\begin{aligned}
\gamma\left(\tfrac{j}{p};\, ct_0^p\right) &= \int_{u=0}^{ct_0^p} u^{\frac{j}{p}-1} e^{-u}\, \mathrm{d}u \\
&= \int_{t=0}^{t_0} (ct^p)^{\frac{j}{p}-1} e^{-ct^p} cpt^{p-1}\, \mathrm{d}t \\
&= \int_{t=0}^{t_0} pc^{\frac{j}{p}} t^{j-1} e^{-ct^p}\, \mathrm{d}t.
\end{aligned}$$

Dividing by $pc^{j/p}$ gives the claimed relation. □

Beta functions. Given real numbers a, b, and $0 \le t_0 \le 1$, the *incomplete Beta function* is defined by

$$B_{t_0}(a,b) = \int_{t=0}^{t_0} t^{a-1}(1-t)^{b-1}\,\mathrm{d}t,$$

and the complete *Beta function* is $B(a,b) = B_1(a,b)$, which can be expressed in terms of complete Gamma functions: $B(a,b) = \Gamma(a)\Gamma(b)/\Gamma(a+b)$.

The Beta functions can be used to integrate over the projection of a sphere in $\mathbb{R}^n$ to a linear subspace $\mathbb{R}^k \hookrightarrow \mathbb{R}^n$, as we now explain. Assuming $\mathbb{R}^k$ is spanned by the first k coordinate vectors of $\mathbb{R}^n$, the projection of a point means dropping coordinates $k+1$ to n. Suppose now that we pick a point $x = (x_1, x_2, \ldots, x_n)$ uniformly on $\mathbb{S}^{n-1}$ by normalizing a vector of n normally distributed random variables: $X_i \sim \mathcal{N}(0,1)$ for $1 \le i \le n$ and $x_j = X_j / \left(\sum_{i=1}^n X_i^2\right)^{1/2}$ for $1 \le j \le n$. Its projection to $\mathbb{R}^k$ is $x' = (x_1, \ldots, x_k, 0, \ldots, 0)$, and the squared distance from the origin is $\|x'\|^2 = \left(\sum_{i=1}^k x_i^2\right) / \left(\sum_{i=1}^n x_i^2\right)$. It can be written as $r^2 = X/(X+Y)$, in which X and Y are χ^2-distributed independent random variables with k and $n-k$ degrees of freedom, respectively. This implies that $r^2 \sim B\left(\frac{k}{n}, \frac{n-k}{n}\right)$ [71, Section 4.2]. We state it as a lemma.

Lemma 2.1.2 (Projection of uniform distribution on the sphere)**.** *Let u be a uniformly random point on the unit sphere in $\mathbb{R}^n$, and let u' be the projection of u to $\mathbb{R}^k \hookrightarrow \mathbb{R}^n$. Then $\|u'\|^2 \sim B\left(\frac{k}{n}, \frac{n-k}{n}\right)$.*

Hypergeometric functions. The family of *hypergeometric functions* takes $p+q$ parameters and one argument and can be defined as a sum of products of Gamma functions, while the *regularized* version of this function is obtained by normalizing by the product of $\Gamma(b_i)$:

$$\begin{aligned}
{}_pF_q\left(a_1,\ldots,a_p;b_1,\ldots,b_q;z\right) &= \sum_{j=0}^{\infty}\left[\prod_{i=1}^{p}\frac{\Gamma(j+a_i)}{\Gamma(a_i)}\right]\left[\prod_{i=1}^{q}\frac{\Gamma(b_i)}{\Gamma(j+b_i)}\right]\frac{z^j}{j!},\\
{}_p\tilde{F}_q\left(a_1,\ldots,a_p;b_1,\ldots,b_q;z\right) &= {}_pF_q\left(a_1,\ldots,a_p;b_1,\ldots,b_q;z\right) \Big/ \prod_{i=1}^{q}\Gamma(b_i)\\
&= \sum_{j=0}^{\infty}\left[\prod_{i=1}^{p}\frac{\Gamma(j+a_i)}{\Gamma(a_i)}\right]\left[\prod_{i=1}^{q}\frac{1}{\Gamma(j+b_i)}\right]\frac{z^j}{j!}.
\end{aligned}$$

We are interested in the type $p = 3$ and $q = 2$. Here convergence of the infinite sum depends on the values of the parameters. We always have convergence for $|z| < 1$, and if $z = 1$, a sufficient condition for convergence is $b_1 + b_2 > a_1 + a_2 + a_3$ [60].

Standard measures. Recall that ν_n and σ_n denote the volume and the surface area of the unit ball in $\mathbb{R}^n$. Using Gamma function, we can write the explicit expressions for these constants $\nu_n = \frac{\pi^{\frac{n}{2}}}{\Gamma\left(\frac{n}{2}+1\right)}$ and $\sigma_n = \frac{2\pi^{\frac{n}{2}}}{\Gamma\left(\frac{n}{2}\right)}$. There are two interesting relations between these constants worth mentioning: $\sigma_n = n\nu_n$ and $\sigma_{n+2} = 2\pi\nu_n$.

Further, using Beta functions we can also write an explicit formula for the spherical cap of geodesic radius η. For $\eta \le \frac{\pi}{2}$, the fraction of the sphere covered by the cap $\mathrm{Cap}_\eta(x)$ is $F(\eta) = \frac{1}{2}B_s(\frac{n}{2},\frac{1}{2}) / B\left(\frac{n}{2},\frac{1}{2}\right)$, in which $s = \sin^2\eta$ is the square of the Euclidean radius measured in $\mathbb{R}^{n+1}$; see [52]. The area of the cap is then

$$\mathrm{Area}(\eta) = \begin{cases} F(\eta)\sigma_{n+1} & \text{for } 0 \le \eta \le \frac{\pi}{2}, \\ \left[1 - F(\pi-\eta)\right]\sigma_{n+1} & \text{for } \frac{\pi}{2} \le \eta \le \pi, \end{cases} \tag{2.1}$$

in which $F(\pi - \eta) = F(\eta)$ because $\sin(\pi - \eta) = \sin \eta$.

One more measure that we will commonly face is the measure of the Grassmanian [39]: $\|\mathcal{L}^n_k\| = \frac{\sigma_n \sigma_{n-1} \cdot \ldots \cdot \sigma_{n-k+1}}{\sigma_1 \sigma_2 \cdot \ldots \cdot \sigma_k}$. To get an intuition for this formula we notice that, for example, $\mathcal{L}^n_{n-1}$ may be identified with the set of normal directions and hence $\|\mathcal{L}^n_{n-1}\| = \frac{\sigma_n}{2}$, half the volume of the $(n-1)$-dimensional sphere.

2.2 Poisson–Delaunay mosaics

As discussed in Section 1.7, for fixed j, the Delaunay centers of j-dimensional simplices in the Poisson–Delaunay mosaic in $\mathbb{R}^n$ form a non-simple point process. At the same time, the Delaunay centers of (ℓ, m)-intervals form a simple point process. With the following theorems we claim that both of these processes are stationary even if we further restrict the Delaunay radius, and give relations between their intensities.

Theorem 9 (Delaunay intervals)**.** *Let X be a stationary Poisson point process with density $\rho > 0$ in $\mathbb{R}^n$. Then there exist constants $C^n_{\ell,m}$, such that for any $r > 0$ (including $r = \infty$) and for any integers $1 \le \ell \le m \le n$, the expected number of intervals in the Poisson–Delaunay mosaic with Delaunay center in a Borel set Ω, lower bound dimension ℓ, upper bound dimension m, and Delaunay radius at most r is given by the lower incomplete Gamma function,*

$$\frac{\gamma(m;\, \rho\nu_n r^n)}{\Gamma(m)} C^n_{\ell,m} \cdot \rho\|\Omega\|,$$

and $C^n_{\ell,m}$ is the intensity of the process of the Delaunay centers of (ℓ, m)-intervals.

Remark. Theorem 9 does not cover the case $\ell = 0$ (because of the degenerate distribution of the Delaunay radius), which is straightforward: all vertices are critical, so the expected number of critical vertices in Ω is $\rho\|\Omega\|$ and there are no intervals with $\ell = 0$ and $m > 0$.

Applying Lemma 1.5.1 to the result of Theorem 9, we get the similar statement for the number of Delaunay j-simplices.

Theorem 10 (Delaunay simplices)**.** *Let X be a stationary Poisson point process with density $\rho > 0$ in $\mathbb{R}^n$. For any $r > 0$ (including $r = \infty$) and for any integer $j > 0$, the expected number of j-simplices in the Poisson–Delaunay mosaic with Delaunay center in a Borel set Ω and Delaunay radius at most r is given by the sum of the incomplete Gamma functions,*

$$\sum_{m=j}^{n} \frac{\gamma(m;\, \rho\nu_n r^n)}{\Gamma(m)} \sum_{\ell=1}^{j} \binom{m-\ell}{m-j} C^n_{\ell,m} \cdot \rho\|\Omega\|.$$

Setting $r = \infty$ we get for the intensity of the process of the Delaunay centers of j-simplices

$$D^n_j = \sum_{m=j}^{n} \sum_{\ell=1}^{j} \binom{m-\ell}{m-j} C^n_{\ell,m}.$$

In Chapter 4 we give explicit expressions for the constants $C^n_{\ell,m}$, see equation (4.3), and compute them in dimensions $n = 2, 3, 4$. The resulting numerical values for are given in Table 2.1. Hence we also have explicit values for D^n_j for $n = 2, 3, 4$; see Table 2.2. This

$C^n_{\ell,m}$	$n=2$			$n=3$				$n=4$				
	$m=0$	1	2	0	1	2	3	0	1	2	3	4
$\ell=0$	1.00	0.00	0.00	1.00	0.00	0.00	0.00	1.00	0.00	0.00	0.00	0.00
1		2.00	1.00		4.00	2.55	1.22		8.00	5.67	3.56	1.67
2			1.00			4.85	3.70			17.67	18.96	11.15
3							1.85				15.41	14.22
4												4.74

Table 2.1: Rounded constants in the expected numbers of critical simplices (*diagonal*) and non-singular intervals (*off-diagonal*) for a Poisson point process in $\mathbb{R}^2$ on the *left*, in $\mathbb{R}^3$ in the *middle*, and in $\mathbb{R}^4$ on the *right*. The exact values can be found in Chapter 5.

D^n_j	$j=0$	1	2	3	4
$n=2$	1.00	3.00	2.00		
3	1.00	7.77	13.54	6.77	
4	1.00	18.89	65.56	79.44	31.78

Table 2.2: Rounded constants in the expected numbers of simplices in a Poisson–Delaunay mosaic. The values are straightforward in two dimensions, they have been found by R. Miles [67] in three dimensions, and except for $j=0,3,4$ they are new in four dimensions. The exact values can be found in Chapter 5.

extends the result of Miles mentioned in [67] to $n = 4$. Figure 2.1 illustrates how the numbers of different simplices and intervals compare to each other at each radius.

Theorem 10 (and Theorem 9) can be equivalently stated in terms of the distribution of the Delaunay radius. Let Ω be a measurable set in $\mathbb{R}^n$ with non-empty interior, and choose uniformly one of the centers of the Delaunay spheres in Ω, conditioning on the existence of such centers. The j-simplex thus chosen is the *typical* j-dimensional Delaunay simplex. Then Theorem 10 can be restated as

Corollary 2.2.1 (Delaunay radius distribution)**.** *Let X be a stationary Poisson point process with density $\rho > 0$ in $\mathbb{R}^n$ and constants $C^n_{\ell,m}$ and D^n_j be the same as above. Then the distribution function of the Delaunay radius of the typical j-dimensional Delaunay simplex for $j > 0$ is a mixed Gamma distribution with distribution function:*

$$G^n_j(r) = \sum_{m=j}^{n} \frac{\gamma(m;\, \rho\nu_n r^n)}{\Gamma(m)} \sum_{\ell=1}^{j} \binom{m-\ell}{m-j} \frac{C^n_{\ell,m}}{D^n_j}, \qquad r \geq 0.$$

It should be noted that it follows that for $j = n$ the Delaunay radius is Gamma distributed. This is in accordance with the Complementary Theorem of Miles [56] (see also Møller [58]), and follows also from the very general paper on Gamma-type results by Baumstark and Last [9], see also Chenavier [18].

While Theorems 9 and 10 make statements about expectations in a fixed region Ω, a standard ergodic argument implies that for a sequence of regions $\Omega_1 \subseteq \Omega_2 \subseteq \ldots$ covering the entire space, the numbers of intervals inside Ω_i, normalized by $\|\Omega_i\|$, converge to the corresponding constants almost surely as random variables, see [54] for details.

It should also be pointed out that Theorem 10 can be converted into results for the dual Poisson–Voronoi tessellation. Then it gives the intensity of the $(n-j)$-dimensional face process of the Poisson–Voronoi tessellation, while the corollary gives the distribution

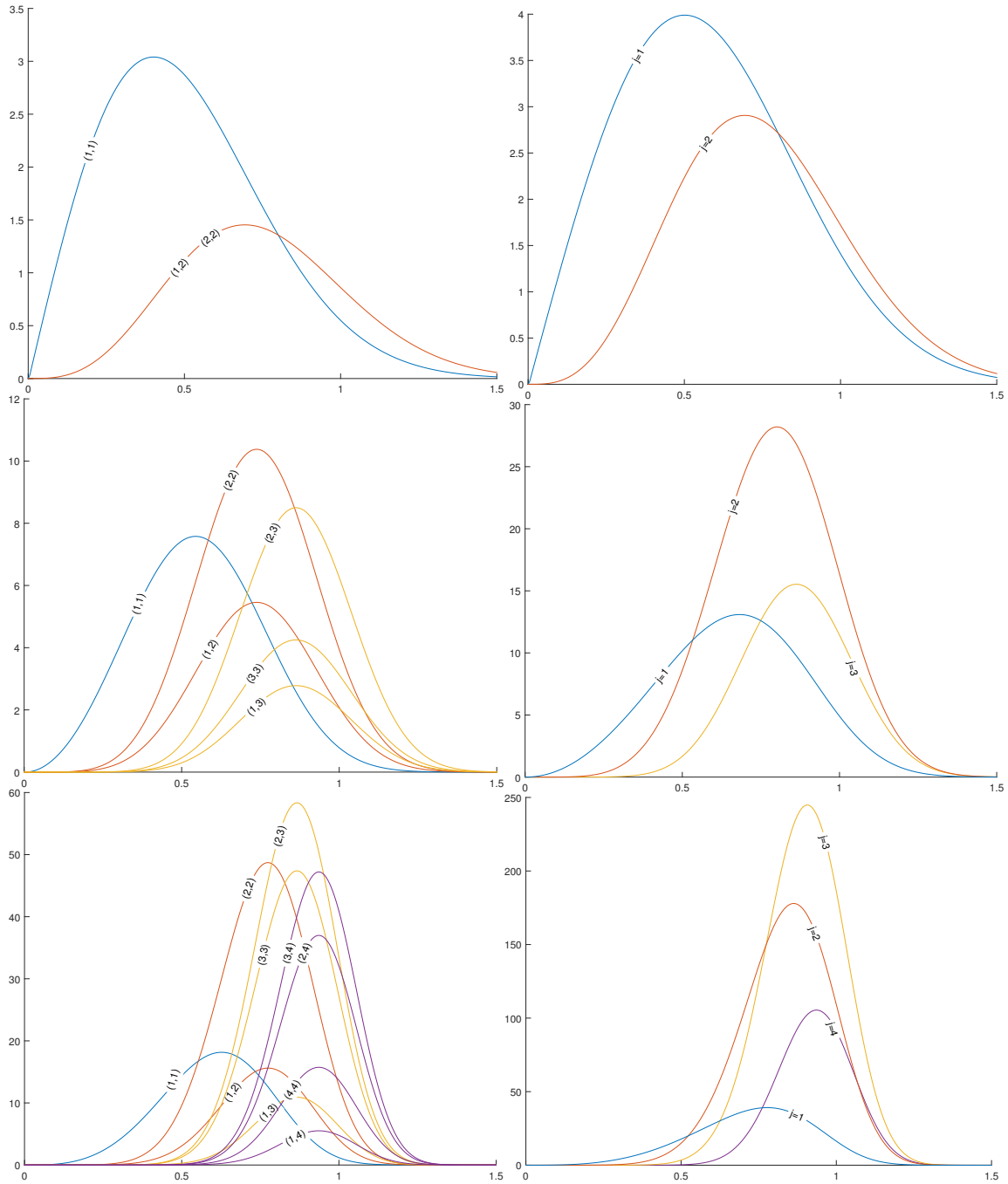

Figure 2.1: *Left*: the densities of distributions of the expected number of intervals as a function of the Delaunay radius ($\rho = 1$). The graphs are obtained by drawing $C^n_{\ell,m}$ times the derivative of $\gamma(m, \nu_n r^n)$ normalized by $\Gamma(m)$, for $1 \leq \ell \leq m \leq n$, with $n = 2, 3, 4$ from *top* to *bottom*. *Right*: the corresponding densities of distributions of the expected number of Delaunay simplices.

of the minimal distance of the typical $(n-j)$-face to the closest point of the Poisson point process.

2.3 Poisson–Čech mosaics

The case of the Čech complex is very similar to the Delaunay analysis.

Theorem 11 (Čech intervals)**.** *Let X be a stationary Poisson point process with density $\rho > 0$ in $\mathbb{R}^n$. For any $r > 0$ (and $r < \infty$) and for any integers $1 \leq \ell \leq m \leq n$, the expected number of intervals of the Poisson–Čech mosaic with lower bound dimension ℓ, upper bound dimension m and their eclosing balls having center in a Borel set Ω and radius at most r is given by the lower incomplete Gamma function,*

$$\frac{\gamma(m;\, \rho\nu_n r^n)}{\Gamma(m)} \check{C}^n_{\ell m} \cdot \rho\|\Omega\|,$$

where $\check{C}^n_{\ell m} = C^n_{\ell,\ell}\binom{m-1}{\ell-1}$ and $C^n_{\ell,\ell}$ are the same as in Theorem 9.

As a corollary we obtain the expected number of simplices in the Čech complex.

Theorem 12 (Čech simplices)**.** *Let X be a stationary Poisson point process with density $\rho > 0$ in $\mathbb{R}^n$. The expected number of j-dimensional simplices of the Poisson–Čech mosaic with smallest enclosing balls having radius at most r and center in Ω is*

$$\sum_{\ell=0}^{\min\{j,n\}} C^n_{\ell,\ell} \sum_{m=j}^{\infty} \binom{m-\ell}{j-\ell}\binom{m-1}{\ell-1} \frac{\gamma(m;\, \rho\nu_n r^n)}{\Gamma(m)}.$$

This sum diverges for $r = \infty$ and converges for $r < \infty$.

Similarly to Theorem 9 the distribution of the radius of the smallest enclosing ball of a typical Čech simplex follows. For completeness we notice that the case $r = \infty$ is trivial: $\check{\mathrm{C}}\mathrm{ech}\, X$ is the complete simplicial complex on X. Hence the expected number of simplices with vertices in Ω is $\mathbb{E}[\binom{|X\cap\Omega|}{m+1}]$. Since $|X \cap \Omega|$ is a Poisson random variable with parameter $\rho\|\Omega\|$, we get

$$\mathbb{E}[\tbinom{|X\cap\Omega|}{m+1}] = \sum_{i=m+1}^{\infty} \binom{i}{m+1} e^{-\rho\|\Omega\|} \frac{(\rho\|\Omega\|)^i}{i!} = \frac{(\rho\|\Omega\|)^{m+1}}{(m+1)!}.$$

Talking about the total number of simplices that contain the center of the smallest enclosing ball inside Ω does not make sense any more: it is infinite.

2.4 Weighted Poisson–Delaunay mosaics

The next theorem is the extension of Theorem 9 to the weighted case.

Theorem 13 (Weighted Delaunay intervals)**.** *Let X be a Poisson point process with density ρ in $\mathbb{R}^n$ and $\mathbb{R}^k \hookrightarrow \mathbb{R}^n$. There are constants $C_{\ell,m}^{k,n}$ such that for any $r \geq 0$, the expected number of intervals of type (ℓ, m) in the k-dimensional weighted Poisson–Delaunay mosaic with their anchored Delaunay spheres having center in a Borel set $\Omega \subseteq \mathbb{R}^k$ and radius at most r is*

$$C_{\ell,m}^{k,n} \cdot \frac{\gamma\big(m+1-\frac{k}{n};\, \rho\nu_n r^n\big)}{\Gamma\big(m+1-\frac{k}{n}\big)} \cdot \rho^{\frac{k}{n}} \|\Omega\|.$$

Here we allow $\ell = 0$ unless $k = n$, in which case it is Theorem 9. The constants $C_{\ell,m}^{k,n}$ are the intensities of the process in $\mathbb{R}^k$ of the anchors of intervals. We give explicit integral expressions for them in (4.4) and compute them for $m = 0$ and $m = 1$, as well as for $k \leq 2$ in Section 4.5. The extension of Theorem 10 is again the corollary of Lemma 1.5.1.

Theorem 14 (Weighted Delaunay simplices)**.** *In the setup of Theorem 13, the expected number of j-dimensional simplices in the weighted Poisson–Delaunay mosaic with their anchored Delaunay spheres having center in a Borel set $\Omega \subseteq \mathbb{R}^k$ and radius at most r is*

$$\left[\sum_{m=j}^{k} \frac{\gamma\big(m+1-\frac{k}{n};\, \rho\nu_n r^n\big)}{\Gamma\big(m+1-\frac{k}{n}\big)} \sum_{\ell=0}^{j} \binom{m-\ell}{m-j} C_{\ell,m}^{k,n}\right] \cdot \rho^{\frac{k}{n}} \|\Omega\|.$$

Setting $r = \infty$ we get for the intensity of the process of the anchors of j-simplices

$$D_j^{k,n} = \sum_{m=j}^{n} \sum_{\ell=1}^{j} \binom{m-\ell}{m-j} C_{\ell,m}^{k,n}.$$

Again, in an equivalent formulation, this theorem states that the radius of the anchored Delaunay sphere of a typical interval is Gamma-distributed, whereas the radius of the anchored Delaunay sphere of a typical simplex is a mixture of Gamma distributions. For $k = n$ we get Theorems 9 and 10. For some values of n, the constants are approximated in Tables 2.3 and 2.4.

	$n=2$	3	4	5	6	7	8	9	…	20	…	∞
$C_{0,0}^{1,n}$	1.00	1.09	1.16	1.22	1.26	1.29	1.32	1.35	…	1.47	…	1.65
$C_{0,1}^{1,n}$	0.27	0.36	0.42	0.45	0.48	0.50	0.51	0.53	…	0.60	…	0.68
$D_0^{1,n}$	1.27	1.46	1.58	1.67	1.74	1.79	1.84	1.87	…	2.07	…	2.33

Table 2.3: The rounded constants in the expressions of the expected number of intervals and simplices of a 1-dimensional weighted Delaunay mosaic. The ratio of the expected number of critical edges over the expected number of regular edges it is monotonically decreasing. It follows that we can infer the ambient dimension from the ratio.

Connection to Boolean model. We want to emphasize one application of the case $k = 1$ of Theorem 13. Let X be a Poisson point process with density ρ in $\mathbb{R}^n$ and consider the union of closed balls of fixed radius r and centers in X, denoted X_r. The obtained random set is sometimes referred to as the *Boolean model* [67]. Write $X_r \cap \Omega$ for the intersection of this set with a line segment $\Omega \subseteq \mathbb{R}^1 \subseteq \mathbb{R}^n$. We claim that the homotopy type of this intersection is the same as that of the weighted Delaunay complex, restricted to Ω. In particular,

	$n=3$	4	5	6	7	8	9	10	...	20	...	1000
$C^{2,n}_{0,0}$	1.11	1.25	1.38	1.49	1.58	1.66	1.73	1.79	...	2.12	...	2.69
$C^{2,n}_{0,1}$	0.26	0.42	0.54	0.63	0.71	0.77	0.82	0.86	...	1.12	...	1.54
$C^{2,n}_{0,2}$	0.09	0.15	0.21	0.25	0.28	0.31	0.33	0.35	...	0.47	...	0.65
$C^{2,n}_{1,1}$	2.47	2.92	3.30	3.61	3.87	4.09	4.28	4.44	...	5.37	...	6.92
$C^{2,n}_{1,2}$	1.46	1.83	2.13	2.37	2.57	2.74	2.89	3.01	...	3.72	...	4.88
$C^{2,n}_{2,2}$	1.37	1.67	1.92	2.12	2.29	2.43	2.55	2.66	...	3.25	...	4.23
$D^{2,n}_{0}$	1.46	1.83	2.13	2.37	2.57	2.74	2.89	3.01	...	3.72	...	4.88
$D^{2,n}_{1}$	4.37	5.48	6.38	7.10	7.71	8.22	8.66	9.03	...	11.16	...	14.65
$D^{2,n}_{2}$	2.92	3.66	4.25	4.74	5.14	5.48	5.77	6.02	...	7.44	...	9.77

Table 2.4: The rounded constants in the expressions of the expected number of intervals and simplices of a 2-dimensional weighted Delaunay mosaic obtained from a Poisson point process in n dimensions.

$\beta_0(X_r \cap \Omega) = \beta_0(\mathrm{WDel}_r(X';\Omega))$, in which X' is the projection of X onto $\mathbb{R}^1$, β_0 counts the connected components and $\mathrm{WDel}_r(X';\Omega)$ is the subcomplex of the weighted Delaunay mosaic that consists of all simplices with radius at most r lying completely within Ω. This follows from the general observation that the weighted Delaunay complex for radius r of a set of points $Y \subseteq \mathbb{R}^k$ with weights $w(y)$ is homotopy equivalent to the union of power balls, $Y_r = \{a \in \mathbb{R}^k \mid \|a-y\|^2 - w(y) \leq r^2\}$, and $Y_r \cap \Omega = X_r \cap \Omega$. Indeed, the weighted Delaunay complex can be defined as the nerve of the decomposition of Y_r with the weighted Voronoi tessellation, so the Nerve Theorem asserts the homotopy equivalence; see [26] for details.

Following the evolution of the nested complexes $\mathrm{WDel}_r(X';\Omega)$, as r goes from 0 to ∞, we observe that every critical vertex creates a new component when it enters the complex, each regular interval does not affect the homotopy type, and every critical edge connects two components; compare with Figure 1.7. It follows that the expected number of components in $X_r \cap \Omega$ is

$$\mathbb{E}[\beta_0(X_r \cap \Omega)] = \mathbb{E}[c^{1,n}_{0,0}(r) - c^{1,n}_{1,1}(r)] \tag{2.2}$$

$$= \tfrac{\sigma_{n-1}\Gamma\left(1-\frac{1}{n}\right)}{n\nu_n^{1-1/n}} \left[\tfrac{\gamma\left(1-\frac{1}{n};\,\rho\nu_n r^n\right)}{\Gamma\left(1-\frac{1}{n}\right)} - \tfrac{\gamma\left(2-\frac{1}{n};\,\rho\nu_n r^n\right)}{\Gamma\left(2-\frac{1}{n}\right)}\right] \cdot \rho^{\frac{1}{n}} \|\Omega\| \tag{2.3}$$

$$= \tfrac{\sigma_{n-1}}{n\nu_n^{1-1/n}} \left[\gamma\left(1-\tfrac{1}{n};\,\rho\nu_n r^n\right) - \tfrac{\gamma\left(2-\frac{1}{n};\,\rho\nu_n r^n\right)}{1-\frac{1}{n}}\right] \cdot \rho^{\frac{1}{n}} \|\Omega\|, \tag{2.4}$$

where we substituted values for $C^{1,n}_{\ell,m}$ from (4.42)–(4.43). We write $A = \rho\nu_n r^n$, use the definition of the incomplete Gamma function, and integrate by parts to get

$$\gamma\left(2-\tfrac{1}{n};\,A\right) = \int_0^A x^{1-\frac{1}{n}} e^{-x}\,\mathrm{d}x = \left[-x^{1-\frac{1}{n}}e^{-x}\right]_0^A + \left(1-\tfrac{1}{n}\right)\int_0^A x^{-\frac{1}{n}} e^{-x}\,\mathrm{d}x \tag{2.5}$$

$$= -A^{1-\frac{1}{n}}e^{-A} + \left(1-\tfrac{1}{n}\right)\gamma\left(1-\tfrac{1}{n};\,A\right). \tag{2.6}$$

Noticing that $A^{1-\frac{1}{n}}\rho^{1/n} = (\rho\nu_n r^n)^{1-\frac{1}{n}}\rho^{1/n} = \rho\nu_n^{1-\frac{1}{n}} r^{n-1}$, we plug (2.6) into (2.4) to obtain

$$\mathbb{E}[\beta_0(X_r \cap \Omega)] = \tfrac{\sigma_{n-1}}{n\nu_n^{1-1/n}} \tfrac{1}{1-\frac{1}{n}} e^{-\rho\nu_n r^n} \rho\nu_n^{1-\frac{1}{n}} r^{n-1}\|\Omega\| = \tfrac{\sigma_{n-1}}{n-1} r^{n-1} e^{-\rho\nu_n r^n}\rho\|\Omega\| \tag{2.7}$$

$$= \nu_{n-1} r^{n-1} e^{-\rho\nu_n r^n}\rho\|\Omega\|, \tag{2.8}$$

where we use the identity $\frac{\sigma_{n-1}}{n-1} = \nu_{n-1}$ in the last transition. In short, (2.8) gives an explicit formula for the expected number of connected components in the Boolean model in $\mathbb{R}^n$ intersected with a line segment of length $\|\Omega\|$. This result is not new and follows after some straightforward computations from [40, Excercise 4.8], but the goal of this derivation is to provide another, more topological view on the problem. The graphs of β_0 for different dimensions n are shown in Figure 2.2. Using Crofton's formula (1.3) and the fact that almost every connected component is a line segment, which meets the boundary of the Boolean model in two points, (2.8) can be transformed into a statement about its expected $(n-1)$-dimensional volume:

$$\overline{V}_{n-1}(X_r) = 2\sqrt{\pi}\frac{\Gamma\left(\frac{n}{2}\right)}{\Gamma\left(\frac{n+1}{2}\right)}\nu_{n-1}r^{n-1}e^{-\rho\nu_n r^n}\rho,$$

in which $\overline{V}_{n-1}(X_r)$ stands for the limit of the $(n-1)$-dimensional volume of the boundary of X_r inside a growing region over the volume of this region; see [67, Section 9] for the detailed discussion of the quantity.

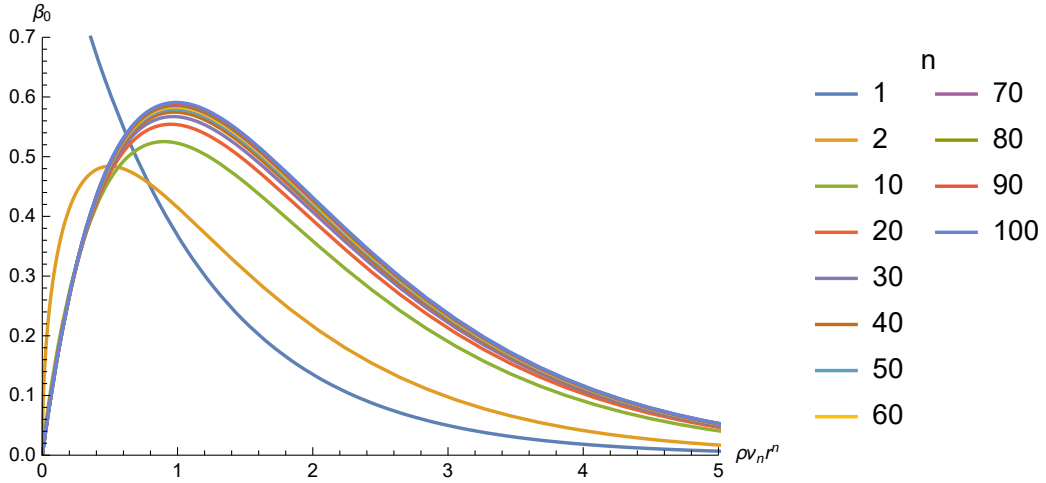

Figure 2.2: Graphs of the expected number of connected components per unit length depending on the radius for different dimensions n. To make sense of putting the curves corresponding to different dimensions on the same plot, they are rescaled, so the parameter on the horizontal axis is $\rho\nu_n r^n$, which stands for the expected number of points inside a ball of radius r in $\mathbb{R}^n$. That said, the curves are $\beta_0(\rho\nu_n r^n) = \mathbb{E}[\beta_0(X_r \cap \Omega)]$ with $\|\Omega\| = 1$.

2.5 Poisson–Delaunay mosaics of higher order

The next two results refer to the order-k Poisson–Delaunay mosaic. Since we neither have a definition nor a description of intervals, we state only the result about the number of cells, deferring the intervals until we define them in the corresponding chapter, see (6.9). The development of the discrete Morse theory for the order-k case in Section 6.3 can also be considered a separate and independent achievement of this work.

Letting G be a j-dimensional cell of the Poisson–Delaunay mosaic of order k, we note that it uniquely determines the smallest sphere centered at a point of the dual order-k Voronoi cell such that the closed ball it bounds contains at least k points of X; see Chapter

6 for details. We call the center and the radius of this ball the *center* and the *radius* of G. To count, we specify a dimension $0 \le j \le n$, a Borel region $\Omega \subseteq \mathbb{R}^n$, and a radius $r \ge 0$, and we write $d_j^{(k,n)}(r)$ for the number of j-cells in $\mathrm{Del}^{(k)}X$ whose center belongs to Ω and whose radius is at most r. We give an explicit formula for the expectation of $d_j^{(k,n)}(r)$.

Theorem 15 (Expected number of cells)**.** *Let X be a stationary Poisson point process with density ρ in $\mathbb{R}^n$, let $k \ge 1$ and $0 < j \le n$. The expected number of j-cells in $\mathrm{Del}^{(k)}X$ with center in a Borel region Ω and radius at most r satisfies*

$$\mathbb{E}[d_j^{(k,n)}(r)] = \rho\|\Omega\| \cdot \sum_{u=j}^{n} \sum_{v=1}^{u} C_{v,u}^n \sum_{g=1}^{g_1} \frac{\gamma(u+k-g;\, \rho\nu_n r^n)}{\Gamma(k-g+1)\Gamma(u)} \sum_{t=t_0}^{t_1} \binom{v+1}{t} \binom{u-v}{t+j-v},$$

in which $g_1 = \min\{k, u\}$, $t_0 = \max\{0, v-j, g-j\}$, and $t_1 = \min\{v+1, u-j, g-1\}$. Further, for $j = 0$ and $k \ge 2$ we have

$$\mathbb{E}[d_0^{(k,n)}(r)] = \rho\|\Omega\| \cdot \sum_{u=1}^{n} \sum_{v=1}^{u} C_{v,u}^n \frac{\gamma(u+k-v-1;\, \rho\nu_n r^n)}{\Gamma(k-v)\Gamma(u)}.$$

The constants $C_{v,u}^n$ are again the same constants defined in (4.3). Setting $r_0 = \infty$, we obtain the expected total number of j-cells in $\mathrm{Del}^{(k)}X$.

Remarks. (1) The case $j = 0$ when $k = 1$ is trivial, because all points of X are 1-Delaunay vertices.

(2) Again, the theorem can be restated in terms of the distribution of the radius of a *typical j-cell*.

(3) Throughout the investigation we always have the special case $j = 0$. The case can be simplified if one considers *degree-k* diagrams instead. Degree-k Voronoi domains split the order-k Voronoi domains into several domains sharing the furthest point.

The second new result for order-k mosaics concerns the expected area of the ℓ-skeleton of an order-k Poisson–Voronoi tessellation. By definition, this is the ℓ-dimensional Lebesgue measure of the union of all ℓ-dimensional faces of order-k Voronoi domains. Since this area is infinite, we normalize by letting $\eta_\ell^{(k,n)}$ be the area of the ℓ-skeleton within a unit volume of space.

Theorem 16 (Expected area)**.** *Let X be a stationary Poisson point process with density $\rho > 0$ in $\mathbb{R}^n$, let $k \ge 1$ and $0 \le \ell < n$. The expected area of the ℓ-skeleton of the order-k Voronoi tessellation of X per unit volume of space is*

$$\mathbb{E}[\eta_\ell^{(k,n)}] = \rho^{\frac{n-\ell}{n}} \sum_{i=\max\{0,k+\ell-n\}}^{k-1} \frac{2^{n-\ell+1}\pi^{\frac{n-\ell}{2}}}{i!n(n-\ell+1)!} \frac{\Gamma\left(\frac{n^2-n\ell+\ell+1}{2}\right)\Gamma\left(1+\frac{n}{2}\right)^{n-\ell+\frac{\ell}{n}}\Gamma\left(n-\ell+i+\frac{\ell}{n}\right)}{\Gamma\left(\frac{n^2-n\ell+\ell}{2}\right)\Gamma\left(\frac{n+1}{2}\right)^{n-\ell}\Gamma\left(\frac{\ell+1}{2}\right)}..$$

For $\ell = n$, we have $\mathbb{E}[\eta_n^{(k,n)}] = \eta_n^{(k,n)} = 1$.

This extends Theorem 10.2.4 in [67] to the order-k case.

2.6 Spherical Poisson–Delaunay mosaics

We conclude the summary of the new results with the Poisson–Delaunay mosaic on the sphere. Recall that in Section 1.8 we defined the normalized radius of a spherical cap with geodesic radius η to be $\bar{\eta} = \eta\rho^{1/n}$. The following theorems count intervals and simplices in this mosaic with bounded radius, or, equivalently, faces of random inscribed polytopes.

Theorem 17 (Spherical Delaunay intervals)**.** *Let X be a Poisson point process with density $\rho > 0$ on $\mathbb{S}^n$. For any integers $1 \leq \ell \leq m \leq n$ and any real number $0 < \eta_0 < \frac{\pi}{2}$, the expected number of intervals of type (ℓ, m) and geodesic radius at most η_0 is*

$$\mathbb{E}[\zeta^n_{\ell,m}, \eta_0] = \rho\sigma_{n+1} \cdot \tfrac{\sigma^m_n}{2\Gamma(m)n^{m-1}} \cdot C^n_{\ell,m} \int_{t=0}^{s} \rho^m t^{\frac{mn-2}{2}} (1-t)^{\frac{n-m-1}{2}} \mathbb{P}_\emptyset(\sqrt{t})\,\mathrm{d}t,$$

in which $s = \sin^2 \eta_0$ is the square of the maximum Euclidean radius, and $\mathbb{P}_\emptyset(r)$ is the probability that a spherical cap with geodesic radius $\eta = \arcsin r$ contains no points of X, namely $\mathbb{P}_\emptyset(r) = e^{-\rho \mathrm{Area}(\eta)}$. Let now $\rho \to \infty$. For any $\bar{\eta}_0 \in [0, +\infty]$, the expected number of intervals of type (ℓ, m) and normalized radius of the Delaunay cap at most $\bar{\eta}_0$ is

$$\mathbb{E}[\zeta^n_{\ell,m}, \bar{\eta}_0] = \rho\sigma_{n+1} \cdot \tfrac{\gamma\left(\bar{\eta}_0^n \nu_n; m\right)}{\Gamma(m)} \cdot C^n_{\ell,m} + o(\rho).$$

Remarks. (1) Constants $C^n_{\ell,m}$ are the same as in Theorem 9.

(2) Theorem 17 does not cover the case $\ell = 0$, i.e., intervals containing vertices, but here the results are straightforward. Specifically, the expected number of critical vertices is $\mathbb{E}[\zeta^n_{0,0}, \eta_0] = \rho\sigma_{n+1}$, for every $\eta_0 \geq 0$, and $\zeta^n_{0,m} = 0$ for every $m \geq 1$.

(3) We will prove that for constant s, the integral is bounded away from both 0 and ∞. This implies that the expected number of intervals is of order $\Theta(\rho)$; compare with [64].

(4) We will also prove that setting $\bar{\eta}_0 = \infty$ in the second equation gives the total number of intervals of type (ℓ, m) as $\mathbb{E}[\zeta^n_{\ell,m}] = \rho\sigma_{n+1} \cdot C^n_{\ell,m} + o(\rho)$. On the other hand, letting $\bar{\eta}_0 \to \infty$, we get the total number of intervals of geodesic radius $\Theta(\rho^{-1/n})$. This implies that the number of intervals with radius $\omega\left(\rho^{-1/n}\right)$ is $o(\rho)$. Note that also the number of intervals with radius $o\left(\rho^{-1/n}\right)$ is $o(\rho)$.

The total number of simplices of dimension j in the Delaunay mosaic is again easy to deduce from the number of intervals. We give only the limit statement.

Theorem 18 (Spherical Delaunay simplices)**.** *Let X be a Poisson point process with density $\rho > 0$ on $\mathbb{S}^n$. For any integer $j \geq 1$ and any non-negative real number $\bar{\eta}_0$, the expected number of j-simplices of $\mathrm{Del}X$ with normalized radius of the Delaunay cap at most $\bar{\eta}_0$ is*

$$\rho\sigma_{n+1} \cdot \sum_{m=j}^{n} \frac{\gamma(\bar{\eta}_0^n \nu_n;\, m)}{\Gamma(m)} \sum_{\ell=0}^{j} \binom{m-\ell}{m-j} C^n_{\ell,m} + o(\rho),$$

Setting

$$G^n_j(\bar{\eta}_0) = \sum_{m=j}^{n} \tfrac{\gamma\left(\bar{\eta}_0^n \nu_n; m\right)}{\Gamma(m)} \sum_{\ell=0}^{j} \binom{m-\ell}{m-j} \frac{C^n_{\ell,m}}{D^n_j},$$

we thus get the distribution of the normalized radius of the Delaunay cap of the typical j-simplex in the limit when $\rho \to \infty$.

Remarks. (1) Observe that $\rho\sigma_{n+1}$ is the expected number of points in X. Comparing with Theorems in Section 2.2, we can notice that the obtained formulas are essentially the same expressions as for the Poisson point process in $\mathbb{R}^n$.

(2) While we state our results for Poisson point processes, very similar expressions can be obtained for the uniform distribution; see Section 7.3.

3. Blaschke–Petkantschin formulas

A commonly used tool for questions concerning random complexes is the mentioned in Section 1.9 Blaschke–Petkantschin formula. The standard approach for working with Poisson–Delaunay mosaics is to study metric properties of Poisson–Voronoi tessellations, and the linear formula suffices for this purpose. We are approaching the problem from the other side, though, and that is why our main tools will be formulas involving spheres, like the one in Theorem 8. In this chapter we summarize and prove new formulas of this type. They are completely self-contained and can be considered as separate results. In the statements, we will use bold notation for sequences of points, like $\mathbf{u} = (u_0, u_1, \dots, u_k)$ and $\mathbf{x} = (x_0, x_1, \dots, x_k)$, we write $\mathrm{Vol}(\mathbf{u})$ for the k-dimensional volume of a k-simplex with vertices at $\mathbf{u}$, and shorten $z + r\mathbf{u}$ for $(z + ru_0, z + ru_1, \dots, z + ru_k)$. The number of points and the ambient dimension can vary between theorems without causing confusion. The integrations are always with respect to the standard measures in the Euclidean space, on the sphere and on Grassmanian [39].

3.1 Smallest circumscribed spheres

The first formula generalizes Theorem 7.3.1 in [67, page 287] to $k \leq n$. It integrates over the smallest circumscribed spheres of k-ples of points.

Theorem 19 (Blaschke–Petkantschin formula for circumscribed spheres)**.** *Let $0 < k \leq n$ and write $S(L)$ for the $(k-1)$-dimensional unit sphere inside $L \in \mathcal{L}^n_k$, Then for every non-negative function f of $k+1$ points in $\mathbb{R}^n$ we have*

$$\int\limits_{\mathbf{x}\in(\mathbb{R}^n)^{k+1}} f(\mathbf{x})\,\mathrm{d}\mathbf{x} = \int\limits_{L\in\mathcal{L}^n_k}\int\limits_{z\in\mathbb{R}^n}\int\limits_{r\geq 0}\int\limits_{\mathbf{u}\in S(L)^{k+1}} f(z+r\mathbf{u})r^{nk-1}(k!\mathrm{Vol}(\mathbf{u}))^{n-k+1}\,\mathrm{d}\mathbf{u}\,\mathrm{d}r\,\mathrm{d}z\,\mathrm{d}L.$$

Proof. We start with the form given in Theorem 7:

$$\int\limits_{\mathbf{x}\in(\mathbb{R}^n)^{k+1}} f(\mathbf{x})\,\mathrm{d}\mathbf{x} = \int\limits_{L\in\mathcal{L}^n_k}\int\limits_{h\in L^\perp}\int\limits_{\mathbf{x}\in L^{k+1}} f(h+\mathbf{x})(k!\mathrm{Vol}(\mathbf{x}))^{n-k}\,\mathrm{d}\mathbf{x}\,\mathrm{d}h\,\mathrm{d}L. \tag{3.1}$$

Using Theorem 8, we expand the innermost integral into

$$k!\int\limits_{z\in L}\int\limits_{r\geq 0}\int\limits_{\mathbf{u}\in S(L)^{k+1}} r^{k^2-1}\mathrm{Vol}(\mathbf{u})f(h+z+r\mathbf{u})(k!\mathrm{Vol}(z+r\mathbf{u}))^{n-k}\,\mathrm{d}\mathbf{u}\,\mathrm{d}r\,\mathrm{d}z. \tag{3.2}$$

Note that $\mathrm{Vol}(z + r\mathbf{u}) = r^k\mathrm{Vol}(\mathbf{u})$, so we get $k^2 - 1 + (n-k)k = nk - 1$ as the final power of the radius. Plugging (3.2) into (3.1) and joining the integration over $L^\perp$ and L, we get the claimed formula. □

3.2 Smallest anchored spheres

The next formula will be used in the analysis of weighted mosaics. Assuming $m+1$ points $\mathbf{x}$ are in general position in $\mathbb{R}^n$, the affine hull of $\mathbf{x}$ is an m-plane, $M = \operatorname{aff}\mathbf{x}$. Furthermore, the set of centers of the spheres that pass through all points of $\mathbf{x}$ is an $(n-m)$-plane, $M^\perp$, orthogonal to M. Generically, the intersection of $M^\perp$ with $\mathbb{R}^k$ is a plane of dimension $k-m$. The center of the smallest anchored sphere passing through $\mathbf{x}$ is the point of this intersection that is the closest to $\mathbf{x}$.

Recall that for a sequence $\mathbf{x}$ of $m+1 \leq k+1$ points in $\mathbb{R}^n$, there is a unique smallest anchored sphere passing through them. We claim that its center lies inside the orthogonal projection P of the m-dimensional affine hull of $\mathbf{x}$ onto $\mathbb{R}^k$. Indeed, orthogonally projecting the center of any anchored sphere passing through $\mathbf{x}$ to P in $\mathbb{R}^k$ we clearly get a point, which is the center of a smaller anchored sphere still passing through $\mathbf{x}$. The following theorem tells us how to integrate over these smallest anchored circumscribed spheres. For $m = k$ it is Theorem 19.

Theorem 20 (Anchored Blaschke–Petkantschin formula)**.** *Let $0 \leq m \leq k \leq n$ and $\alpha = n(m+1)-(k+1)$. Then every measurable non-negative function $f\colon (\mathbb{R}^n)^{m+1} \to \mathbb{R}$ satisfies*

$$\int\limits_{\mathbf{x}\in(\mathbb{R}^n)^{m+1}} f(\mathbf{x})\,\mathrm{d}\mathbf{x} = \int\limits_{y\in\mathbb{R}^k}\int\limits_{P\in\mathcal{L}^k_m}\int\limits_{r\geq 0}\int\limits_{\mathbf{u}\in(S)^{m+1}} f(y+r\mathbf{u})r^\alpha[m!\mathrm{Vol}_m(\mathbf{u}')]^{k-m+1}\,\mathrm{d}\mathbf{u}\,\mathrm{d}r\,\mathrm{d}P\,\mathrm{d}y,$$

in which $\mathcal{L}^k_m$ is the Grassmannian of (linear) m-planes in $\mathbb{R}^k$, $\mathbf{u}'$ is the projection of $\mathbf{u}$ to P, and S is short for the unit sphere in $P\times\mathbb{R}^{n-k}$.

Proof. As in the previous proof, we first settle the case $m = k$ and then combine it with the linear Blaschke–Petkantscin formula to get the result.

Lemma 3.2.1 (Blaschke–Petkantschin for top-dimensional simplices)**.** *Let $0 \leq k \leq n$. Then every measurable non-negative function $f\colon (\mathbb{R}^n)^{k+1} \to \mathbb{R}$ satisfies*

$$\int\limits_{\mathbf{x}\in(\mathbb{R}^n)^{k+1}} f(\mathbf{x})\,\mathrm{d}\mathbf{x} = \int\limits_{y\in\mathbb{R}^k}\int\limits_{r\geq 0}\int\limits_{\mathbf{u}\in(\mathbb{S}^{n-1})^{k+1}} f(y+r\mathbf{u})r^{(n-1)(k+1)}k!\mathrm{Vol}_k(\mathbf{u}')\,\mathrm{d}\mathbf{u}\,\mathrm{d}r\,\mathrm{d}y,$$

in which $\mathbf{u}'$ is the projection of $\mathbf{u}$ to $\mathbb{R}^k$, $\mathrm{Vol}_k(\mathbf{u}')$ is the Lebesgue measure of the k-simplex, and we use the standard spherical measure on $\mathbb{S}^{n-1}$.

Proof. We follow the proof of Theorem 7.3.1 in [67], with just slight modifications. Recall first that we choose the coordinates in $\mathbb{R}^n$ so that the projection of $x = (x_1, x_2, \ldots, x_n)$ to $\mathbb{R}^k \hookrightarrow \mathbb{R}^n$ is $x' = (x_1, \ldots, x_k, 0, \ldots, 0)$. The claimed relation is a change of variables: on the right-hand side, we represent the points $\mathbf{x}$ by the center $y \in \mathbb{R}^k \hookrightarrow \mathbb{R}^n$ of the anchored sphere passing through these points, its radius r, and k points $\mathbf{u}$ on the unit sphere $\mathbb{S}^{n-1} \hookrightarrow \mathbb{R}^n$. This change of variables is the mapping $\varphi\colon \mathbb{R}^k\times[0,\infty)\times(\mathbb{S}^{n-1})^{k+1} \to (\mathbb{R}^n)^{k+1}$ defined by $\varphi(y, r, \mathbf{u}_0, \mathbf{u}_1, \ldots, \mathbf{u}_k) = (y+r\mathbf{u}_0, y+r\mathbf{u}_1, \ldots, y+r\mathbf{u}_k)$, we note that φ is bijective up to a measure 0 subset of the domain. We claim the Jacobian of φ is $J(y, r, \mathbf{u}) = r^{(n-1)(k+1)}k!\mathrm{Vol}_k(\mathbf{u}')$, in which $\mathbf{u}' = (\mathbf{u}'_0, \mathbf{u}'_1, \ldots, \mathbf{u}'_k)$ is the projection of $\mathbf{u}$ to $\mathbb{R}^k$. To prove it at a particular point $(y, r, \mathbf{u})$, we choose local coordinates around every point $\mathbf{u}_i$ on the sphere. We choose them such that the matrix $[\mathbf{u}_i\dot{\mathbf{u}}_i]$ is orthogonal, for every $0 \leq i \leq k$, in

which $\dot{\mathbf{u}}_i$ is the $n \times (n-1)$ matrix of partial derivatives with respect to the $n-1$ local coordinates. This is the same parametrization as in [67]. With this, the Jacobian is the absolute value of the $n(k+1) \times n(k+1)$ determinant:

$$J(y,r,\mathbf{u}) = \operatorname{abs} \left| \begin{array}{cc:ccc:c} E_{n,k} & \mathbf{u}_0 & r\dot{\mathbf{u}}_0 & 0 & \dots & 0 \\ E_{n,k} & \mathbf{u}_1 & 0 & r\dot{\mathbf{u}}_1 & \dots & 0 \\ \vdots & \vdots & \vdots & \vdots & \ddots & \vdots \\ E_{n,k} & \mathbf{u}_k & 0 & 0 & \dots & r\dot{\mathbf{u}}_k \end{array} \right|,$$

where we write the matrix in block notation, with $E_{n,k}$ the $n \times k$ matrix with all elements zero and ones in the diagonal. Similarly, $\mathbf{u}_i$ is a column vector of length n, $r\dot{\mathbf{u}}_i$ is an $n \times (n-1)$ matrix, and 0 is the zero matrix of appropriate size, which in this case is an $n \times (n-1)$ matrix. Like in [67], we extract r from $(k+1)(n-1)$ columns, and use the fact that transposing the matrix does not affect the determinant to get

$$\left(\frac{J(y,r,\mathbf{u})}{r^{(k+1)(n-1)}}\right)^2 = \left| \begin{array}{cccc} E_{k,n} & E_{k,n} & \dots & E_{k,n} \\ \mathbf{u}_0^T & \mathbf{u}_1^T & \dots & \mathbf{u}_k^T \\ \hdashline \dot{\mathbf{u}}_0^T & 0 & \dots & 0 \\ 0 & \dot{\mathbf{u}}_1^T & \dots & 0 \\ \vdots & \vdots & \ddots & \vdots \\ 0 & 0 & \dots & \dot{\mathbf{u}}_k^T \end{array} \right| \cdot \left| \begin{array}{cc:ccc:c} E_{n,k} & \mathbf{u}_0 & \dot{\mathbf{u}}_0 & 0 & \dots & 0 \\ E_{n,k} & \mathbf{u}_1 & 0 & \dot{\mathbf{u}}_1 & \dots & 0 \\ \vdots & \vdots & \vdots & \vdots & \ddots & \vdots \\ E_{n,k} & \mathbf{u}_k & 0 & 0 & \dots & \dot{\mathbf{u}}_0 \end{array} \right|.$$

The orthogonality of the matrices $[\mathbf{u}_i \dot{\mathbf{u}}_i]$ implies that $\mathbf{u}_i^T \mathbf{u}_i = 1$, $\dot{\mathbf{u}}_i^T \dot{\mathbf{u}}_i = E_{n-1,n-1}$, whereas $\mathbf{u}_i^T \dot{\mathbf{u}}_i$ is the zero row vector of length $n-1$, and $\dot{\mathbf{u}}_i^T \mathbf{u}_i$ is the zero column vector of length $n-1$, for each $0 \le i \le k$. We can therefore multiply the matrices and get

$$\left(\frac{J(y,r,\mathbf{u})}{r^{(k+1)(n-1)}}\right)^2 = \left| \begin{array}{cc:ccc} (k+1)E_{k,k} & \sum \mathbf{u}_i' & \dot{\mathbf{u}}_0' & \dots & \dot{\mathbf{u}}_k' \\ \sum \mathbf{u}_i'^T & k+1 & 0 & \dots & 0 \\ \hdashline \dot{\mathbf{u}}_0'^T & 0 & E_{n-1,n-1} & \dots & 0 \\ \vdots & \vdots & \vdots & \ddots & \vdots \\ \dot{\mathbf{u}}_k'^T & 0 & 0 & \dots & E_{n-1,n-1} \end{array} \right|, \tag{3.3}$$

in which we write $\mathbf{u}_i'$ for the vector consisting of the first k coordinates of $\mathbf{u}_i$. Similarly, $\dot{\mathbf{u}}_i'$ is the $k \times (n-1)$ matrix obtained from $\dot{\mathbf{u}}_i$ by dropping the bottom $n-k$ rows. As written, the $n(k+1) \times n(k+1)$ matrix in (3.3) is a $(k+3) \times (k+3)$ matrix of blocks, not all of the same size. To zero out the last $k+1$ blocks in the first row, we subtract the third row times $\dot{\mathbf{u}}_0'$, the fourth row times $\dot{\mathbf{u}}_1'$, and so on. The determinant is therefore the product of the determinants of the upper left 2×2 block matrix and the lower right $(k+1) \times (k+1)$ block matrix, the latter being 1. To further simplify the 2×2 block matrix, we use $[\mathbf{u}_i \dot{\mathbf{u}}_i][\mathbf{u}_i \dot{\mathbf{u}}_i]^T = E_{n,n}$, which implies $[\mathbf{u}_i' \dot{\mathbf{u}}_i'][\mathbf{u}_i' \dot{\mathbf{u}}_i']^T = E_{k,k}$, and we write the matrix as a product of two matrices:

$$\left(\frac{J(y,r,\mathbf{u})}{r^{(k+1)(n-1)}}\right)^2 = \left| \begin{array}{cc} (k+1)E_{k,k} - \sum \dot{\mathbf{u}}_i' \dot{\mathbf{u}}_i'^T & \sum \mathbf{u}_i' \\ \sum \mathbf{u}_i'^T & k+1 \end{array} \right| \tag{3.4}$$

$$= \left| \begin{array}{cc} \sum \mathbf{u}_i' \mathbf{u}_i'^T & \sum \mathbf{u}_i' \\ \sum \mathbf{u}_i'^T & k+1 \end{array} \right| = \left| \begin{bmatrix} \mathbf{u}_0' & \mathbf{u}_1' & \dots & \mathbf{u}_k' \\ 1 & 1 & \dots & 1 \end{bmatrix} \begin{bmatrix} \mathbf{u}_0'^T & 1 \\ \vdots & \vdots \\ \mathbf{u}_1'^T & 1 \\ \mathbf{u}_k'^T & 1 \end{bmatrix} \right|, \tag{3.5}$$

in which we get from (3.4) to (3.5) using $\dot{\mathbf{u}}'_i\dot{\mathbf{u}}'^T_i = E_{k,k} - \mathbf{u}'_i\mathbf{u}'^T_i$. Finally, the determinant of the vectors $\mathbf{u}'_i$ with appended 1 is $k!$ times the k-dimensional volume of $\mathbf{u}'$. Hence, $J(y, r, \mathbf{u}) = r^{(k+1)(n-1)}k!\mathrm{Vol}_k(\mathbf{u}')$, as claimed. This completes the proof. □

We are now ready to prove the theorem. For $P \in \mathcal{L}^k_m$, we write $P \times \mathbb{R}^{n-k} \in \mathcal{L}^n_{m+n-k}$ for the $(m + n - k)$-plane whose orthogonal projection to $\mathbb{R}^k$ is P. The first application of Blaschke–Petkantschin formula integrates over all (affine) m-planes in $\mathbb{R}^k$, spanned by the projections of $\mathbf{x}$ to $\mathbb{R}^k$:

$$\int\limits_{\mathbf{x}\in(\mathbb{R}^n)^{m+1}} f(\mathbf{x})\,\mathrm{d}\mathbf{x} = \int\limits_{P\in\mathcal{L}^k_m}\int\limits_{h\in P^\perp}\int\limits_{\mathbf{x}\in(P\times\mathbb{R}^{n-k})^{m+1}} f(h+\mathbf{x})[m!\mathrm{Vol}_m(\mathbf{x}')]^{k-m}\,\mathrm{d}\mathbf{x}\,\mathrm{d}h\,\mathrm{d}P.$$

For every m-plane P in $\mathbb{R}^k$, we consider the vertical $(m+n-k)$-plane $P \times \mathbb{R}^{n-k}$ in $\mathbb{R}^n$ and apply Lemma 3.2.1 inside it. Recalling that S is the unit sphere in $P \times \mathbb{R}^{n-k}$, this gives

$$\int\limits_{\mathbf{x}\in(\mathbb{R}^n)^{m+1}} f(\mathbf{x})\,\mathrm{d}\mathbf{x} = \int\limits_{P\in\mathcal{L}^k_m}\int\limits_{h\in P^\perp}\int\limits_{z\in P}\int\limits_{r\geq 0}\int\limits_{\mathbf{u}\in(S)^{m+1}} f(h+z+r\mathbf{u})r^{(m+n-k-1)(m+1)}$$
$$m!\mathrm{Vol}_m(\mathbf{u}')[m!\mathrm{Vol}_m(r\mathbf{u}')]^{k-m}\,\mathrm{d}\mathbf{u}\,\mathrm{d}r\,\mathrm{d}z\,\mathrm{d}h\,\mathrm{d}P.$$

Note that $\mathrm{Vol}_m(r\mathbf{u}') = r^m\mathrm{Vol}_m(\mathbf{u}')$, which implies that the final power of r is $(m+n-k-1)(m+1)+m(k-m) = \alpha$. Finally, we get the claimed relation by setting $y = z + h$ and exchanging the integral over $P \in \mathcal{L}^k_m$ with the integral over $y \in \mathbb{R}^k$. □

3.3 Circles on the sphere

The last formula we prove lives in another space: it integrates over smallest circumscribed caps of points on the sphere $\mathbb{S}^n \subseteq \mathbb{R}^{n+1}$. To express the result, we write $P^\perp$ for the $(n-k+1)$-plane orthogonal to the k-plane P, both passing through the origin in $\mathbb{R}^{n+1}$, and we write S_P for the unit $(k-1)$-sphere in P.

Theorem 21 (Blaschke–Petkantschin formula on the sphere)**.** *Let n be a positive integer, $1 \leq k \leq n$, and $f\colon (\mathbb{S}^n)^{k+1} \to \mathbb{R}$ a non-negative measurable function. Then*

$$\int\limits_{\mathbf{x}\in(\mathbb{S}^n)^{k+1}} f(\mathbf{x})\,\mathrm{d}\mathbf{x} = \int\limits_{P\in\mathcal{L}^{n+1}_k}\int\limits_{p\in P^\perp} r^{kn-2}\int\limits_{\mathbf{u}\in(S_P)^{k+1}} f(p+r\mathbf{u})\,[k!\mathrm{Vol}(\mathbf{u})]^{n-k+1}\,\mathrm{d}\mathbf{u}\,\mathrm{d}p\,\mathrm{d}P,$$

in which $r^2 = 1 - \|p\|^2$, implicitly assuming $\|p\| \leq 1$, If f is rotationally symmetric, we define $f_r(\mathbf{u}) = f(p + r\mathbf{u})$, in which $\mathbf{u}$ is a k-simplex on $\mathbb{S}^{k-1} \subseteq \mathbb{R}^k$, and p is any point with $\|p\|^2 = 1 - r^2 \leq 1$ in the $(n-k+1)$-plane orthogonal to $\mathbb{R}^k \subseteq \mathbb{R}^{n+1}$. With this notation, we have

$$\int\limits_{\mathbf{x}\in(\mathbb{S}^n)^{k+1}} f(\mathbf{x})\,\mathrm{d}\mathbf{x} = \tfrac{\sigma_{n+1}}{2}\|\mathcal{L}^n_k\|\int\limits_{t=0}^{1} t^{\frac{kn-2}{2}}(1-t)^{\frac{n-k-1}{2}}\int\limits_{\mathbf{u}\in(\mathbb{S}^{k-1})^{k+1}} f_{\sqrt{t}}(\mathbf{u})\,[k!\mathrm{Vol}(\mathbf{u})]^{n-k+1}\,\mathrm{d}\mathbf{u}\,\mathrm{d}t.$$

Proof. We first argue that f may be assumed to be continuous. Consider the subset M of $\mathcal{L}^{n+1}_k \times \mathbb{R}^{n+1} \times (\mathbb{R}^{n+1})^{k+1}$ consisting of all triplets $(P, p, \mathbf{u})$ such that $p \in P^\perp$, $\|p\| < 1$, and $\mathbf{u} \in (S_P)^{k+1}$. Clearly, M is a submanifold of the product space with a natural measure. Recall that $r^2 = 1 - \|p\|^2$ and consider the mapping $T\colon M \to (\mathbb{S}^n)^{k+1}$ defined by

$T(P, p, \mathbf{u}) = p + r\mathbf{u}$. It is a bijection up to a set of measure 0. By Theorem 20.3 in [42], there exists a corresponding Jacobian $J\colon M \to \mathbb{R}$, meaning that every integrable function f satisfies $\int_{\mathbf{x}\in(\mathbb{S}^n)^{k+1}} f(\mathbf{x})\,\mathrm{d}\mathbf{x} = \int_{y\in M} f(T(y))J(y)\,\mathrm{d}y$. For non-negative f, the right-hand side integral can be split using Fubini's theorem. The existence of the Jacobian is thus settled, and to find its values, we may assume that f be continuous.

The main idea in the rest of the proof is to thicken $\mathbb{S}^n$ to an $(n+1)$-dimensional annulus, to apply the original Blaschke–Petkantschin formula to this annulus, and to take the limit when we shrink the annulus back to $\mathbb{S}^n$. We write $\mathbb{A}^{n+1}_{1+\varepsilon} = (1+\varepsilon)\mathbb{B}^{n+1} \setminus \operatorname{int}\mathbb{B}^{n+1}$ for the $(n+1)$-dimensional annulus with inner radius 1 and outer radius $1+\varepsilon$. We begin by extending f from the sphere to the annulus. Specifically, for points $y_i \in \mathbb{A}^{n+1}_{1+\varepsilon}$, we set

$$F(y_0, y_1, \ldots, y_k) = f\left(y_0/\|y_0\|, y_1/\|y_1\|, \ldots, y_k/\|y_k\|\right).$$

Since f is continuous on the $(k+1)$-fold product of spheres, by assumption, F is continuous on the $(k+1)$-fold product of annuli. Because F is continuous on a compact set and therefore bounded and uniformly continuous, we have

$$\begin{aligned}\int\limits_{\mathbf{x}\in(\mathbb{S}^n)^{k+1}} f(\mathbf{x})\,\mathrm{d}\mathbf{x} &= \lim_{\varepsilon\to 0} \tfrac{1}{\varepsilon^{k+1}} \int\limits_{\mathbf{y}\in(\mathbb{A}^{n+1}_{1+\varepsilon})^{k+1}} F(\mathbf{y})\,\mathrm{d}\mathbf{y} \\ &= \lim_{\varepsilon\to 0} \tfrac{1}{\varepsilon^{k+1}} \int\limits_{P\in\mathcal{L}^{n+1}_k} \int\limits_{p\in P^\perp} \int\limits_{\mathbf{u}\in A^{k+1}} F(\mathbf{u})[k!\mathrm{Vol}(\mathbf{u})]^{n-k+1}\,\mathrm{d}\mathbf{u}\,\mathrm{d}p\,\mathrm{d}P, \end{aligned} \tag{3.6}$$

in which $A = \mathbb{A}^{n+1}_{1+\varepsilon} \cap [p+P]$ is the k-dimensional slice of the $(n+1)$-dimensional annulus defined by P and p. We obtain the second line by applying the standard Blaschke–Petkantschin formula in $\mathbb{R}^{n+1}$ to the function $F(\mathbf{y})$ times the indicator function of the $(k+1)$-fold product of annuli, and then absorb the indicator into the integration domain. To continue, we investigate the slice of the annulus whose $(k+1)$-fold product is the innermost integration domain; see Figure 3.1. Write $h = \|p\|$ for the height of the slice, which is non-empty for $0 \le h \le 1+\varepsilon$. A is a (possibly degenerate) k-dimensional annulus, with squared inner radius $r^2 = \max\{0, 1-h^2\}$ and squared outer radius $r_\varepsilon^2 = (1+\varepsilon)^2 - h^2$. We split the integration domain into three regions: $h \le 1-\varepsilon^{-0.2}$, $1-\varepsilon^{0.2} < h \le 1$, and $1 < h \le 1+\varepsilon$.

We first show that the contribution of the region $1-\varepsilon^{0.2} < h \le 1$ is small. To get started, note that $r_\varepsilon - r = (r_\varepsilon^2 - r^2)/(r_\varepsilon + r) = (2\varepsilon+\varepsilon^2)/(r_\varepsilon+r)$. For small ε, this implies $r_\varepsilon - r \le \mathrm{const}\cdot\varepsilon/r_\varepsilon$, in which we deliberately avoid the computation of the constant. With this, we can bound the k-dimensional volume of A. Assuming $k \ge 2$, we get $\mathrm{Vol}(A) = \nu_k(r_\varepsilon^k - r^k) = \nu_k(r_\varepsilon - r)(r_\varepsilon^{k-1} + r_\varepsilon^{k-2}r + \ldots + r^{k-1}) \le \mathrm{const}\cdot\varepsilon r_\varepsilon^{k-2}$, in which the constant depends only on k and n. As noted before, the inequality also holds for $k=1$. Since $h > 1-\varepsilon^{0.2}$, we also get $r_\varepsilon^2 < (1+\varepsilon)^2 - (1-\varepsilon^{0.2})^2 \le \varepsilon^2 + 2\varepsilon + 2\varepsilon^{0.2} - \varepsilon^{0.4}$ for small ε, which implies $r_\varepsilon < \mathrm{const}\cdot\varepsilon^{0.1}$. Clearly, the k-dimensional volume of any k-simplex with vertices inside A can not exceed a constant times the k-th power of the diameter of A, which is $2r_\varepsilon$, implying $\mathrm{Vol}(\mathbf{u}) \le \mathrm{const}\cdot r_\varepsilon^k$. Recalling that F is bounded, we thus get

$$\left| \int\limits_{P\in\mathcal{L}^{n+1}_k} \int\limits_{\substack{p\in P^\perp \\ \|p\|<1-\varepsilon^{0.2}}} \tfrac{1}{\varepsilon^{k+1}} \int\limits_{u\in A^{k+1}} F(\mathbf{u})[k!\mathrm{Vol}(\mathbf{u})]^{n-k+1}\,\mathrm{d}\mathbf{u}\,\mathrm{d}p\,\mathrm{d}P \right|$$

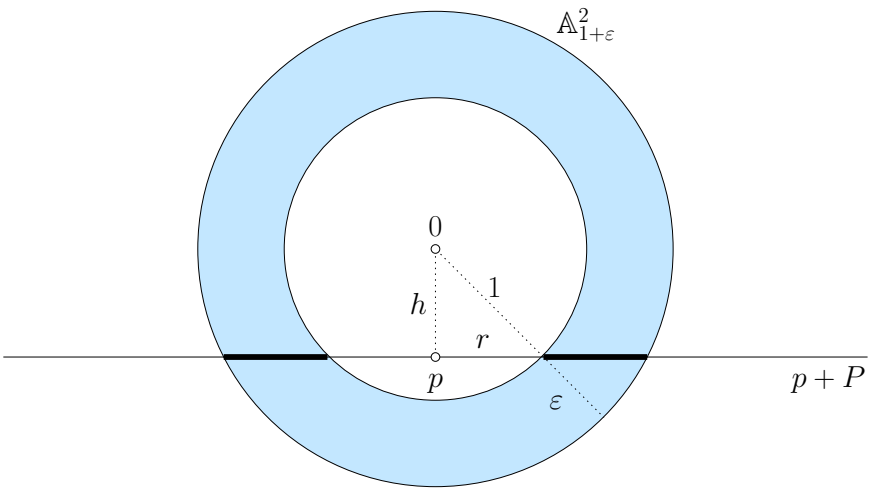

Figure 3.1: For $h = \|p\| < 1$, the slice of the $(n+1)$-dimensional annulus is a k-dimensional annulus. In this picture, $n+1 = 2$ and $k = 1$.

$$\begin{aligned}
&\leq \text{const} \int_{h=1-\varepsilon^{0.2}}^{1} \tfrac{1}{\varepsilon^{k+1}} \mathrm{Vol}(A)^{k+1} \mathrm{Vol}(\mathbf{u})^{n-k+1} \,\mathrm{d}h \\
&\leq \text{const} \int_{h=1-\varepsilon^{0.2}}^{1} \tfrac{1}{\varepsilon^{k+1}} (\varepsilon r_\varepsilon^{k-2})^{k+1} r_\varepsilon^{k(n-k+1)} \,\mathrm{d}h \\
&\leq \text{const} \int_{h=1-\varepsilon^{0.2}}^{1} r_\varepsilon^{kn-2} \,\mathrm{d}h \;\leq\; \text{const} \cdot \varepsilon^{0.2} \cdot \varepsilon^{0.1(kn-2)} \;\to\; 0.
\end{aligned} \tag{3.7}$$

Here we use the bound on r_ε for the last inequality, and $kn \geq 1$ to see that the expression tends to zero. Next consider the region $1 < h \leq 1+\varepsilon$, in which A is a ball of radius r_ε, so $\mathrm{Vol}(A) = \nu_k r_\varepsilon^k$. We have $\mathrm{Vol}(\mathbf{u}) \leq \nu_k r_\varepsilon^k$, as before, and $r_\varepsilon^2 \leq (1+\varepsilon)^2 - 1$, which implies $r_\varepsilon \leq \text{const} \cdot \sqrt{\varepsilon}$. With this, we can again establish the vanishing of the integral as $\varepsilon \to 0$:

$$\begin{aligned}
&\left| \int_{P \in \mathcal{L}_k^{n+1}} \int_{\substack{p \in P^\perp \\ 1 \leq \|p\| \leq 1+\varepsilon}} \tfrac{1}{\varepsilon^{k+1}} \int_{u \in A^{k+1}} F(\mathbf{u}) [k! \mathrm{Vol}(\mathbf{u})]^{n-k+1} \,\mathrm{d}\mathbf{u} \,\mathrm{d}p \,\mathrm{d}P \right| \\
&\qquad \leq \text{const} \int_{h=1}^{1+\varepsilon} \tfrac{1}{\varepsilon^{k+1}} \mathrm{Vol}(A)^{k+1} \mathrm{Vol}(\mathbf{u})^{n-k+1} \,\mathrm{d}h \\
&\qquad \leq \text{const} \int_{h=1}^{1+\varepsilon} \tfrac{1}{\varepsilon^{k+1}} r_\varepsilon^{k(n+2)} \,\mathrm{d}h \;\leq\; \text{const} \cdot \varepsilon \cdot \varepsilon^{(kn-2)/2} \;\to\; 0.
\end{aligned} \tag{3.8}$$

We have thus established that the relevant region is $0 \leq h \leq 1 - \varepsilon^{0.2}$, and we are ready to investigate its contribution. First, we claim that the width of the annulus A is

$$r_\varepsilon - r = r\sqrt{1 + \tfrac{2\varepsilon+\varepsilon^2}{r^2}} - r = \tfrac{\varepsilon}{r} + o(\varepsilon). \tag{3.9}$$

To get the right-hand side of (3.9), we use the Taylor expansion of $g(x) = (1+x)^{1/2} = 1 + \frac{1}{2}x - \frac{1}{2}x^2 + \ldots$, and $r > \varepsilon^{0.1}$ as well as $x = (2\varepsilon + \varepsilon^2)/r^2 < 3\varepsilon^{0.8}$, which we get from the

assumed $h \leq 1-\varepsilon^{0.2}$. observing that $\varepsilon^2/(2r^2) = O(\varepsilon^{1.8})$, we get $rg(x) - r = \frac{\varepsilon}{r} + O(r\varepsilon^{1.8}) + O(r\varepsilon^{1.6})$ and therefore (3.9). Using the fact that $F(\mathbf{u})$ is equal to $f(\mathbf{u})$ when all points lie on the inner sphere and the uniform continuity of F and writing S_r for the $(k-1)$-sphere with center p and radius r in $P \in \mathcal{L}_k^{n+1}$, we get

$$\int\limits_{\mathbf{u}\in A^{k+1}} \tfrac{1}{\varepsilon^{k+1}} F(\mathbf{u})[k!\mathrm{Vol}(\mathbf{u})]^{n-k+1}\,\mathrm{d}\mathbf{u} \left(\tfrac{1}{r}\right)^{k+1} \int\limits_{\mathbf{u}\in(S_r)}^{k+1} f(\mathbf{u})[k!\mathrm{Vol}(\mathbf{u})]^{n-k+1}\,\mathrm{d}\mathbf{u} + o(1), \quad (3.10)$$

in which the integration domain on the right is the k-fold product of the $(k-1)$-sphere with center p and radius r in P, and $o(1)$ is uniform over p and P. Substituting (3.7), (3.8), and (3.10) into (3.6), we finally get

$$\begin{aligned}
&\int\limits_{\mathbf{x}\in(\mathbb{S}^n)^{k+1}} f(\mathbf{x})\,\mathrm{d}\mathbf{x} \\
&\quad= \lim_{\varepsilon\to 0} \int\limits_{P\in\mathcal{L}_k^{n+1}} \int\limits_{\substack{p\in P^\perp \\ \|p\|\leq 1-\varepsilon^{0.2}}} \left[\tfrac{1}{r^{k+1}} \int\limits_{\mathbf{u}\in(S_r)^{k+1}} f(\mathbf{u})[k!\mathrm{Vol}(\mathbf{u})]^{n-k+1}\,\mathrm{d}\mathbf{u} + o(1) \right] \mathrm{d}p\,\mathrm{d}P \quad (3.11)\\
&\quad= \int\limits_{P\in\mathcal{L}_k^{n+1}} \int\limits_{p\in P^\perp} \left(\tfrac{1}{r}\right)^{k+1} \int\limits_{\mathbf{u}\in(S_r)^{k+1}} f(\mathbf{u})[k!\mathrm{Vol}(\mathbf{u})]^{n-k+1}\,\mathrm{d}\mathbf{u}\,\mathrm{d}p\,\mathrm{d}P \quad (3.12)\\
&\quad= \int\limits_{P\in\mathcal{L}_k^{n+1}} \int\limits_{p\in P^\perp} r^{kn-2} \int\limits_{\mathbf{u}\in(S_P)^{k+1}} f(p+r\mathbf{u})[k!\mathrm{Vol}(\mathbf{u})]^{n-k+1}\,\mathrm{d}\mathbf{u}\,\mathrm{d}p\,\mathrm{d}P, \quad (3.13)
\end{aligned}$$

in which we drop the $\|p\| \leq 1-\varepsilon^{0.2}$ condition in (3.11) for the implicitly assumed $\|p\| \leq 1$ when passing to (3.12), which we can do because the difference vanishes in the limit and (3.13) is obtained by rescaling and translating the sphere in (3.12). Indeed, the power of r is a consequence of scaling the volume of the k-simplex, adjusting the volume of the integration domain, and subtracting the power we have already in (3.12): $k(n-k+1) + (k-1)(k+1) - (k+1) = kn-2$. This proves the first relation claimed in Theorem 21.

To get the second relation, we simplify the first by exploiting the rotational symmetry of f. Recalling that $r^2 = 1-\|p\|^2$, it makes sense to define $f_r(\mathbf{u}) = f(p+r\mathbf{u})$ on the $(k+1)$-fold product of $S_P \subseteq \mathbb{S}^n$ because the direction of p does not matter for a fixed height. Neither does P influence the function for a fixed height, so we can define f_r on $(\mathbb{S}^{k-1})^{k+1}$. Thus

$$\begin{aligned}
\int\limits_{\mathbf{x}\in(\mathbb{S}^n)^{k+1}} f(\mathbf{x})\,\mathrm{d}\mathbf{x} &= \|\mathcal{L}_k^{n+1}\| \int\limits_{p\in\mathbb{B}^{n-k+1}} r^{kn-2} \int\limits_{\mathbf{u}\in(\mathbb{S}^{k-1})^{k+1}} f_r(\mathbf{u})[k!\mathrm{Vol}(\mathbf{u})]^{n-k+1}\,\mathrm{d}\mathbf{u}\,\mathrm{d}p \quad (3.14)\\
&= \|\mathcal{L}_k^{n+1}\|\sigma_{n-k+1} \int\limits_{h=0}^{1} h^{n-k} r^{kn-2} \int\limits_{\mathbf{u}\in(\mathbb{S}^{k-1})^{k+1}} f_r(\mathbf{u})[k!\mathrm{Vol}(\mathbf{u})]^{n-k+1}\,\mathrm{d}\mathbf{u}\,\mathrm{d}h \quad (3.15)\\
&= \tfrac{\sigma_{n+1}}{2}\|\mathcal{L}_k^{n}\| \int\limits_{t=0}^{1} t^{\frac{kn-2}{2}} (1-t)^{\frac{n-k-1}{2}} \int\limits_{\mathbf{u}\in(\mathbb{S}^{k-1})^{k+1}} f_r(\mathbf{u})[k!\mathrm{Vol}(\mathbf{u})]^{n-k+1}\,\mathrm{d}\mathbf{u}\,\mathrm{d}t, \quad (3.16)
\end{aligned}$$

in which $t = r^2 = 1-h^2$. We get (3.14) from (3.13) because every $P \in \mathcal{L}_k^{n+1}$ contributes the same to the integral. Similarly, we get (3.15) from (3.14) by integrating over the range

of heights and compensating for the different sizes of the corresponding spheres, aka expressing the integral in polar coordinates. Finally, we get (3.16) from (3.15) by substituting t for r^2, $1-t$ for h^2, and $\mathrm{d}t$ for $-2h\,\mathrm{d}h$, noting that the minus sign is absorbed by reversing the limits of integration. This proves the second relation in Theorem 21. □

4. Constants

In this chapter we define the constants $C^n_{\ell,k}$ and $C^{k,n}_{\ell,m}$ used in the statements of theorems in Chapter 2. Their definition involves certain expectations of volumes of inscribed simplices, and we compute the values of $C^n_{\ell,k}$ for $n \leq 4$ and of $C^{k,n}_{\ell,m}$ for $k \leq 2$.

4.1 Spherical expectations

Denote by $\mathbf{u} = (u_0, u_1, \ldots, u_m)$ a sequence of $m+1$ random points independently chosen according to the uniform distribution on the unit sphere in $\mathbb{R}^m$, and write $\mathrm{Vol}(\mathbf{u})$ for the m-dimensional volume of the m-simplex spanned by the u_i. We define

$$E^n_{\ell,m} = \mathbb{E}[\mathrm{Vol}(\mathbf{u})^{n-m+1}\mathbf{1}_{m-\ell}(\mathbf{u})], \tag{4.1}$$

in which

$$\mathbf{1}_j(\mathbf{u}) = \begin{cases} 1 & \text{if exactly } j \text{ facets of } \mathbf{u} \text{ are visible from } 0, \\ 0 & \text{otherwise;} \end{cases}$$

recall the definition of visibility in Section 1.5.

Similarly, denote by $\mathbf{v} = (v_0, v_1, \ldots, v_m)$ a sequence of $m+1$ random points independently chosen according to the uniform distribution on the unit sphere in $\mathbb{R}^{m+n-k}$ and write $\mathbf{v}'$ for the orthogonal projection of $\mathbf{v}$ onto any fixed subspace $\mathbb{R}^m$. Write $\mathrm{Vol}(\mathbf{v}')$ for the m-dimensional volume of the m-simplex spanned by the v_i. Then the corresponding constants for the weighted case are defined as

$$E^{k,n}_{\ell,m} = \mathbb{E}[\mathrm{Vol}(\mathbf{v}')^{k-m+1}\mathbf{1}_{m-\ell}(\mathbf{v}')]. \tag{4.2}$$

Note that 0 is usually not the circumcenter of the projected simplex, but we still ask if a facet of projected simplex is visible from 0. The main constants $C^n_{\ell,m}$ and $C^{k,n}_{\ell,m}$ are then given by

$$C^n_{\ell,m} = \frac{\sigma_n \cdot \sigma_{n-1} \cdot \ldots \cdot \sigma_{n-m+1}}{\sigma_1 \cdot \sigma_2 \cdot \ldots \cdot \sigma_m} \frac{\Gamma(m) m!^{n-m} \sigma_m^{m+1}}{(m+1) n \nu_n^m} E^n_{\ell,m}, \tag{4.3}$$

$$C^{k,n}_{\ell,m} = \frac{\sigma_k \sigma_{k-1} \cdot \ldots \cdot \sigma_{k-m+1}}{\sigma_1 \sigma_2 \cdot \ldots \cdot \sigma_m} \frac{\Gamma\left(m+1-\frac{k}{n}\right) m!^{k-m} \sigma_{m+n-k}^{m+1}}{(m+1) n \nu_n^{m+1-\frac{k}{n}}} E^{k,n}_{\ell,m}. \tag{4.4}$$

Of course, for $k = n$ we have $E^n_{\ell,m} = E^{n,n}_{\ell,m}$ and $C^n_{\ell,m} = C^{n,n}_{\ell,m}$. Further, we trivially have $E^n_{0,0} = E^{k,n}_{0,0} = 1$. Now we turn to the less trivial cases.

4.2 General relations between constants

The constants are now fully defined, and the rest of the chapter is devoted to computing them. Assume for this section that the theorems stated in Chapter 2 are proved for the constants defined in (4.3) and (4.4). Then the expected number of simplices of dimension j in (weighted) Poisson–Delaunay mosaic with $\rho = 1$ in any Borel region is the constant D_j^n ($D_j^{k,n}$) times the volume of the region. The expected number of critical simplices of dimension j in the corresponding complexes is similarly $C_{j,j}^n$ ($C_{j,j}^{k,n}$) times the volume of the region. Now we incorporate the combinatorial structure of the complex to collect the relations between the constants. All of the following statements appeared in the text before in different contexts, and we collect them all together for a convenient reference. First we state them for the unweighted case:

$$D_0^n = 1, \tag{4.5}$$

$$D_n^n = \frac{2^{n+1}\pi^{\frac{n}{2}}}{n(n+1)!}\frac{\Gamma\left(\frac{n^2+1}{2}\right)\Gamma\left(1+\frac{n}{2}\right)^n\Gamma(n)}{\Gamma\left(\frac{n^2}{2}\right)\Gamma\left(\frac{n+1}{2}\right)^n\Gamma\left(\frac{1}{2}\right)}, \tag{4.6}$$

$$D_{n-1}^n = \frac{n+1}{2}D_n^n, \tag{4.7}$$

$$0 = \sum_{j=0}^{n}(-1)^j D_j^n, \tag{4.8}$$

$$0 = \sum_{j=0}^{n}(-1)^j C_{j,j}^n, \tag{4.9}$$

$$C_{0,m}^n = \mathbf{1}_{\{m=0\}}, \tag{4.10}$$

$$D_j^n = \sum_{\ell=0}^{j}\sum_{m=j}^{n}\binom{m-\ell}{m-j}C_{\ell,m}^n. \tag{4.11}$$

The first four relations come from Theorems 1 and 2, (4.9) is the first Morse relation from page 9, (4.10) reflects the fact that all vertices are critical, and the last one is Lemma 1.5.1. Note that this relations are enough to get D_j^n for $n \leq 3$. Similar relations hold for $D_j^{k,n}$. We don't know the intensity of vertices any more, the expression for the number of top-dimensional simplices comes from Theorem 3, and the rest is the same:

$$D_k^{k,n} = \frac{\sigma_1\sigma_{n+1}}{\sigma_{k+1}\sigma_{n-k+1}}\frac{2^{k+1}\pi^{k/2}}{n(k+1)!}\frac{\Gamma\left(\frac{kn+n-k+1}{2}\right)}{\Gamma\left(\frac{kn+n-k}{2}\right)}\frac{\Gamma\left(\frac{n+2}{2}\right)^{k+1-\frac{k}{n}}}{\Gamma\left(\frac{n+1}{2}\right)^k}\frac{\Gamma\left(k+1-\frac{k}{n}\right)}{\Gamma\left(\frac{n-k+1}{2}\right)}, \tag{4.12}$$

$$D_{k-1}^{k,n} = \frac{k+1}{2}D_k^{k,n}, \tag{4.13}$$

$$0 = \sum_{j=0}^{n}(-1)^j D_j^{k,n}, \tag{4.14}$$

$$0 = \sum_{j=0}^{n}(-1)^j C_{j,j}^k n, \tag{4.15}$$

$$D_j^{k,n} = \sum_{\ell=0}^{j}\sum_{m=j}^{k}\binom{m-\ell}{m-j}C_{\ell,m}^{k,n}. \tag{4.16}$$

We do not focus on subtleties at the boundary in the weighted case either, as they can be resolved in the same way as in the unweighted case, see the discussion after Theorem 2.

4.3 Reflections

To get hands on the explicit values of constants, we incorporate a trick developed by Wendel in [72].

Volume decomposition. Although there was some ambiguity in the previous notation concerning ambient dimension, in this section we write $\mathbf{u} = (u_0, u_1, \ldots, u_m)$ for a sequence of $m+1$ affinely independent points in $\mathbb{R}^m$. Recall that for each $0 \leq i \leq m$ we write $\mathbf{u}_i$ for the m-simplex obtained by substituting 0 for u_i, called a *cone* over the i-th facet, and $V_i = \mathrm{Vol}(\mathbf{u}_i)$ for its m-dimensional volume. We faced the cones in Theorems 4 and 5, but now the simplex $\mathbf{u}$ is not necessarily inscribed. Expressing the origin in terms of the points, $0 = \sum_{i=0}^m \zeta_i u_i$ with $\sum_{i=0}^m \zeta_i = 1$, we see that the facet opposite to u_i is visible from 0 iff $\zeta_i < 0$, and it can be verified that actually ζ_i is a signed volume of the corresponding cone. The coefficients ζ_i are called *barycentric coordinates* of 0 with respect to $\mathbf{u}$. Writing $\mathrm{sgn}(\zeta_i)$ for the sign of the i-th barycentric coordinate, we therefore have

$$\mathrm{Vol}(\mathbf{u}) = \sum_{i=0}^{m} \mathrm{sgn}(\zeta_i) V_i. \tag{4.17}$$

This formula is easy to see, for example, as each ray originating from 0 that intersects a simplex enters crossing a visible (front) facet and leaves crossing an invisible (back) facet, and the formula above subtracts from the total length of the ray before it leaves the simplex the part which lies outside.

The multiplicative group $\mathbb{Z}_2 = \{-1, 1\}$ acts on $\mathbb{R}^m$ by reflecting $x \in \mathbb{R}^m$ to $-x$. This action is naturally extended to the action of $\mathbb{Z}_2^{m+1}$ on $(m+1)$-tuples of points: for any vector $\mathbf{t} = (t_0, t_1, \ldots, t_m)$, with $t_i \in \{-1, 1\}$ for $0 \leq i \leq m$, we call $\mathbf{tu} = (t_0 u_0, t_1 u_1, \ldots, t_m u_m)$ the *reflection* with *signature* $\mathbf{t}$ of $\mathbf{u}$, and we write $\#\mathbf{t}$ for the number of indices i with $t_i = -1$. Importantly, the reflection of a vertex does not affect the volume of any cone. We write $V_{\mathbf{t}} = V_{\mathbf{t}}(\mathbf{u}) = \sum_{i=0}^m t_i V_i$ for the sum of positive and negative cone volumes. Assuming 0 is contained in the interior of the m-simplex $\mathbf{u}$, the following lemma shows that it is the signed volume of $\mathbf{tu}$.

Lemma 4.3.1 (Volume decomposition)**.** *Let $\mathbf{u} \in (\mathbb{R}^m)^{m+1}$ such that 0 is contained in the interior of the m-simplex. Then $\mathrm{Vol}(\mathbf{tu}) = |V_{\mathbf{t}}(\mathbf{u})|$, for every $\mathbf{t} \in \{-1, 1\}^{m+1}$.*

Proof. We reflect the vertices one by one to obtain $\mathbf{tu}$ from $\mathbf{u}$ and argue by induction on $\#\mathbf{t}$. By assumption, no facet of $\mathbf{u}$ is visible from 0, so $\mathrm{Vol}(\mathbf{u}) = \sum_{i=0}^m V_i$, which settles the base case. Assume without loss of generality that $\mathbf{t} = (-1, \ldots, -1, 1, \ldots, 1)$ with $\#\mathbf{t} = j$, and $\mathbf{t}' = (-1, \ldots, -1, 1, \ldots, 1)$ with $\#\mathbf{t}' = j-1$. By induction, the volume of $\mathbf{t}'\mathbf{u}$ is $\pm V_{\mathbf{t}'}(\mathbf{u})$, i.e., either $\mathrm{Vol}(\mathbf{t}'\mathbf{u}) = -V_0 - \ldots - V_{j-1} + V_j + \ldots + V_m$ or $\mathrm{Vol}(\mathbf{t}'\mathbf{u}) = V_0 + \ldots + V_{j-1} - V_j - \ldots - V_m$, depending on which of the two expressions is positive. Reflecting u_j either changes the orientation of the inscribed m-simplex, meaning that the reflection of u_j lies on the other side of the hyperplane spanned by the remaining vertices, or it does not. In case the orientation is changed, the reflection changes the visibility of exactly one facet, namely the one opposite to u_j, and by (4.17) we get either $\mathrm{Vol}(\mathbf{tu}) = -V_0 - \ldots - V_{j-1} - V_j + V_{j+1} + \ldots + V_m$ or $\mathrm{Vol}(\mathbf{tu}) = V_0 + \ldots + V_{j-1} + V_j - V_{j+1} - \ldots - V_m$. In case the orientation is preserved, the reflection changes the visibility of every facet but one, namely the one opposite to u_j, and again by (4.17) we get either $\mathrm{Vol}(\mathbf{tu}) = V_0 + \ldots + V_{j-1} + V_j - V_{j+1} - \ldots - V_m$ or $\mathrm{Vol}(\mathbf{tu}) = -V_0 - \ldots - V_{j-1} - V_j + V_{j+1} + \ldots + V_m$. In all cases we have $\mathrm{Vol}(\mathbf{tu}) = |V_{\mathbf{t}}(\mathbf{u})|$. □

Visibility. There are several useful consequences of Lemma 4.3.1, which we now state. Note that for almost every m-simplex, there are precisely two signatures for which the corresponding reflections produce a m-simplex that contains the origin. Indeed, to produce one, we reflect every vertex opposite a facet visible from 0, and to produce the other, we reflect every vertex opposite a facet that is not visible from 0. In this way we get all barycentric coordinates of 0 to be positive, which is equivalent to containing 0 in the interior. If the first simplex corresponds to $\mathbf{t} = (t_0, t_1, \ldots, t_m)$, then the second corresponds to $-\mathbf{t} = (-t_0, -t_1, \ldots, -t_m)$, which we refer to as the *complementary* signature.

Corollary 4.3.2 (Reflections and visibility)**.** *Let $\mathbf{u} \in (\mathbb{R}^m)^{m+1}$ such that 0 is contained in the interior of the m-simplex, and let $\mathbf{t} \in \{-1, 1\}^{m+1}$.*

1. *After reflecting a subset of the vertices, the visible facets are either the ones opposite to the reflected vertices, or all others. Specifically, if $V_{\mathbf{t}}(\mathbf{u}) > 0$, then there are $\#\mathbf{t}$ visible facets, each one opposite a reflected vertex, and if $V_{\mathbf{t}}(\mathbf{u}) < 0$, then there are $m - \#\mathbf{t} + 1$ visible facets, each one opposite a non-reflected vertex.*

2. *The simplices $\mathbf{tu}$ and $-\mathbf{tu}$ are central reflections of each other; in particular, they have the same volume and the same indices of facets visible from 0.*

Fact 1 in Corollary 4.3.2 is a direct consequence of (4.17) and Lemma 4.3.1, and Fact 2 is clear for geometric reasons. The following simple facts will be useful in our computations.

Lemma 4.3.3 (Visibility of facets)**.** *Let $\mathbf{u} \in (\mathbb{R}^m)^{m+1}$ such that 0 is contained in the interior of the m-simplex, and let $\mathbf{t} \in \{-1, 1\}^{m+1}$.*

1. *The origin, 0, is contained in the interior of the m-simplex $\mathbf{tu}$ iff $\#\mathbf{t} = 0$ or $m + 1$.*

2. *$\#\mathbf{t} = 0$ implies $V_{\mathbf{t}}(\mathbf{u}) > 0$ and, equivalently, $\#\mathbf{t} = m + 1$ implies $V_{\mathbf{t}}(\mathbf{u}) < 0$.*

3. *If a set of facets of $\mathbf{tu}$ is visible from 0, then there is no signature $\mathbf{t}'$ such that the complementary set of facets is visible from 0 in $\mathbf{t}'\mathbf{u}$.*

4. *If $\mathbf{u}$ is an inscribed simplex, i.e., $\mathbf{u} \in (\mathbb{S}^{m-1})^{m+1}$, then $\#\mathbf{t} = 1$ implies $V_{\mathbf{t}}(\mathbf{u}) > 0$ and, equivalently, $\#\mathbf{t} = m$ implies $V_{\mathbf{t}}(\mathbf{u}) < 0$.*

Proof. By assumption on $\mathbf{u}$, the only signatures for which all terms $t_i V_i$ have the same sign are the ones for which $\#\mathbf{t} = 0$ or $\#\mathbf{t} = m + 1$. Fact 1 follows and implies Fact 2.

To see Fact 3, we express $\mathrm{Vol}(\mathbf{tu})$ using (4.17), getting a negative coefficient for every visible facet. Nevertheless, the sum of signed cone volumes is positive. If the visibility of all facets could be reversed, (4.17) would give a negative volume, which is a contradiction. Fact 4 follows: if $\mathbf{u}$ is a simplex on the sphere, then reflecting any vertex u_i we obtain a simplex with a single visible facet, the one opposite to u_i. Hence, by Fact 3, it is impossible to see the complementary m facets all at once from 0. □

Fact 1 of Lemma 4.3.3 was used in [72] to compute the probability that all points of a finite set sampled independently and uniformly on a sphere lie inside a hemisphere. Fact 4 will allow us to compute many of the values of $E^n_{\ell,m}$, but, unfortunately, it can not be applied for $E^{k,n}_{\ell,m}$, because the points are inside a ball and not on the sphere any more.

Spherical expectations and cone volumes. We will now rewrite the expectation in the definition (4.1) of $E^n_{\ell,m}$ using the cone volumes. The probability space for the random variable $\mathbf{u}$ is $\mathcal{P} = (\{\mathbb{S}^{m-1}, \mathfrak{U}\})^{\otimes(m+1)}$, in which $\mathfrak{U}$ is the uniform measure on the sphere, and the random variables u_i are just the projections onto i-th coordinate. Note that every inscribed simplex, $\mathbf{u}$, corresponds to a unique point configuration $\bar{\mathbf{u}} \in \mathbb{RP}^{m-1}$ obtained by projecting u_i from the sphere to the projective space. Likewise, every m-simplex with vertices in $\mathbb{RP}^{m-1}$ corresponds to 2^{m+1} m-simplices inscribed in $\mathbb{S}^{m-1}$. This allows us to decompose the probability space as $\mathcal{P} = (\{\mathbb{RP}^{m-1}, \mathfrak{U}'\} \otimes \{\{-1,1\}, \mathfrak{B}\})^{\otimes(m+1)}$, in which $\mathfrak{U}'$ is the uniform measure on the projective space and $\mathfrak{B}$ is the uniform measure on $\mathbb{Z}_2$. In other words, we decompose the uniform measure on the sphere as the measure on orbits under the action of $\mathbb{Z}_2^{m+1}$ times the Haar measure on the group. Write $\mathbb{E}_{\mathbf{u}}$ for the expectation taken over the sphere, $\mathbb{E}_{\bar{\mathbf{u}}}$ for the expectation over the projective space and $\mathbb{E}_{\bar{\mathbf{u}},\mathbf{t}}$ for the expectation over the projective space and the group. We use the probabilistic formalism only locally, to decompose the expectation in (4.1) further into expectations involving volumes of cones. We recall that the volume of $\mathbf{tu}$ is either $V_{\mathbf{t}}(\mathbf{u})$ or $-V_{\mathbf{t}}(\mathbf{u})$. For each $1 \le \ell \le m \le n$, we write the expectation in (4.1) as

$$
\begin{aligned}
E^n_{\ell,m} &= \mathbb{E}_{\mathbf{u}}[\mathrm{Vol}(\mathbf{u})^{n-m+1}\mathbf{1}_{m-\ell}(\mathbf{u})] && (4.18)\\
&= \mathbb{E}_{\bar{\mathbf{u}},\mathbf{t}}[|V_{\mathbf{t}}(\bar{\mathbf{u}})|^{n-m+1}\mathbf{1}_{m-\ell}(\bar{\mathbf{u}},\mathbf{t})] && (4.19)\\
&= \tfrac{1}{2^{m+1}} \sum_{\#\mathbf{t}=m-\ell} \mathbb{E}_{\bar{\mathbf{u}}}[|V_{\mathbf{t}}(\bar{\mathbf{u}})|^{n-m+1}\mathbf{1}_{V_{\mathbf{t}}(\bar{\mathbf{u}})>0}] + \tfrac{1}{2^{m+1}} \sum_{\#\mathbf{t}=\ell+1} \mathbb{E}_{\bar{\mathbf{u}}}[|V_{\mathbf{t}}(\bar{\mathbf{u}})|^{n-m+1}\mathbf{1}_{V_{\mathbf{t}}(\bar{\mathbf{u}})<0}] && (4.20)\\
&= \tfrac{1}{2^{m}} \sum_{\#\mathbf{t}=m-\ell} \mathbb{E}_{\bar{\mathbf{u}}}[V_{\mathbf{t}}(\bar{\mathbf{u}})^{n-m+1}\mathbf{1}_{V_{\mathbf{t}}(\bar{\mathbf{u}})>0}] && (4.21)\\
&= \tfrac{1}{2^{m}}\binom{m+1}{m-\ell}\, \mathbb{E}_{\mathbf{u}}[V_{\mathbf{t}_{m-\ell}}(\mathbf{u})^{n-m+1}\mathbf{1}_{V_{\mathbf{t}_{m-\ell}}(\mathbf{u})>0}], && (4.22)
\end{aligned}
$$

in which $\mathbf{t}_{m-\ell}$ in (4.22) is an arbitrary signature with $\#\mathbf{t} = m-\ell$. The transition to (4.19) is possible because for a fixed $\mathbf{t}$, $V_{\mathbf{t}}$ is the same for all simplices in an orbit, and the transition to (4.20) is justified by the first fact in Corollary 4.3.2. We get (4.21) by observing that the two sums in (4.20) are over complementary signatures, and we get (4.22) because relabeling the vertices does not change the expected volume. We can remove the bar in the last transition again because $V_{\mathbf{t}_{m-\ell}}$ is the same along the orbits.

The same relation also holds for $E^{k,n}_{\ell,m}$. Indeed, the same reasoning can be repeated for any rotationally invariant measure on $\mathbb{R}^m$ with the only addition that we need to multiply the probability space by the measure on the $\mathbb{R}^+$ corresponding to the norm of the vector. The projection used in the definition of $E^{k,n}_{\ell,m}$ in (4.2) obviously gives a random simplex in $\mathbb{R}^m$ (actually, inside the unit ball in $\mathbb{R}^m$) with rotationally invariant probability measure.

4.4 Computations of constants in the unweighted case

We extract the explicit factor from (4.3) and rewrite it as

$$C^n_{\ell,m} = \mathrm{Factor}(m,n)E^n_{\ell,m}.$$

Note that it depends only on m and n. To compute the coefficient for small values of m and n, it is helpful to recall that the measures of the unit spheres are $\sigma_1 = 2$, $\sigma_2 = 2\pi$, $\sigma_3 = 4\pi$, $\sigma_4 = 2\pi^2$; see Table 4.1. Our remaining job is to compute the $E^n_{\ell,m}$.

$\mathrm{Factor}(m,n)$	$m=1$	2	3	4
$n=2$	1	$\frac{4}{3}\pi$		
3	1	$2\pi^2$	18π	
4	1	$\frac{64}{3}\pi$	1536	$\frac{768}{5}\pi^2$

Table 4.1: Values of Factor

4.4.1 Two dimensions

As a warm-up exercise, we begin with a Poisson point process in $\mathbb{R}^2$. We have $C^2_{0,0} = 1$ and $C^2_{0,k} = 0$ for $k > 0$ because all vertices are critical. To compute the remaining constants, we need the spherical expectations given in (4.22):

$$2E^2_{1,1} = \mathbb{E}[(V_0 + V_1)^2] = 2\mathbb{E}[V_0^2] + 2\mathbb{E}[V_0 V_1],$$

in which we get the right-hand side because expectations do not change under re-indexing. The expectation is with respect to the uniform distribution on $\mathbb{S}^0$, which is a pair of points. We have $V_0 = V_1 = 1$ and therefore $2E^2_{1,1} = 4$. We also need

$$\begin{aligned} \tfrac{4}{3}E^2_{1,2} &= \mathbb{E}[V_0 + V_1 - V_2] = \mathbb{E}[V_0], \\ 4E^2_{2,2} &= \mathbb{E}[V_0 + V_1 + V_2] = 3\mathbb{E}[V_0], \end{aligned}$$

which both satisfy $\#\mathbf{t} \leq 1$, so Lemma 4.3.3 applies and we can remove the indications, which we did. These two expectations are with respect to the uniform distribution on $\mathbb{S}^1$. Using (1.1) to compute $\mathbb{E}[V_0]$, we get $\frac{4}{3}E^2_{1,2} = \mathrm{Mnt}_1(2,2;1) = \frac{1}{\pi}$, and similarly $4E^2_{2,2} = 3\mathrm{Mnt}_1(2,2;1) = \frac{3}{\pi}$. Retrieving $\mathrm{Factor}(1,2) = 1$ and $\mathrm{Factor}(2,2) = \frac{4\pi}{3}$ from Table 1.1, we can now use (4.3) to get the corresponding constants:

$$\begin{aligned} C^2_{1,1} &= \mathrm{Factor}(1,2) \cdot E^2_{1,1} = 1 \cdot \tfrac{1}{2} \cdot 4 = 2, \\ C^2_{1,2} &= \mathrm{Factor}(2,2) \cdot E^2_{1,2} = \tfrac{4\pi}{2} \cdot \tfrac{3}{4} \cdot \tfrac{1}{\pi} = 1, \\ C^2_{2,2} &= \mathrm{Factor}(2,2) \cdot E^2_{2,2} = \tfrac{4\pi}{2} \cdot \tfrac{1}{4} \cdot 3\tfrac{1}{\pi} = 1. \end{aligned}$$

This justifies the entries of the left matrix in Table 2.1. Note that $C^2_{0,0} - C^2_{1,1} + C^2_{2,2} = 0$, which agrees with the discrete Morse relation (4.9). Indeed, it makes sense to use this relation as a check of correctness as we have refrained from using it during the derivation of the constants.

Remark. The computations for the critical edges generalize to n dimensions. Indeed, in this case we have $\mathrm{Factor}(1,n) = 1$ and $2E^2_{1,1} = \mathbb{E}[(V_0 + V_1)^n] = 2^n$, which gives

$$C^n_{1,1} = \mathrm{Factor}(1,n) \cdot E^n_{1,1} = 2^{n-1}. \tag{4.23}$$

Simplices in the Poisson–Delaunay mosaic. For completeness, we also compute the expected numbers of simplices in the 2-dimensional Poisson–Delaunay mosaic, which are of course known:

$$\begin{aligned} D^2_0 &= C^2_{0,0} = 1, \\ D^2_1 &= C^2_{1,1} + C^2_{1,2} = 3, \\ D^2_2 &= C^2_{1,2} + C^2_{2,2} = 2. \end{aligned}$$

We have $D^2_0 - D^2_1 + D^2_2 = 0$, which is consistent with the Euler relation in the plane. Note that $D^2_2 = 2$ and $C^2_{2,2} = 1$ imply that about half the Delaunay triangles are critical. The geometric reason behind this fact is an observation by Miles [54] that a Delaunay triangle is acute with probability $\frac{1}{2}$.

4.4.2 Three dimensions

We have $C^3_{0,0} = 1$ and $C^3_{0,m} = 0$ for $m > 0$ because every vertex is critical, and we know $C^3_{1,1} = 4$ for the critical edges from (4.23). To compute the remaining constants in $\mathbb{R}^3$, we need some spherical expectations:

$$\begin{aligned}\tfrac{4}{3}E^3_{1,2} &= \mathbb{E}[(V_0 + V_1 - V_2)^2] = 3\mathbb{E}[V_0^2] - 2\mathbb{E}[V_0V_1],\\ 4E^3_{2,2} &= \mathbb{E}[(V_0 + V_1 + V_2)^2] = 3\mathbb{E}[V_0^2] + 6\mathbb{E}[V_0V_1],\end{aligned}$$

in which the expectations are with respect to the uniform distribution on the circle. We get $\mathbb{E}[V_0^2] = \mathrm{Mnt}_1(2,2;2) = \frac{1}{8}$ from (1.1) and $\mathbb{E}[V_0V_1] = \mathrm{Mnt}_2(2;1,1) = \frac{1}{\pi^2}$ from (1.2); see also Table 1.1. Using again Lemma 4.3.3 to omit indicators, we furthermore have

$$\begin{aligned}2E^3_{2,3} &= \mathbb{E}[V_0 + V_1 + V_2 - V_3] = 2\mathbb{E}[V_0],\\ 8E^3_{3,3} &= \mathbb{E}[V_0 + V_1 + V_2 + V_3] = 4\mathbb{E}[V_0],\end{aligned}$$

in which the expectations are with respect to the uniform distribution on the 2-dimensional sphere. For now we skip the computation of $\frac{8}{6}E^3_{1,3} = \mathbb{E}[|V_0 + V_1 - V_2 - V_3|]$. We get $\mathbb{E}[V_0] = \mathrm{Mnt}_1(3,3;1) = \frac{\pi}{48}$ from (1.1). Multiplying the spherical expectation with the corresponding factors in (4.3), we get the corresponding entries of the middle matrix in Table 2.1:

$$\begin{aligned}C^3_{1,2} &= \mathrm{Factor}(2,3)\cdot E^3_{1,2} = 2\pi^2\cdot\tfrac{3}{4}\cdot(3\tfrac{1}{8} - 2\tfrac{1}{\pi^2}) = \tfrac{9}{16}\pi^2 - 3 = 2.55\ldots,\\ C^3_{2,2} &= \mathrm{Factor}(2,3)\cdot E^3_{2,2} = 2\pi^2\cdot\tfrac{1}{4}\cdot(3\tfrac{1}{8} + 6\tfrac{1}{\pi^2}) = \tfrac{3}{16}\pi^2 + 3 = 4.85\ldots,\\ C^3_{2,3} &= \mathrm{Factor}(3,3)\cdot E^3_{2,3} = 18\pi\cdot\tfrac{1}{2}\cdot 2\tfrac{\pi}{48} = \tfrac{3}{8}\pi^2 = 3.70\ldots,\\ C^3_{3,3} &= \mathrm{Factor}(3,3)\cdot E^3_{3,3} = 18\pi\cdot\tfrac{1}{8}\cdot 4\tfrac{\pi}{48} = \tfrac{3}{16}\pi^2 = 1.85\ldots.\end{aligned}$$

We can compute the remaining $C^3_{1,3}$ either by Euler formula or from (4.6), which gives the constant in the number of 3-simplices in the Poisson–Delaunay mosaic as $D^3_3 = \frac{24}{35}\pi^2$. This gives

$$C^3_{1,3} = \tfrac{69}{560}\pi^2 = 1.21\ldots,$$

which completes the justification of the entries of the middle matrix in Table 2.1. We use (4.9) to check the numbers of critical simplices and get $C^3_{0,0} - C^3_{1,1} + C^3_{2,2} - C^3_{3,3} = 0$, as required.

Simplices in the Poisson–Delaunay mosaic. While the expected numbers of simplices in the Poisson–Delaunay mosaic in $\mathbb{R}^3$ are known [67], it is easy to compute them from the above constants:

$$\begin{aligned}D^3_0 &= C^3_{0,0} = 1,\\ D^3_1 &= C^3_{1,1} + C^3_{1,2} + C^3_{1,3} = \tfrac{24}{35}\pi^2 + 1 = 7.76\ldots,\\ D^3_2 &= C^3_{1,2} + C^3_{2,2} + 2C^3_{1,3} + C^3_{2,3} = \tfrac{48}{35}\pi^2 = 13.53\ldots,\\ D^3_3 &= C^3_{1,3} + C^3_{2,3} + C^3_{3,3} = \tfrac{24}{35}\pi^2 = 6.76\ldots.\end{aligned}$$

This completes the entries in the second row of Table 2.2. As a final check of correctness, we compute the alternating sum, which gives $D^3_0 - D^3_1 + D^3_2 - D^3_3 = 0$, as required.

4.4.3 Four dimensions

In four dimensions, we compute most of the constants directly, but use knowledge of D_4^4 and D_3^4 to get $C_{1,4}^4$ and $C_{2,4}^4$. We have $C_{0,0}^4 = 1$ and $C_{0,m}^4 = 0$ for $m > 0$ because every vertex is critical, and $C_{1,1}^4 = 8$ by (4.23), so we proceed to the remaining constants. We will also require expressions (4.6) and (4.7) for $n = 4$:

$$D_4^4 = \tfrac{32\pi^{3/2}}{80} \tfrac{\Gamma(17/2)}{\Gamma(8)} \left[\tfrac{\Gamma(3)}{\Gamma(5/2)}\right]^4 = \tfrac{286}{9} = 31.77\ldots, \tag{4.24}$$

$$D_3^4 = \tfrac{5}{2}\tfrac{286}{9} = \tfrac{715}{9} = 79.44\ldots. \tag{4.25}$$

Triangles as upper bounds. Here we count the critical triangles and edge-triangle pairs. Starting with $C_{1,2}^4$, we have $\#\mathbf{t} = 1$ reflection, and by Lemma 4.3.3 this implies $V_{\mathbf{t}} > 0$. We therefore get

$$\begin{aligned}
\tfrac{4}{3}E_{1,2}^4 &= \mathbb{E}[(V_0 + V_1 - V_2)^3] \\
&= \mathbb{E}[V_0^3 + V_1^3 - V_2^3 + 3(V_0^2V_1 - V_0^2V_2 + V_1^2V_0 - V_1^2V_2 + V_2^2V_0 + V_2^2V_1) - 6V_0V_1V_2] \\
&= \mathbb{E}[V_0^3] + 6\mathbb{E}[V_0^2V_1] - 6\mathbb{E}[V_0V_1V_2].
\end{aligned}$$

From (1.1) and (1.2) we get $\mathbb{E}[V_0^3] = \mathrm{Mnt}_1(2,2;3) = \frac{1}{6\pi}$ and $\mathbb{E}[V_0^2V_1] = \mathrm{Mnt}_2(2;2,1) = \frac{1}{8\pi}$. Note that V_0 and V_1 are independent in two dimensions, so we also have $\mathbb{E}[V_0^2V_1] = \mathbb{E}[V_0^2]\ \mathbb{E}[V_1] = \mathrm{Mnt}_1(2,2;2)\ \mathrm{Mnt}_1(2,2;1)$, which gives the same result. For the remaining term, we need a convenient description of the three points uniformly chosen on the unit circle. Fixing u_0, we parametrize u_1 and u_2 by the angles $\alpha, \beta \in [-\pi, \pi]$ they form with u_0. In this setup, we have $V_0 = \frac{1}{2}|\sin(\alpha - \beta)|$, $V_1 = \frac{1}{2}|\sin\beta|$, $V_2 = \frac{1}{2}|\sin\alpha|$, where α and β are uniformly distributed over $[-\pi, \pi]$. We notice that this also implies that V_i and V_j are independent whenever $i \neq j$. The moment can now be computed as

$$\begin{aligned}
\mathbb{E}[V_0V_1V_2] &= \tfrac{1}{8}\ \mathbb{E}[|\sin\alpha||\sin\beta||\sin(\alpha-\beta)|] \\
&= \tfrac{1}{8}\tfrac{1}{4\pi^2} \int_{\alpha=-\pi}^{\pi} \int_{\beta=-\pi}^{\pi} |\sin\alpha||\sin\beta||\sin(\alpha-\beta)|\,\mathrm{d}\alpha\,\mathrm{d}\beta \\
&= \tfrac{1}{8\pi^2} \int_{\alpha=0}^{\pi} \int_{\beta=0}^{\pi} \sin\alpha\sin\beta|\sin(\alpha-\beta)|\,\mathrm{d}\alpha\,\mathrm{d}\beta,
\end{aligned}$$

in which the last equality is true because the expression does not change under transformations $\alpha \mapsto \alpha+\pi$ and $\beta \mapsto \beta+\pi$. Computing the integral either by splitting cases or using any mathematical software, we see that the moment evaluates to $\frac{3}{32\pi}$. Next, we proceed to the critical triangles, computing $C_{2,2}^4$. For this, we need

$$4E_{22}^4 = \mathbb{E}[(V_0 + V_1 + V_2)^3] = 3\mathbb{E}[V_0^3] + 18\mathbb{E}[V_0^2V_1] + 6\mathbb{E}[V_0V_1V_2].$$

Plugging these results into (4.3), we get

$$\begin{aligned}
C_{1,2}^4 &= \mathrm{Factor}(2,4) \cdot E_{12}^4 = \tfrac{64\pi}{3} \cdot \tfrac{3}{4} \cdot (\tfrac{1}{6\pi} + 6\tfrac{1}{8\pi} - 6\tfrac{3}{32\pi}) = \tfrac{17}{3} = 5.66\ldots, \\
C_{2,2}^4 &= \mathrm{Factor}(2,4) \cdot E_{22}^4 = \tfrac{64\pi}{3} \cdot \tfrac{1}{4} \cdot (3\tfrac{1}{6\pi} + 18\tfrac{1}{8\pi} + 6\tfrac{3}{32\pi}) = \tfrac{53}{3} = 17.66\ldots.
\end{aligned}$$

Tetrahedra as upper bounds. Here we count the critical tetrahedra, triangle-tetrahedron pairs, and edge-tetrahedron quadruplets. Starting with $C_{1,3}^4$, we need the second moment

of the volumes of cones with two visible facets. Setting $\mathbf{t} = (1, 1, -1, -1)$ and recalling that $-\mathbf{t} = (-1, -1, 1, 1)$, we get

$$\begin{aligned}
\tfrac{4}{3}E^4_{13} &= \mathbb{E}[(V_0 + V_1 - V_2 - V_3)^2 \mathbf{1}_{V_\mathbf{t} > 0}] \\
&= \tfrac{1}{2}\left(\mathbb{E}[(V_0 + V_1 - V_2 - V_3)^2 \mathbf{1}_{V_\mathbf{t} > 0}] + \mathbb{E}[(-V_0 - V_1 + V_2 + V_3)^2 \mathbf{1}_{V_{-\mathbf{t}} > 0}]\right) \\
&= \tfrac{1}{2}\left(\mathbb{E}[(V_0 + V_1 - V_2 - V_3)^2 \mathbf{1}_{V_\mathbf{t} > 0}] + \mathbb{E}[(V_0 + V_1 - V_2 - V_3)^2 \mathbf{1}_{V_\mathbf{t} < 0}]\right) \\
&= \tfrac{1}{2}\left(\mathbb{E}[(V_0 + V_1 - V_2 - V_3)^2]\right) \\
&= 2\mathbb{E}[V_0^2] - 2\mathbb{E}[V_0 V_1].
\end{aligned}$$

We get $\mathbb{E}[V_0^2] = \mathrm{Mnt}_1(3, 3; 2) = \frac{1}{162}$ from (1.1), and $\mathbb{E}[V_0 V_1] = \mathrm{Mnt}_2(3; 1, 1) = \frac{1}{216}$ from (1.2). Moving on to $C^4_{2,3}$ and to $C^4_{3,3}$, we need

$$\begin{aligned}
2E^4_{23} &= \mathbb{E}[(V_0 + V_1 + V_2 - V_3)^2] = 4\mathbb{E}[V_0^2], \\
8E^4_{33} &= \mathbb{E}[(V_0 + V_1 + V_2 + V_3)^2] = 4\mathbb{E}[V_0^2] + 12\mathbb{E}[V_0 V_1].
\end{aligned}$$

Plugging these results into (4.3), we get

$$\begin{aligned}
C^4_{1,3} &= \mathrm{Factor}(3, 4) \cdot E^4_{13} = 1536 \cdot \tfrac{3}{4} \cdot (2\tfrac{1}{162} - 2\tfrac{1}{216}) = \tfrac{32}{9} = 3.55\ldots, \\
C^4_{2,3} &= \mathrm{Factor}(3, 4) \cdot E^4_{23} = 1536 \cdot \tfrac{1}{2} \cdot 4\tfrac{1}{162} = \tfrac{512}{27} = 18.96\ldots, \\
C^4_{3,3} &= \mathrm{Factor}(3, 4) \cdot E^4_{33} = 1536 \cdot \tfrac{1}{8} \cdot (4\tfrac{1}{162} + 12\tfrac{1}{216}) = \tfrac{416}{27} = 15.40\ldots.
\end{aligned}$$

4-simplices as upper bounds. Here we count the critical 4-simplices and the intervals they form with tetrahedra, triangles, and edges as lower bounds. For $C^4_{3,4}$ and $C^4_{4,4}$, we need

$$\begin{aligned}
\tfrac{16}{5}E^4_{34} &= \mathbb{E}[V_0 + V_1 + V_2 + V_3 - V_4] = 3\mathbb{E}[V_0], \\
16E^4_{44} &= \mathbb{E}[V_0 + V_1 + V_2 + V_3 + V_4] = 5\mathbb{E}[V_0].
\end{aligned}$$

We get $\mathbb{E}[V_0] = \mathrm{Mnt}_1(4, 4; 1) = \frac{8}{81\pi^2}$ from (1.1), and using (4.3), we get

$$\begin{aligned}
C^4_{3,4} &= \mathrm{Factor}(4, 4) \cdot E^4_{34} = \tfrac{768\pi^2}{5} \cdot \tfrac{5}{16} \cdot 3\tfrac{8}{81\pi^2} = \tfrac{128}{9} = 14.22\ldots, \\
C^4_{4,4} &= \mathrm{Factor}(4, 4) \cdot E^4_{44} = \tfrac{768\pi^2}{5} \cdot \tfrac{1}{16} \cdot 5\tfrac{8}{81\pi^2} = \tfrac{128}{27} = 4.74\ldots.
\end{aligned}$$

To avoid the complications that arise from having more than one reflection, we compute $C^4_{1,4}$ and $C^4_{2,4}$ using the linear relations connecting the Delaunay simplices with the intervals. Since all constants other than the two sought after ones are known, either from the above calculations or from (4.24) and (4.25), this leads to a system of two linear equations: $3C^4_{1,4} + 2C^4_{2,4} = \frac{737}{27}$ and $C^4_{1,4} + C^4_{2,4} = \frac{346}{27}$. Solving them, we get

$$\begin{aligned}
C^4_{1,4} &= \tfrac{5}{3} = 1.66\ldots, \\
C^4_{2,4} &= \tfrac{301}{27} = 11.14\ldots.
\end{aligned}$$

We use (4.9) to check the number of critical simplices and get $C^4_{0,0} - C^4_{1,1} + C^4_{2,2} - C^4_{3,3} + C^4_{4,4} = 0$, as required.

Simplices in the Poisson–Delaunay mosaic. Finally, we count the total number of simplices in the Poisson–Delaunay mosaic. Using the linear relations that connect the Delaunay simplices with the intervals, we get

$$D_0^4 = C_{0,0}^4 = 1, \tag{4.26}$$
$$D_1^4 = C_{1,1}^4 + C_{1,2}^4 + C_{1,3}^4 + C_{1,4}^4 = \tfrac{170}{9} = 18.88\ldots, \tag{4.27}$$
$$D_2^4 = C_{1,2}^4 + C_{2,2}^4 + 2C_{1,3}^4 + C_{2,3}^4 + 3C_{1,4}^4 + C_{2,4}^4 = \tfrac{590}{9} = 65.55\ldots, \tag{4.28}$$
$$D_3^4 = C_{1,3}^4 + C_{2,3}^4 + C_{3,3}^4 + 3C_{1,4}^4 + 2C_{2,4}^4 + C_{3,4}^4 = \tfrac{715}{9} = 79.44\ldots, \tag{4.29}$$
$$D_4^4 = C_{1,4}^4 + C_{2,4}^4 + C_{3,4}^4 + C_{4,4}^4 = \tfrac{286}{9} = 31.77\ldots. \tag{4.30}$$

This completes the justification of the numbers in Tables 2.1 and 2.2. We note that we did not use the Euler Relations to derive any of the constants. We can therefore use it to check whether the computations are possibly correct. Indeed, we get $D_0^4 - D_1^4 + D_2^4 - D_3^4 + D_4^4 = 0$, as required.

4.5 Computations of constants in the weighted case

We now return to (4.4) and aim at computing the constants $E_{\ell,m}^{k,n}$. Recall that it is the expectation of the random variable

$$U_{\ell,m}^{k,n} = \mathbf{1}_{m-\ell}(\mathbf{u}')\mathrm{Vol}_m(\mathbf{u}')^{k-m+1}, \tag{4.31}$$

where $\mathbf{u}$ is a sequence of $m+1$ random points uniformly and independently distributed on the unit sphere in $\mathbb{R}^{m+n-k}$, and $\mathbf{u}'$ is the corresponding sequence of points projected to $\mathbb{R}^m \hookrightarrow \mathbb{R}^{m+n-k}$. Instead of working with the original points, we prefer to study their projections to $\mathbb{R}^m$, whose distribution was determined in Section 2.1. In this section we find explicit expressions for $C_{0,0}^{k,n}$, $C_{0,1}^{k,n}$, $C_{1,1}^{k,n}$, $C_{0,2}^{2,n}$, $C_{1,2}^{2,n}$ and $C_{2,2}^{2,n}$. Since the interval structure is very reach, we were not able to go beyond $k=2$ in computing $D_j^{k,n}$.

4.5.1 Number of intervals

Critical vertices. For $m=0$, we count intervals of type $(0,0)$ or, equivalently, critical vertices. Since $E_{0,0}^{k,n} = U_{0,0}^{k,n} = 1$, for all $k \le n$, we get from (4.4)

$$C_{0,0}^{k,n} = \sigma_{n-k}\frac{\Gamma\left(1-\frac{k}{n}\right)}{n\nu_n^{1-k/n}}. \tag{4.32}$$

Vertex-edge pairs. Next we count the intervals of type $(0,1)$ or, equivalently, the regular vertex-edge pairs. For this, we need the expectation of $U_{0,1}^{k,n}$: picking two random points on the unit sphere in $\mathbb{R}^{n-k+1}$ and projecting them to $\mathbb{R}^1 \hookrightarrow \mathbb{R}^{n-k+1}$, this is the expectation when we get the k-th power of the distance between the projected points, if they lie on the same side of the origin, and we get 0, otherwise. Writing $\mathbf{u}_0', \mathbf{u}_1' \in [-1,1]$ for the projected points and $x = |\mathbf{u}_0'|$, $y = |\mathbf{u}_1'|$ for their absolute values, we note that the signs and magnitudes are independent. It follows that we get zero with probability $\frac{1}{2}$, so the desired expectation is

$$\mathbb{E}[U_{0,1}^{k,n}] = \tfrac{1}{2}\mathbb{E}[|x-y|^k] = \mathbb{E}[(x-y)^k \mathbf{1}_{x>y}]. \tag{4.33}$$

We can therefore restrict our attention to the half of the unit sphere that projects to $[0,1]$. To integrate over this hemisphere, we use that x^2 and y^2 are by Lemma 2.1.2 independent Beta-distributed random variables. Setting $a = x^2$ and $b = y^2$, we have

$$\mathbb{E}[U_{0,1}^{k,n}] = \frac{1}{B\left(\frac{n-k}{2}, \frac{1}{2}\right)^2} \int_{a=0}^{1} \int_{b=0}^{a} [\sqrt{a} - \sqrt{b}]^k a^{-\frac{1}{2}} (1-a)^{\frac{n-k-2}{2}} b^{-\frac{1}{2}} (1-b)^{\frac{n-k-2}{2}} \,\mathrm{d}a \,\mathrm{d}b \tag{4.34}$$

$$= \frac{4}{B\left(\frac{n-k}{2}, \frac{1}{2}\right)^2} \int_{x=0}^{1} \int_{y=0}^{x} [x-y]^k (1-x^2)^{\frac{n-k-2}{2}} (1-y^2)^{\frac{n-k-2}{2}} \,\mathrm{d}x \,\mathrm{d}y \tag{4.35}$$

$$= \frac{\Gamma(k+1)\Gamma\left(\frac{n-k+1}{2}\right)^2}{2^k \sqrt{\pi} \Gamma\left(\frac{n-k}{2}\right)} \cdot {}_3\tilde{F}_2\left(\tfrac{1}{2}, 1, \tfrac{k-n+2}{2}; \tfrac{k+3}{2}, \tfrac{n+2}{2}; 1\right), \tag{4.36}$$

in which ${}_3\tilde{F}_2$ is the regularized hypergeometric function defined in Section 2.1 and we use the Mathematica software to get from (4.35) to (4.36). As mentioned at the end of this appendix, $\frac{k+3}{2} + \frac{n+2}{2} > \frac{1}{2} + 1 + \frac{k-n+2}{2}$ is a sufficient condition for the convergence of the infinite sum that defines the value of the regularized hypergeometric function. This is equivalent to $n > 0$, which is always satisfied. Plugging (4.36) into (4.4), we get an expression for the corresponding constant:

$$C_{0,1}^{k,n} = \frac{\sigma_{n-k+1}^2 \sigma_k \Gamma\left(2 - \frac{k}{n}\right)}{4n\nu_n^{2-k/n}} \frac{\Gamma(k+1)\Gamma\left(\frac{n-k+1}{2}\right)^2}{2^k \sqrt{\pi} \Gamma\left(\frac{n-k}{2}\right)} \cdot {}_3\tilde{F}_2\left(\tfrac{1}{2}, 1, \tfrac{k-n+2}{2}; \tfrac{k+3}{2}, \tfrac{n+2}{2}; 1\right). \tag{4.37}$$

Critical edges. Next we count the intervals of type $(1,1)$ or, equivalently, the critical edges. Here the expectation of $U_{1,1}^{k,n}$ is relevant: picking two points on the unit sphere in $\mathbb{R}^{n-k+1}$ and projecting them to $\mathbb{R}^1 \hookrightarrow \mathbb{R}^{n-k+1}$, this is the expectation in which we get the k-th power of the distance between the projected points, if they lie on opposite sides of the origin, and we get 0, otherwise. Using again that the signs and magnitude of the projected points are independent, we note that this expectation is $\mathbb{E}[U_{1,1}^{k,n}] = \frac{1}{2}\mathbb{E}[(x+y)^k]$. Setting $a = x^2$, $b = y^2$, and integrating as before, we get

$$\mathbb{E}[U_{1,1}^{k,n}] = \frac{1}{B\left(\frac{n-k}{2}, \frac{1}{2}\right)^2} \int_{a=0}^{1} \int_{b=0}^{1} \left[\sqrt{a} + \sqrt{b}\right]^k a^{-\frac{1}{2}} (1-a)^{\frac{n-k-2}{2}} b^{-\frac{1}{2}} (1-b)^{\frac{n-k-2}{2}} \,\mathrm{d}a \,\mathrm{d}b \tag{4.38}$$

$$= \frac{1}{B\left(\frac{n-k}{2}, \frac{1}{2}\right)^2} \int_{a=0}^{1} \int_{b=0}^{1} \sum_{i=0}^{k} \binom{k}{i} a^{\frac{i-1}{2}} b^{\frac{k-i-1}{2}} (1-a)^{\frac{n-k-2}{2}} (1-b)^{\frac{n-k-2}{2}} \,\mathrm{d}a \,\mathrm{d}b \tag{4.39}$$

$$= \frac{1}{B\left(\frac{n-k}{2}, \frac{1}{2}\right)^2} \sum_{i=0}^{k} \binom{k}{i} B\left(\tfrac{n-k}{2}, \tfrac{i+1}{2}\right) B\left(\tfrac{n-k}{2}, \tfrac{k-i+1}{2}\right). \tag{4.40}$$

Plugging (4.40) into (4.4), we get the expression for the corresponding constant:

$$C_{1,1}^{k,n} = \frac{\sigma_{n-k+1}^2 \sigma_k \Gamma\left(2 - \frac{k}{n}\right)}{8n\nu_n^{2-k/n} B\left(\frac{n-k}{2}, \frac{1}{2}\right)^2} \sum_{i=0}^{k} \binom{k}{i} B\left(\tfrac{n-k}{2}, \tfrac{i+1}{2}\right) B\left(\tfrac{n-k}{2}, \tfrac{k-i+1}{2}\right). \tag{4.41}$$

4.5.2 Constants in low dimensions

Projection to a line. We now investigate the constants for $k = 1$. From (4.32), (4.37), (4.41) we get

$$C_{0,0}^{1,n} = C_{1,1}^{1,n} = \frac{\sigma_{n-1}\Gamma\left(1-\frac{1}{n}\right)}{n\nu_n^{1-1/n}}, \tag{4.42}$$

$$C_{0,1}^{1,n} = \frac{\sigma_{n-1}^2\sqrt{\pi}\Gamma\left(2-\frac{1}{n}\right)}{n(n-1)\nu_n^{2-1/n}}\left[\frac{2\Gamma(n-1)}{\Gamma\left(n-\frac{1}{2}\right)} - \frac{\Gamma\left(\frac{n-1}{2}\right)}{\Gamma\left(\frac{n}{2}\right)}\right]. \tag{4.43}$$

Equation (4.16) provides values

$$D_0^{1,n} = C_{0,0}^{1,n} + C_{0,1}^{1,n} \tag{4.44}$$

$$D_1^{1,n} = C_{1,1}^{1,n} + C_{0,1}^{1,n}. \tag{4.45}$$

Of course, these two values are the same. Note however, that when we introduce the radius threshold, the numbers of vertices and edges diverge; see Theorem 13. Some values are computed in Table 2.3. This case can actually be analyzed purely geometrically; see [30].

Projection to a plane. In $k = 2$ dimensions, the formulas provide sufficient information to compute all constants governing the expectations of the six types of intervals. We get three constants from (4.32), (4.37), (4.41):

$$C_{0,0}^{2,n} = \frac{\sigma_{n-2}\Gamma\left(1-\frac{2}{n}\right)}{n\nu_n^{1-2/n}}, \tag{4.46}$$

$$C_{0,1}^{2,n} = \frac{\sigma_{n-1}^2\sqrt{\pi}\Gamma\left(2-\frac{2}{n}\right)}{4n\nu_n^{2-2/n}}\frac{\Gamma\left(\frac{n-1}{2}\right)^2}{\Gamma\left(\frac{n-2}{2}\right)} \cdot {}_3\tilde{F}_2\left(\tfrac{1}{2}, 1, \tfrac{4-n}{2}; \tfrac{5}{2}, \tfrac{n+2}{2}; 1\right), \tag{4.47}$$

$$C_{1,1}^{2,n} = \frac{\sigma_{n-1}^2\Gamma\left(2-\frac{2}{n}\right)\pi}{2n\nu_n^{2-2/n}} \cdot \left[\frac{1}{n-1} + \frac{\Gamma\left(\frac{n-1}{2}\right)^2}{\pi\Gamma\left(\frac{n}{2}\right)^2}\right]. \tag{4.48}$$

The critical simplices satisfy the Morse relation (4.15): $C_{0,0}^{2,n} - C_{1,1}^{2,n} + C_{2,2}^{2,n} = 0$, which gives us the constant for the critical triangles. Relation (4.13) and (4.16) give further: $C_{0,2}^{2,n} + C_{1,2}^{2,n} + C_{2,2}^{2,n} = 2(C_{0,0}^{2,n} + C_{0,1}^{2,n} + C_{0,2}^{2,n})$. Finally, we get a relation for the number of weighted Delaunay triangles from (4.12), which we restate for $k = 2$:

$$D_2^{2,n} = \frac{2\sigma_{n+1}}{3n\sigma_{n-1}}\frac{\Gamma\left(\frac{3n-1}{2}\right)}{\Gamma\left(\frac{3n-2}{2}\right)}\frac{\Gamma\left(\frac{n+2}{2}\right)^{3-\frac{2}{n}}}{\Gamma\left(\frac{n+1}{2}\right)^2}\frac{\Gamma\left(3-\frac{2}{n}\right)}{\Gamma\left(\frac{n-1}{2}\right)}. \tag{4.49}$$

Combining $C_{0,2}^{2,n} + C_{1,2}^{2,n} + C_{2,2}^{2,n} = D_2^{2,n}$ with the two linear relations mentioned above, we get

$$C_{0,2}^{2,n} = -C_{0,0}^{2,n} - C_{0,1}^{2,n} + \tfrac{1}{2}D_2^{2,n}, \tag{4.50}$$

$$C_{1,2}^{2,n} = C_{0,0}^{2,n} + C_{0,1}^{2,n} - C_{2,2}^{2,n} + \tfrac{1}{2}D_2^{2,n}, \tag{4.51}$$

$$C_{2,2}^{2,n} = -C_{0,0}^{2,n} + C_{1,1}^{2,n}. \tag{4.52}$$

Explicit expressions are complicated, so we give numerical approximations in Table 2.4.

5. Poisson–Delaunay, Poisson–Čech and weighted Poisson–Delaunay complexes

In this chapter we prove three theorems stated in Chapter 2, namely Theorem 9, Theorem 11 and Theorem 13 Note that Theorem 9 is a special case $k = n$ of Theorem 13, so we start with proving the latter.

5.1 Expected size of the weighted Delaunay complex

Recall that to count the type (ℓ, m) intervals, we focus our attention by restricting the center of the Delaunay sphere to a region $\Omega \subseteq \mathbb{R}^k$ and the radius to be less than or equal r_0. By Lemma 1.5.4, any sequence $\mathbf{x} = (\mathbf{x}_0, \mathbf{x}_1, \ldots, \mathbf{x}_m)$ of $m+1$ points in $X \subseteq \mathbb{R}^n$ defines such an interval if it satisfies the following conditions:

1. the smallest anchored sphere passing through $\mathbf{x}$ is empty, and we write $\mathbb{P}_\emptyset(\mathbf{x})$ for the probability of this event;
2. the center z of this sphere lies in Ω, and we write $\mathbf{1}_\Omega(\mathbf{x})$ for the indicator;
3. the radius r of this sphere is bounded from above by r_0, and we write $\mathbf{1}_{r_0}(\mathbf{x})$ for the indicator;
3. exactly $m - \ell$ facets of the projection $\mathbf{x}'$ of the m-simplex $\mathbf{x}$ are visible from z, and we write $\mathbf{1}_{m-\ell}(\mathbf{x}')$ for the indicator.

Combining these conditions with the Slivnyak–Mecke formula (Lemma 1.6.1), we get an integral expression for the expected number of type (ℓ, m) intervals, which we partially evaluate using Theorem 20 and Lemma 2.1.1:

$$\mathbb{E}[c^{k,n}_{\ell,m}(r_0)] = \tfrac{1}{(m+1)!} \int\limits_{\mathbf{x}\in(\mathbb{R}^n)^{m+1}} \mathbb{P}_\emptyset(\mathbf{x})\mathbf{1}_\Omega(\mathbf{x})\mathbf{1}_{r_0}(\mathbf{x})\mathbf{1}_{m-\ell}(\mathbf{x}')\,\mathrm{d}\mathbf{x} \tag{5.1}$$

$$= \|\Omega\|\|\mathcal{L}^k_m\|\rho^{m+1}\tfrac{m!^{k-m+1}}{(m+1)!} \int\limits_{r\le r_0} e^{-\rho\nu_n r^n} r^\alpha\,\mathrm{d}r \int\limits_{\mathbf{u}\in(S)^{m+1}} \mathbf{1}_{m-\ell}(\mathbf{u}')\mathrm{Vol}_m(\mathbf{u}')^{k-m+1}\,\mathrm{d}\mathbf{u} \tag{5.2}$$

$$= \|\Omega\|\rho^{\frac{k}{n}}\tfrac{m!^{k-m}}{m+1}\|\mathcal{L}^k_m\|\tfrac{\gamma\left(m+1-\frac{k}{n};\rho\nu_n r_0^n\right)}{n\nu_n^{m+1-\frac{k}{n}}} \int\limits_{\mathbf{u}\in(S)^{m+1}} \mathbf{1}_{m-\ell}(\mathbf{u}')\mathrm{Vol}_m(\mathbf{u}')^{k-m+1}\,\mathrm{d}\mathbf{u} \tag{5.3}$$

$$= C_{\ell,m}^{k,n} \cdot \frac{\gamma\left(m+1-\frac{k}{n}; \rho\nu_n r_0^n\right)}{\Gamma\left(m+1-\frac{k}{n}\right)} \cdot \|\Omega\| \rho^{\frac{k}{n}}. \tag{5.4}$$

Specifically, we get (5.2) by noting $\mathbb{P}_\emptyset(\mathbf{x}) = e^{-\rho\nu_n r^n}$, applying Theorem 20 to the right-hand side of (5.1), collapsing the indicators, using rotational invariance, and writing S for the unit sphere in $\mathbb{R}^{m+n-k}$. We get (5.3) from (5.2) by applying Lemma 2.1.1 with $j = \alpha + 1 = n(m+1) - k$, $c = \rho\nu_n$, $p = n$, $t_0 = r_0$, which asserts that the integral over the radius evaluates to the fraction involving the incomplete Gamma function. We get (5.4) by defining the constant

$$C_{\ell,m}^{k,n} = \frac{m!^{k-m} \|\mathcal{L}_m^k\| \Gamma\left(m+1-\frac{k}{n}\right)}{(m+1) n \nu_n^{m+1-\frac{k}{n}}} \int\limits_{\mathbf{u} \in (S)^{m+1}} \mathbf{1}_{m-\ell}(\mathbf{u}') \mathrm{Vol}_m(\mathbf{u}')^{k-m+1} \, \mathrm{d}\mathbf{u}. \tag{5.5}$$

We finish noticing that the last integral is by definition in (4.2) equal to $\sigma_{m+n-k}^{m+1} E_{\ell,m}^{k,n}$, justifying that (4.4) and (5.5) indeed define the same constant.

5.2 Expected size of the Poisson–Čech complex

Recall the characterization of intervals of Čech complex in Lemma 1.5.3. It stated that any sequence $\mathbf{x} = (\mathbf{x}_0, \mathbf{x}_1, \ldots, \mathbf{x}_m)$ of $m+1$ points in $X \subseteq \mathbb{R}^n$ defines such an interval if it satisfies the following conditions:

1. the ball, bounded by the smallest $(n-1)$-sphere passing through $\mathbf{x}$, has exactly $m-\ell$ points of X in its interior, and we write $\mathbb{P}_{m-\ell}[\mathbf{x}]$ for the probability of this event;
2. the center z of this sphere lies in Ω, and we write $\mathbf{1}_\Omega(\mathbf{x})$ for the indicator;
3. the radius r of this sphere is bounded from above by r_0, and we write $\mathbf{1}_{r_0}(\mathbf{x})$ for the indicator;
3. no facets of $\mathbf{x}$ are visible, and we write $\mathbf{1}_0(\mathbf{x}')$ for the indicator.

Similarly to (5.1) we thus get for the number of Čech (ℓ, m)-intervals with the smallest enclosing ball having center in Ω and radius not greater than r_0:

$$\mathbb{E}[\check{c}_{\ell,m}^n(r_0)] = \tfrac{1}{(\ell+1)!} \rho^{\ell+1} \int\limits_{\mathbf{x} \in (\mathbb{R}^n)^{\ell+1}} \mathbb{P}_{m-\ell}[\mathbf{x}] \; \mathbf{1}_0(\mathbf{x}) \; \mathbf{1}_\Omega(\mathbf{x}) \; \mathbf{1}_{r_0}(\mathbf{x}) \, \mathrm{d}\mathbf{x},$$

where $\mathbb{P}_{m-\ell}[\mathbf{x}] = \frac{(\rho\nu_n r^n)^{m-\ell}}{(m-\ell)!} e^{-\rho\nu_n r^n}$ is the probability that there are exactly $m-\ell$ points inside the ball. The complete analysis (5.1)-(5.4) carries over and, recalling that $C_{\ell,m}^n = C_{\ell,m}^{m,n}$, we obtain for the expected number of (ℓ, m)-intervals

$$\mathbb{E}[\check{c}_{\ell,m}^n(r_0)] = C_{\ell,\ell}^n \tfrac{\gamma\left(m; \rho\nu_n r_0^n\right)}{(m-\ell)!\Gamma(\ell)} \rho \|\Omega\|.$$

Note that we express the number of Čech intervals in terms of the number of Delaunay (or Čech) *critical* simplices. This is so, because by Lemma 1.5.3 the geometric characterization of Čech intervals is similar to the critical Delaunay simplices. Using notation similar to the

notation used in the Delaunay case, we write for the expected density of (ℓ, m)-intervals of $\check{C}(X, \infty)$:

$$\check{C}^n_{\ell m} = C^n_{\ell,\ell} \frac{\Gamma(m)}{\Gamma(\ell)(m-\ell)!} = C^n_{\ell,\ell} \binom{m-1}{\ell-1},$$
$$\mathbb{E}[\check{c}^n_{\ell,m}(r_0)] = \check{C}^n_{\ell m} \frac{\gamma(m;\, \rho\nu_n r_0^n)}{\Gamma(m)} = C^n_{\ell,\ell} \binom{m-1}{\ell-1} \frac{\gamma(m;\, \rho\nu_n r_0^n)}{\Gamma(m)}.$$

For $\ell > n$ we have $\check{C}^n_{\ell m} = 0$.

Čech simplices. If we use Lemma 1.5.1, we get the expected total number of j-simplices in $\check{\mathrm{C}}\mathrm{ech}_{r_0} X$ restricted to Ω as

$$\sum_{\ell=0}^{\min\{j,n\}} \sum_{m=j}^{\infty} \binom{m-\ell}{j-\ell} \check{c}^n_{\ell,m}(r_0) = \sum_{\ell=0}^{\min\{j,n\}} C^n_{\ell,\ell} \sum_{m=j}^{\infty} \binom{m-\ell}{j-\ell} \binom{m-1}{\ell-1} \frac{\gamma(m, \rho\nu_n r_0^n)}{\Gamma(m)}$$

We want to show that this sum converges for $r_0 < \infty$ to justify that we can change the order of summation and take expectations. It can be either obtained by an asymptotic analysis or by the following argument, which claims that the sum should indeed be finite. The expected number of Čech j-simplices, whose smallest enclosing ball has radius not greater than r_0 and intersects the boundary of Ω is not more than the number of $(j+1)$-ples of points, that are located inside a ball of radius r_0 in the r_0-neighborhood of $\partial\Omega$. In general, the expected number of $(j+1)$-ples of points, whose smallest enclosing ball intersect any Borel region $\mathbb{H}$ is not more than

$$\tfrac{1}{(j+1)!} \int_{x_0 \in \mathbb{H}_{r_0}} \int_{x_1,\dots,x_j \in B(x_0, 2r_0)} 1\, \rho^{j+1}\, \mathrm{d}x_0 \dots\, \mathrm{d}x_j \le C \tfrac{1}{(j+1)!} r_0^{n\cdot j} \rho^{j+1} \|\mathbb{H}_{r_0}\|,$$

where $\mathbb{H}_{r_0}$ is the r_0-neighborhood of $\mathbb{H}$. Setting $\mathbb{H} = \partial\Omega$, we get that the number of j-simplices intersecting it is $\frac{1}{(j+1)!}(\rho r_0^n)^{(j+1)} o(\|\Omega\|)$. Hence for a fixed j the answer does not depend on the way we restrict the complex to Ω up to $o(\|\Omega\|)$, and since this little-oh is uniform over j, it happens for all j simultaneously; compare with Section 5.3.

As opposed to the Delaunay case, the convergence is not uniform over the radius, so the argument does not work for $r_0 = \infty$.

5.3 Boundary effect on Poisson–Delaunay mosaics

Recall that K_0 is the nerve of the Voronoi diagram restricted to Ω, and $K_1 \subseteq K_0$ contains all Delaunay simplices whose Delaunay spheres have the center inside Ω. In this section, we show that the difference between K_0 and K_1 is small when Ω is a ball. For simplicity we work with the unweighted Poisson–Delaunay complex here, but similar statements can be achieved for other complexes as well.

Big spheres. We need an auxiliary lemma implying that only a vanishing fraction of the n-simplices in the Poisson–Delaunay mosaic have Delaunay spheres with radii larger than some positive threshold. Note that for n-simplices the Delaunay sphere is the unique circumscribed sphere. To simplify the discussion, we call the closed ball bounded by the Delaunay sphere of an n-simplex its *Delaunay ball*. Letting $\mathbb{H} \subseteq \mathbb{R}^n$ be bounded and $r_0 > 0$, we write $\#(\mathbb{H}, r_0)$ for the number of n-simplices in the Poisson–Delaunay mosaic whose Delaunay spheres have center in $\mathbb{H}$ and radius larger than r_0.

Lemma 5.3.1 (Big spheres). *There exist positive constants c, α, β, all depending only on n, such that for any bounded Borel set $\mathbb{H} \subseteq \mathbb{R}^n$ and any fixed $r_0 > 0$, $\mathbb{E}[\#(\mathbb{H}, r_0)] \leq c\|\mathbb{H}\|e^{-\alpha\rho r_0^\beta}$.*

Proof. Arguing as in Section 5.1, with the only difference that z is now integrated over $\mathbb{H}$ and r from r_0 to infinity and the sphere is not anchored, we can write

$$\mathbb{E}[\#(\mathbb{H}, r_0)] = c_0\|\mathbb{H}\| \int_{r=r_0}^{\infty} e^{-\rho r^n \nu_n} r^{n^2-1}\,\mathrm{d}r = c_0'\|\mathbb{H}\|\Gamma(n, \rho r_0^n \nu_n),$$

in which c_0 and c_0' are constants that depends only on n, and $\Gamma(n,x) = \Gamma(n) - \gamma(n,x)$ is the upper incomplete Gamma function. Noticing that $\Gamma(n, \rho r_0^n \nu_n) = o\big(e^{-0.9\rho r_0^n \nu_n}\big)$, see for example [61], completes the proof. □

Size of boundary. We are now ready to give an upper bound on the number of simplices in K_0 that are not in K_1, which we need for bound on the Euler characteristic of K_1; see the definition of K_1 on page 15. Every simplex $Q \in K_0 \setminus K_1$ corresponds to an intersection of Voronoi domains, $\mathrm{Vor}(Q)$, that has points inside as well as outside Ω. Let $x \in \mathrm{Vor}(Q) \cap \Omega$ and $y \in \mathrm{Vor}(Q) \setminus \Omega$. We argue that both points are contained in the union of Delaunay balls of the n-simplices that share Q. Indeed, all these Delaunay balls contain all points of Q, and for each $q \in Q$ there is a vertex of $\mathrm{Vor}(Q)$ that is closer to x than to q, so the Delaunay ball centered at this vertex contains x. The same argument applies to y. Since the union contains points on both sides of $\partial\Omega$, at least one of these Delaunay balls has a non-empty intersection with $\partial\Omega$.

Writing $\#(\partial\Omega)$ for the number of n-simplices whose Delaunay balls have a non-empty intersection with $\partial\Omega$, we prove that it grows slower than the number of n-simplices whose Delaunay balls are centered inside Ω. The discussion above implies that the difference between two complexes is $|K_0 \setminus K_1| < 2^{n+1}\#(\partial\Omega)$, so to get $|K_0 \setminus K_1| = o(\rho\|\Omega\|)$, it is enough to prove the following.

Lemma 5.3.2 (Boundary size). *Let X be a Poisson point process with density ρ in $\mathbb{R}^n$. Let $\Omega = \mathbb{B}(R)$ be a ball of radius R centered at the origin. Then $\mathbb{E}[\#(\partial\Omega)] = o(1)\rho\|\Omega\|$ as $R \to \infty$.*

Proof. Without loss of generality assume $\rho = 1$. Fix $0 < \delta < 1$. It suffices to count the n-simplices with Delaunay centers outside Ω and to prove that the number of such n-simplices whose Delaunay balls intersect $\partial\Omega$ is $O(R^{n-1+\delta})$. Assume $R > 1$ and let $\mathbb{A}$ be the set of points at distance at most R^δ from $\partial\Omega$. For a ball with center z outside Ω to intersect Ω, one of the following must happen:

1. $z \in \mathbb{A}$;
2. $z \in \mathbb{B}(2R) \setminus \mathbb{A}$ and its radius exceeds R^δ;
3. $z \notin \mathbb{B}(2R)$ and its radius exceeds R.

As proved in [67] and reproved in Section 5.1, the expected number of n-simplices in $\mathrm{Del}X$ with Delaunay center in $\mathbb{A}$ is $O(\|\mathbb{A}\|) = O(R^{n-1+\delta})$. This settles Case 1. Applying Lemma 5.3.1, we see that the expected number of n-simplices with Delaunay center in $\mathbb{B}(2R)$ and Delaunay radius larger than R^δ is $O(R^n e^{-\alpha R^{\delta\beta}})$, in which α and β are positive constants. This settles Case 2. Finally, we decompose the complement of $\mathbb{B}(2R)$ into annuli of the form

$\mathbb{H}_i = \mathbb{B}(iR + 2R) \setminus \mathbb{B}(iR + R)$, for $i \geq 1$. To intersect $\Omega = \mathbb{B}(R)$, a ball centered inside $\mathbb{H}_i$ must have radius exceeding iR. Writing $\mathbb{H} = \bigcup_{i=1}^{\infty} \mathbb{H}_i$ for the union of annuli and $\#(\mathbb{H}, \Omega)$ for the number of n-simplices with Delaunay center in $\mathbb{H}$ whose Delaunay ball intersects Ω, we get an upper bound on the expected number:

$$\begin{aligned}
\mathbb{E}[\#(\mathbb{H}, \Omega)] &\leq \sum_{i=1}^{\infty} \mathbb{E}[\#(\mathbb{H}_i, iR)] \\
&\leq \sum_{i=1}^{\infty} c\|\mathbb{H}_i\| e^{-\alpha(iR)^\beta} \qquad (5.6) \\
&\leq c' R^n e^{-\alpha R^\beta} \sum_{i=0}^{\infty} i^n e^{-\alpha i^\beta}, \qquad (5.7)
\end{aligned}$$

where we use Lemma 5.3.1 to get (5.6), and $\|\mathbb{H}_i\| = O(i^n R^n)$ as well as $\alpha(iR)^\beta \geq \alpha i^\beta$ to get (5.7). Since the last sum converges, we get $\mathbb{E}[\#(\mathbb{H}, \Omega)] = O(R^n e^{-\alpha R^\beta})$, which settles Case 3. □

REMARKS. (1) Besides $|K_0 \setminus K_1| = o(1)\rho\|\Omega\|$, Lemma 5.3.2 implies that the number of vertices of K_0 outside Ω is $o(1)\rho\|\Omega\|$.

(2) Actually, we have proved that for any $\varepsilon > 0$, $\mathbb{E}[\#(\partial\Omega)] = o(1)\rho\|\partial\Omega\|^{1+\varepsilon}$. Also, one can apply the Markov's inequality to show that the convergence happens in probability.

6. Poisson–Delaunay complexes of higher order

In this chapter we spend most of the time characterizing faces of order-k Delaunay and Voronoi mosaics and developing the discrete Morse theory, which can be applied to count them. Theorems 16 and 15 will be proved in the first and the last sections correspondingly.

6.1 Faces of higher order Voronoi diagrams and skeleta volumes

Recall that the order-k Voronoi diagram of $X \subseteq \mathbb{R}^n$ is defined as the collection of order-k Voronoi domains, which are identified by the closest k points of X. In the order-1 case, we could thus say that a point $p \in \mathbb{R}^n$ belongs to the Voronoi domain of a point $x \in X$ if the unique open ball bounded by the sphere centered at p and passing through x does not contain any points of X. It gives an alternative description for Delaunay simplices as simplices having an empty circumscribed sphere. We want to generalize this description for the order-k case. We start with the order-k Voronoi polyhedra, which will be transformed into equivalent characterization of the order-k Delaunay cells in the next section. Also, Theorem 16 will follow from these considerations.

Delaunay spheres. Let $X \subseteq \mathbb{R}^n$ be locally finite. For a point $p \in \mathbb{R}^n$ and a positive integer k, the *order-k Delaunay sphere* of p, denoted $\Sigma_k(p)$, is the smallest sphere centered at $p \in \mathbb{R}^n$ such that the number of points of X that lie inside or on the sphere is at least k. It will be convenient to have short notation for the points strictly inside and on the sphere, as well as their numbers. Observing that $\operatorname{conv}\Sigma_k(p)$ is the closed ball with boundary $\Sigma_k(p)$, we define

$$\operatorname{In}(p) = X \cap \operatorname{int}\operatorname{conv}\Sigma_k(p) \text{ and } \operatorname{in}(p) = |\operatorname{In}(p)|, \tag{6.1}$$
$$\operatorname{On}(p) = X \cap \Sigma_k(p) \text{ and } \operatorname{on}(p) = |\operatorname{On}(p)|. \tag{6.2}$$

By definition, $\operatorname{in}(p) + \operatorname{on}(p) \geq k$, and by minimality of the radius, $\operatorname{on}(p) \geq 1$ and $\operatorname{in}(p) \leq k-1$. The $\operatorname{in}(p)$ points in $\operatorname{In}(p)$ are the unique $\operatorname{in}(p)$ nearest points to p, the $\operatorname{on}(p)$ points in $\operatorname{On}(p)$ are all at the same distance from p, while all other points of X are further. This gives a following characterization of the order-k Voronoi domains:

Lemma 6.1.1 (Incident Voronoi domains)**.** *Let $X \subseteq \mathbb{R}^n$ be locally finite and in general position, and let $Q \subseteq X$ with $|Q| = k$. A point $p \in \mathbb{R}^n$ belongs to $\operatorname{dom}_k(Q)$ iff $\operatorname{In}(p) \subseteq Q \subseteq \operatorname{In}(p) \cup \operatorname{On}(p)$.*

Equivalence relation. We want to strengthen the previous lemma by including polyhedra other than the Voronoi domains. Recall that the interiors of the order-k Voronoi polyhedra partition $\mathbb{R}^n$. To reconstruct this partition, we say that $p, q \in \mathbb{R}^n$ are *equivalent* if their order-k Delaunay spheres identify the same subsets of X. More formally, we distinguish between the cases in which there are k or more than k points inside or on the Delaunay sphere:

$$p \sim_X q \text{ if } \begin{cases} \mathrm{In}(p) \cup \mathrm{On}(p) = \mathrm{In}(q) \cup \mathrm{On}(q) & \text{for } \mathrm{in}(p) + \mathrm{on}(p) = \mathrm{in}(q) + \mathrm{on}(q) = k, \\ \mathrm{In}(p) = \mathrm{In}(q), \mathrm{On}(p) = \mathrm{On}(q) & \text{for } \mathrm{in}(p) + \mathrm{on}(p) = \mathrm{in}(q) + \mathrm{on}(q) > k. \end{cases}$$

We claim that the equivalence classes of $\sim_X$ are precisely the (relative) interiors of the order-k Voronoi polyhedra.

Lemma 6.1.2 (Interiors of order-k Voronoi polyhedra)**.** *Let $X \subseteq \mathbb{R}^n$ be locally finite and in general position. Then $p, q \in \operatorname{int} F$, for a common face F of $\mathrm{Vor}^{(k)}(X)$, iff $p \sim_X q$.*

Proof. We first show that $p \sim_X q$ implies that the two points belong to the interior of a common order-k Voronoi polyhedron. In the first case, when $\mathrm{in}(p) + \mathrm{on}(p) = \mathrm{in}(q) + \mathrm{on}(q) = k$, this is clear because $Q = \mathrm{In}(p) \cup \mathrm{On}(p) = \mathrm{In}(q) \cup \mathrm{On}(q)$ is the unique set of k nearest points in X, so $p, q \in \operatorname{int} \mathrm{dom}_k(Q)$, which is an order-$k$ Voronoi n-polyhedron. In the second case, when $\mathrm{in}(p) + \mathrm{on}(p) = \mathrm{in}(q) + \mathrm{on}(q) > k$, we let $i = \mathrm{in}(p) = \mathrm{in}(q)$ and note that $i < k$. The points in $\mathrm{In}(p) = \mathrm{In}(q)$ are the unique i nearest points, and we can add any $k - i$ points from $\mathrm{On}(p) = \mathrm{On}(q)$ to get a complete set of k nearest points. There are $\binom{\mathrm{on}(p)}{k-i} = \binom{\mathrm{on}(q)}{k-i}$ such choices, and by Lemma 6.1.1 each gives an order-k Voronoi domain, that together exhaust the domains that contain p or q on their boundaries. The set of points at equal distance from $\mathrm{on}(p) = \mathrm{on}(q)$ points of X is a plane of dimension $n + 1 - \mathrm{on}(p) = n + 1 - \mathrm{on}(q)$, which implies that this is also the dimension of the order-k Voronoi polyhedron whose interior contains p and q.

We second show that $p \nsim_X q$ implies that p and q belong to the interiors of different order-k Voronoi polyhedra. Assume the contrary. We note that the dimension of the order-k Voronoi polyhedron whose interior contains p is n, if $\mathrm{in}(p)+\mathrm{on}(p) = k$, and $n+1-\mathrm{on}(p)$, if $\mathrm{in}(p) + \mathrm{on}(p) > k$, and similar for q. In the first case, we would thus need $\mathrm{in}(q) + \mathrm{on}(q) = k$ to match the dimensions of the domains, but then $\mathrm{In}(p) \cup \mathrm{On}(p) \neq \mathrm{In}(q) \cup \mathrm{On}(q)$, so p and q belong to different domains. In the second case, we would need $\mathrm{on}(q) = \mathrm{on}(p)$ to have the same dimension of the polyhedra. Hence, $\mathrm{In}(p) \neq \mathrm{In}(q)$ or $\mathrm{In}(p) = \mathrm{In}(q)$ and $\mathrm{On}(p) \neq \mathrm{On}(q)$. In either case, we get a different collection of order-k Voronoi domains for p than for q. □

Proof of Theorem 16. Recall that the proof of Lemma 6.1.2 determines the dimension of the order-k Voronoi polyhedron whose interior contains a point $p \in \mathbb{R}^n$ as n, if $\mathrm{in}(p) + \mathrm{on}(p) = k$, and as $n + 1 - \mathrm{on}(p)$, if $\mathrm{in}(p) + \mathrm{on}(p) > k$. Equivalently, p belongs to the interior of an order-k Voronoi ℓ-polyhedron iff

$$\ell = n \text{ and } \mathrm{in}(p) + \mathrm{on}(p) = k \text{ or} \tag{6.3}$$

$$0 \leq \ell \leq n - 1 \text{ and } \mathrm{on}(p) = n - \ell + 1 \text{ and } k + \ell - n \leq \mathrm{in}(p) \leq k - 1. \tag{6.4}$$

These relations suffice to extend the analysis in [67] from skeletons of order-1 to skeletons of order-k Voronoi tessellations. For $0 \leq \ell \leq n-1$, they can be obtained as in [67, Theorem 10.2.4], which is the special case $k = 1$ of Theorem 16. The sole difference is that we use

the probability that there are i points in the interior of the ball instead of 0, and sum over all admissible values of i, thus getting $\Gamma\big(n-\ell+i+\frac{\ell}{n}\big)/i!$ instead of $\Gamma\big(n-\ell+\frac{\ell}{n}\big)$ in the numerator. This is precisely the expression in the statement of Theorem 16. For $\ell=0$ this gives the expected number of vertices in the order-k Poisson–Voronoi mosaic. The case $\ell=n$ is trivial: we obviously have $\mathbb{E}[\eta_n^{(k,n)}]=\eta_n^{(k,n)}=1$. Theorem 16 is thus proved.

6.2 Faces of higher order Delaunay mosaics

In this section, we are more specific about the dual of the order-k Voronoi tessellation. As mentioned in Section 1.4, each vertex of the order-k Delaunay mosaic is the average of the k points that generate a non-empty order-k Voronoi domain. Each $(n-j)$-polyhedron of $\mathrm{Vor}^{(k)}(X)$ is shared by a number of Voronoi domains, each domain corresponds to a vertex, and the polyhedron corresponds to the j-cell in $\mathrm{Del}^{(k)}X$ that is the convex hull of these vertices. Since $\mathrm{Vor}^{(k)}(X)$ is not necessarily normal, $\mathrm{Del}^{(k)}X$ is not necessarily simplicial.

Barycenter polytopes. We introduce a class of convex polytopes that is slightly richer than the class of simplices. As we will see later, this class contains all polytopes we generically encounter in order-k Delaunay mosaics. Let Δ^n be an n-dimensional simplex and recall that it has $\binom{n+1}{g}$ faces of dimension $g-1$, for $1\leq g\leq n+1$. The corresponding *generation-g barycenter polytope* is the convex hull of the barycenters of all $(g-1)$-faces, denoted Δ^n_g. For $g=n+1$ the corresponding polytopes consist of a single point, but for other values of g they are n-dimensional. For $g=1$ and $g=n$ the polytopes are n-simplices, namely the convex hull of the $n+1$ vertices, $\Delta^n_1=\Delta^n$, and the convex hull of the barycenters of the $n+1$ $(n-1)$-faces, Δ^n_n. For $2\leq g\leq n-1$, the barycenter polytope is not a simplex, and the first such case is Δ^3_2, which is an octahedron; see Figure 6.1.

Characterization. If X is in general position, which we assume, then every cell of $\mathrm{Del}^{(k)}X$ is a barycenter polytope. To prove this, we consider a u-dimensional cell G of $\mathrm{Del}^{(k)}X$ and recall that all interior points of its dual $(n-u)$-dimensional polyhedron F of $\mathrm{Vor}^{(k)}(X)$ are equivalent. In other words, there are sets $I=\mathrm{In}(F)$ and $U=\mathrm{On}(F)$ that uniquely determine F as the polyhedron whose interior points p satisfy $I=\mathrm{In}(p)$ and $U=\mathrm{On}(p)$.

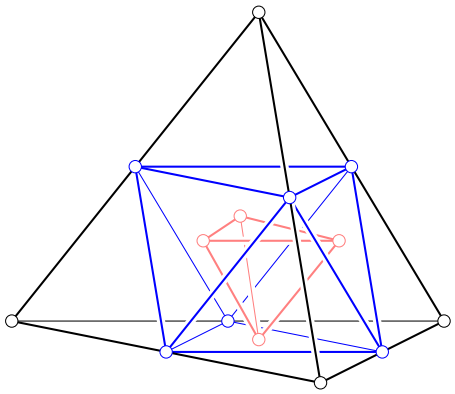

Figure 6.1: Three barycenter polytopes in $\mathbb{R}^3$: the generation-1 tetrahedron, the generation-2 octahedron, and the generation-3 tetrahedron.

We rewrite (6.3) and (6.4) to get constraints on the sizes of the two sets:

$$|I| + |U| = k \quad \text{if } u = 0, \tag{6.5}$$

$$|U| = u + 1 \text{ and } k - u \leq |I| \leq k - 1 \quad \text{if } u > 0. \tag{6.6}$$

The vertices of $\mathrm{Del}^{(k)}X$ are governed by a different relation, (6.5), from the remainder of the cells. Focusing on the cells of dimension $0 < u \leq n$, we note that (6.6) allows for a range of u possible sizes of the set I. These correspond to the generations of the barycenter polytopes, as we now explain. Let $i = |I|$ and define $g = k - i$, noting that (6.6) implies $1 \leq g \leq u$. By Lemma 6.1.2, F is the intersection of $\binom{u+1}{g}$ order-k Voronoi domains corresponding to $Q = I \cup U_{in}$, in which $U_{in} \subseteq U$ with $|U_{in}| = g$. So its dual cell G is the convex hull of the centers of masses x_Q of these sets, as discussed in Section 1.4. Writing x_Q as

$$x_Q = \tfrac{1}{k}\left[\sum_{x\in I} x + \sum_{x\in U_{in}} x\right] = \tfrac{k-g}{k} x_I + \tfrac{g}{k} x_{U_{in}}, \tag{6.7}$$

we see that the convex hull of the x_Q is therefore a translated and scaled copy of a generation-g barycenter polytope, namely the convex hull of the points $x_{U_{in}}$. Since $|U| = u+1$, this polytope is u-dimensional, as expected. To summarize, we have a complete description of the cells in an order-k Delaunay mosaic.

Lemma 6.2.1 (Order-k Delaunay cells)**.** *Let $X \subseteq \mathbb{R}^n$ be locally finite and in general position, and let $I, U \subseteq X$ with $I \cap U = \emptyset$. If $|I| + |U| = k$, then there is a point $p \in \mathbb{R}^n$ with $\mathrm{In}(p) \cup \mathrm{On}(p) = I \cup U$ iff $x_{I\cup U}$ is a vertex of $\mathrm{Del}^{(k)}X$. If $|I| + |U| \geq k + 1$, then there is a point $p \in \mathbb{R}^n$ with $\mathrm{In}(p) = I$ and $\mathrm{On}(p) = U$ iff the u-dimensional generation-g barycenter polytope defined by I and U belongs to $\mathrm{Del}^{(k)}X$, in which $u = |U| - 1$ and $g = k - |I|$.*

6.3 Relaxed discrete Morse theory

In the previous section we found out that all cells of the order-k Delaunay mosaic are defined by the order-k Delaunay spheres of points in the dual Voronoi face. This description is not unique though: several spheres can define the same cell. We want to resolve this non-uniqueness by choosing the unique smallest one. This rather informal description is a starting point for developing a version of discrete Morse theory, which would generalize the standard discrete Morse theory [36, 37, 8] to the order-k case.

Radius function. Recall that every j-cell $G \in \mathrm{Del}^{(k)}X$ corresponds to an $(n-j)$-polyhedron F of $\mathrm{Vor}^{(k)}(X)$. By Lemma 6.1.2, for any point $p \in \operatorname{int} F$, the Delaunay sphere $\Sigma_k(p)$ passes through the same $j+1$ points $\mathrm{On}(p) = \mathrm{On}(F)$, and G is a scaled and translated copy of a barycenter polytope defined by $\mathrm{On}(p)$. Since this is the smallest sphere centered at p such that the closed ball it bounds contains at least k points of X, the definition does not depend on F, and its radius, $r_k(p)$, is continuous as function of p. Noting that F is compact, we can therefore introduce $\mathcal{R}_k \colon \mathrm{Del}^{(k)}X \to \mathbb{R}$ defined by

$$\mathcal{R}_k(G) = \min\{r_k(p) \mid p \in F \text{ and } F \text{ dual to } G\},$$

and call it the *radius function* of $\mathrm{Del}^{(k)}X$. We further call the point $p \in F$, which attains the minimum, the *center* of G. This agrees with the definitions used in the statement of

Theorem 15. Note that if the center p of G lies in the interior of a Voronoi face F', then $r_k(p)$ is the radius of $\Sigma_k(p)$, which determines F' in the sense of Lemma 6.1.2. A very important observation is that $\mathrm{On}(F) \subseteq \mathrm{On}(p) = \mathrm{On}(F')$ and $\mathrm{In}(F') \subseteq \mathrm{In}(F) \subseteq \mathrm{In}(F') \cup \mathrm{On}(F')$, because all k-tuples of points of X, whose order-k Voronoi domains intersect in F, are involved in forming F'. With this it is also easy to find out, which Voronoi polyhedra of any fixed dimension, not necessarily n, intersect in F'.

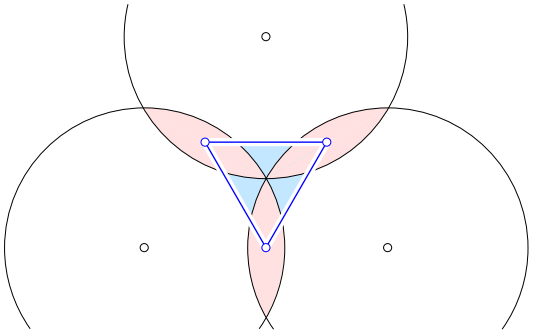

Figure 6.2: The radius function partitions the order-2 Delaunay mosaic of the three points into four relaxed intervals: three contain a vertex each, and the fourth relaxed interval contains the triangle together with its three edges.

The discrete Morse theory of [36] requires that level sets of the radius function are singletons and pairs, while the generalized discrete Morse theory of [37] allows intervals, which are maximal sets of faces of a cell that share a common face. The level sets of $\mathcal{R}_k$ are not necessarily of this type, as we now show. Let X consist of three points spanning an equilateral triangle with unit length edges in the plane. The order-2 Delaunay mosaic consists of the triangle spanned by the midpoints of the three edges, together with its edges and vertices. Observe that $r_0 = 1/2$ is the radius assigned to its three vertices, and $r_1 = \sqrt{3}/3$ is assigned to the triangle together with its three edges; see Figure 6.2. Indeed, the closed disks of radius r centered at the points in X have pairwise intersections iff $r \geq r_0$, and they have a non-empty common intersection iff $r \geq r_1$. Each vertex of the order-2 Delaunay mosaic has its own center in the interior of the corresponding Voronoi 2-polyhedron, but the triangle and its three edges share the center at the circumcenter of the triangle. The triangle together with its edges is not an interval, so $\mathcal{R}_k$ is not a generalized discrete Morse function, and we refer to it as a *relaxed discrete Morse function*. This function indeed contains some topological meaning, see [32], so the term is not chosen randomly.

Relaxed intervals. The radius function $\mathcal{R}_k$ is monotonic, by which we mean that $\mathcal{R}_k(G) \leq \mathcal{R}_k(G')$ whenever G is a face of G'. Equality is possible, namely when the order-k Voronoi face F', dual to G', contains the center of G, which lies in $F \setminus \operatorname{int} F$. By definition, a *relaxed interval* of $\mathcal{R}_k$ is a maximal collection of cells in $\mathrm{Del}^{(k)}X$ that share the center, and hence the function value. Thus, every level set of $\mathcal{R}_k$ is a disjoint union of relaxed intervals.

The previous example begs the question how much more general the relaxed intervals are compared to the intervals. Each relaxed interval has a unique *upper bound*, which is a cell $G \in \mathrm{Del}^{(k)}X$, whose dual Voronoi polyhedron, F, contains the center p of G in its interior. Write $U = \mathrm{On}(p)$ and $u = |U| - 1$. The dimension of G is thus u, unless $\mathrm{in}(p) + \mathrm{on}(p) = k$, in which case it is 0. Considering any partition of U into three sets, $U = U_{in} \cup U_{on} \cup U_{out}$ with $U_{on} \neq U$, we can slightly perturb the sphere $\Sigma_k(p)$ into a sphere

Σ, with $\Sigma \cap X = U_{on}$ and $\operatorname{int} \Sigma \cap X = U_{in} \cup \operatorname{In}(p)$. If the sizes of these two sets satisfy the requirements for the order-k Delaunay sphere, they define a cell of $\operatorname{Del}^{(k)} X$, which is a face of G. On the other hand, every face of G *induces* such a partition. We thus get a corresponding between such partitions and faces of G, which is one-to-one unless $|U_{in} \cup U_{on} \cup \operatorname{In}(p)| = k$, otherwise we get the same vertex for different partitions with the same $U_{in} \cup U_{on}$. We are particularly interested in distinguishing the faces that share the center, p, from the other faces of G. The crucial concept is again the visibility of facets of $\operatorname{conv} U$ from p, as defined in Section 1.5.

Recall that the center p of G lies in the interior of the dual Voronoi polyhedron by assumption. It follows that p lies in the affine hull of U. Equivalently, the u-sphere with center p that passes through the $u+1$ points of $U = \operatorname{On}(p)$ is a great-sphere of $\Sigma_k(p)$, and $\Sigma_k(p)$ is the smallest circumscribed sphere of U. The convex hull of U is a u-simplex, and recall that we say that a facet of U is *visible* from p if the affine hull of the facet, which is a $(u-1)$-plane, separates p from $\operatorname{conv} U$ within the affine hull of U, which is a u-plane. Let V be the intersection of all visible facets of U, and write $|V| = v+1$. In particular, $V = U$ if there are no visible facets. Notice that v is also the number of invisible facets minus 1, because a vertex belongs to V iff the facet opposite to the vertex is invisible, and observe that $v \geq 1$ because the $u+1$ points of U lie on a sphere around p; compare also with Lemma 4.3.3. With these notions, we can identify the partitions of U corresponding to faces of G that belong to the same relaxed interval.

Lemma 6.3.1 (Visibility and relaxed intervals)**.** *Let $X \subseteq \mathbb{R}^n$ be locally finite and in general position. Let $G \in \operatorname{Del}^{(k)} X$ with corresponding order-k Delaunay sphere $\Sigma_k(p)$ be the upper bound of a relaxed interval of the radius function. A face G' of G belongs to the same relaxed interval iff the partition $\operatorname{On}(p) = U_{in} \cup U_{on} \cup U_{out}$ induced by G' satisfies $U_{in} \subseteq V \subseteq U_{in} \cup U_{on}$.*

Proof. Write $U = \operatorname{On}(p)$. Let q be the center of G', and recall that G, G' belong to the same relaxed interval iff $p = q$. The following two conditions must hold, else $p \neq q$.

(i) If an invisible face of $\operatorname{conv} U$ contains U_{on}, then the opposite vertex must be in U_{in}.

(ii) If a visible face of $\operatorname{conv} U$ contains U_{on}, then the opposite vertex must be in U_{out}.

To see (i), we would move the center, p, normal to and slightly toward the facet while adjusting the radius so the sphere keeps passing through all vertices of the facet. This generates a smaller sphere for the same partition of U, hence $p \neq q$. The symmetric argument proves (ii). Now (i) is equivalent to $U_{in} \subseteq V$, and (ii) is equivalent to $U \setminus V \subseteq U_{out}$. Hence $p = q$ implies $U_{in} \subseteq V \subseteq U_{in} \cup U_{on}$. The converse is also true because the two conditions prohibit a smaller sphere in the normal directions of all facets. These directions span all directions in the affine hull of U. □

The only case when the induced decomposition is not necessarily unique, is when G' is a vertex. In particular, if the upper bound cell G is a vertex itself, an additional requirement that $V = U$ appears, because otherwise we would get that some of its faces, namely itself, belong to a different relaxed interval.

6.4 Counting intervals and simplices

In this section, we count the cells in the relaxed intervals that arise in the partition of order-k Delaunay mosaics. We then use the result to prove Theorem 15.

Cells in relaxed intervals. As explained in the previous section, every relaxed interval has a unique upper bound, which is a cell $G \in \mathrm{Del}^{(k)}X$ whose center, $p \in \mathbb{R}^n$, is contained in the interior of the dual Voronoi polyhedron. The order-k Delaunay sphere of this point, $\Sigma_k(p)$, completely determines G; see (6.7). Ignoring the case in which G is a vertex, we assume that $\mathrm{in}(p) + \mathrm{on}(p) \geq k+1$, in which case $u = \mathrm{on}(p) - 1 \geq 1$ is the dimension of G and $g = k - \mathrm{in}(p)$ is its generation. To get the number of vertices of G, we count the partitions $U = U_{in} \cup U_{out}$ of $U = \mathrm{On}(p)$ with $|U_{in}| = g$, where we artificially move U_{on} into U_{in} because we are interested only in their union; compare with (6.5). To get the number of j-faces, for $0 < j < u$, we count the partitions $U = U_{in} \cup U_{on} \cup U_{out}$ that satisfy $|U_{on}| = j+1$ and $g - j \leq |U_{in}| \leq g-1$; compare with (6.6). To further limit the number to the cells in the relaxed interval of G, we restrict to $U_{in} \subseteq V \subseteq U_{in} \cup U_{on}$, in which $V \subseteq U$ with $|V| = v+1$ contains the vertices that belong to all visible facets of U.

For $j = 0$, the last condition is equivalent to $U_{in} = V$. So, we have $N^u_{v,g}(0) = 1$ if $g = v+1$ and 0 otherwise. When $j > 0$ the dimension requirement is that $|U_{on}| = j+1$. Writing $t = |U_{in}|$, we can formulate the question purely combinatorially, first choosing the union $U_{in} \cup U_{on} \subseteq U$ such that $V \subseteq U_{in} \cup U_{on}$ and second choosing $U_{in} \subseteq V$: *how many ways are there to pick* $(t+j+1)-(v+1)$ *from* $(u+1)-(v+1)$ *points and then* t *from* $v+1$ *points?*

$$N^u_{v,g}(j) = \sum_{t=t_0}^{t_1} \binom{u-v}{t+j-v}\binom{v+1}{t}, \tag{6.8}$$

in which $t_0 = \max\{0, v-j, g-j\}$ and $t_1 = \min\{v+1, u-j, g-1\}$ are obtained from $0 \leq t \leq v+1$, $0 \leq j - v + t \leq u - v$, and $g - j \leq t \leq g-1$. The first two conditions assert that the binomial coefficients make sense, while the last one is the geometric requirement for the number of points inside the sphere.

Intrinsic characterization of relaxed intervals. Let $U \subseteq X \subseteq \mathbb{R}^n$ with $|U| = u+1 \leq n+1$ be a simplex, such that the smallest circumscribed sphere Σ of U has at most $k-1$ and at least $k-u-1$ points inside. Letting p be the center of this sphere, we notice that $\Sigma = \Sigma_k(p)$ and $\mathrm{On}(p) = U$. If $\mathrm{on}(p) + \mathrm{in}(p) > k$, it defines a cell G of $\mathrm{Del}^{(k)}X$, which is a barycenter polytope of type Δ^u_g, for $g = k - \mathrm{in}(p)$. By Lemma 6.3.1, this cell is the upper bound of a relaxed interval of the radius function $\mathcal{R}_k$, which contains the cells that share p as their center. The lemma also asserts that the interval is fully described by the the set of vertices of U that belong to all visible facets. Writing V for this set and $v = |V| - 1$ for its dimension, we call (v, u, g) the *type* of the relaxed interval. It is fully defined by U.

If $\mathrm{on}(p) + \mathrm{in}(p) = k$, then p belongs to the interior of the order-k Voronoi domain of $\mathrm{On}(p) \cup \mathrm{In}(P)$. By Lemma 6.3.1 and the remark after it, p is the center of this domain iff it lies in the interior of U. In this case, we get a critical vertex, with $V = U$ and $g = u+1$. The type of this interval is thus defined as $(u, u, u+1)$. This should not be confusing because vertices with different relaxed interval types are really different kinds of vertices in the mosaic.

Proof of Theorem 15. We now apply the developed theory to get the expected number of j-cells in the Poisson–Delaunay mosaic of order k. Let X be a stationary Poisson point process with density ρ in $\mathbb{R}^n$. Using the intrinsic characterization, we want to compute the expected numbers of intervals of type (v, u, g), while restricting the radius from above. Write $s^{(k,n)}_{v,u,g}(r_0)$ for the number of tuples of $u+1$ points in X, whose smallest circumspheres have $k-g$ points inside, have their center in some region $\Omega \subseteq \mathbb{R}^n$, and have radius at most

r_0. As the previous discussion shows, it is the same as the number $c^{(k,n)}_{v,u,g}(r_0)$ of intervals of type (v,u,g) with center in Ω and radius at most r_0, when $1 \le g \le \max\{u,k\}$ or $v = u = g-1$. For $u > 0$, the Slivnyak–Mecke formula (Lemma 1.6.1) helps to take advantage of such description and express the expected number of such intervals as

$$\mathbb{E}[s^{(k,n)}_{v,u,g}(r_0)] = \tfrac{1}{(u+1)!} \int\limits_{\mathbf{x}\in(\mathbb{R}^n)^{u+1}} \mathbf{1}_\Omega(\mathbf{x})\mathbf{1}_{r_0}(\mathbf{x})\mathbf{1}_{u-v}(\mathbf{x})\mathbb{P}_{k-g}(\mathbf{x})\rho^{u+1}\,\mathrm{d}\mathbf{x},$$

in which $\mathbb{P}_{k-g}(\mathbf{x}) = (\rho\nu_n r^n)^{k-g}e^{-\rho\nu_n r^n}/(k-g)!$ is the probability that the smallest circumsphere of $\mathbf{x}$ has $k-g$ points of X inside, $\mathbf{1}_\Omega(\mathbf{x})$ indicates whether the center of this sphere belongs to Ω, $\mathbf{1}_{r_0}(\mathbf{x})$ indicates whether its radius is at most r_0, and $\mathbf{1}_{u-v}(\mathbf{x})$ indicates whether $\mathbf{x}$ has $u-v$ visible facets. This notation mimics the notation in Chapter 5, in particular, we write $\mathbf{x}$ for a sequence of $u+1$ points, which is better suited for integration than the set U of $u+1$ points. This formula effectively differs from (5.1) only in the way that we use $\mathbb{P}_{k-g}(\mathbf{x})$ instead of $\mathbb{P}_0(\mathbf{x}) = \mathbb{P}_\emptyset(\mathbf{x})$, and k in (5.1) is equal to n. To avoid redundancy, we do not rewrite the steps (5.1)–(5.4), but rather focus on the difference. Specifically, instead of $\int_{r=0}^{r_0} r^{nk-1}e^{-\rho r^n\nu_n} = \frac{\gamma\left(k;\,\rho\nu_n r_0^n\right)}{n(\rho\nu_n)^k}$ in (5.2), we have

$$\int\limits_{r=0}^{r_0} r^{nu-1}\frac{(\rho r^n\nu_n)^{k-g}}{(k-g)!}e^{-\rho r^n\nu_n} = \frac{(\rho\nu_n)^{k-g}}{(k-g)!}\frac{\gamma(u+k-g;\,\rho\nu_n r_0^n)}{n(\rho\nu_n)^{u+k-g}} = \frac{\gamma(u+k-g;\,\rho\nu_n r_0^n)}{(k-g)!n(\rho\nu_n)^u}.$$

Repeating (5.1)–(5.4), we get

$$\mathbb{E}[s^{(k,n)}_{v,u,g}(r_0)] = \frac{\gamma(u+k-g;\,\rho\nu_n r_0^n)}{(k-g)!\Gamma(u)}C^n_{v,u}\cdot\rho\|\Omega\|, \tag{6.9}$$

in which the constant $C^n_{v,u}$ is the same constant as defined in (4.3) The case $u = 0$ is exceptional, because the smallest circumscribed sphere of any single vertex has radius 0 and has no points inside, so the only non-zero value is $\mathbb{E}[s^{(1,n)}_{0,0,1}(r_0)] = \rho\|\Omega\|$ for all $r_0 \ge 0$, independent of the radius. Turning back to the number of relaxed intervals, we thus have $\mathbb{E}[c^{(k,n)}_{v,u,g}(r_0)] = \mathbb{E}[s^{(k,n)}_{v,u,g}(r_0)]$ for admissible values of parameters, i.e., for $1 \le g \le \min\{k,u\}$ or $v = u = g-1$, and 0 otherwise. The result agrees with Theorem 9 for $k = 1$.

Now that we have expressions for the number of relaxed intervals of all types, it is not difficult to count the j-cells in the order-k Delaunay mosaic whose value under the radius function is at most r_0:

$$\mathbb{E}[d^{(k,n)}_j(r_0)] = \sum_{u=j}^{n}\sum_{v=0}^{u}\sum_{g=1}^{\min\{k,u+1\}} N^u_{v,g}(j)\cdot\mathbb{E}[c^{(k,n)}_{v,u,g}(r_0)].$$

For $j > 0$, we can use (6.8) and (6.9) to get

$$\mathbb{E}[d^{(k,n)}_j(r_0)] = \sum_{u=j}^{n}\sum_{v=1}^{u}\sum_{g=1}^{g_1}\sum_{t=t_0}^{t_1}\binom{v+1}{t}\binom{u-v}{t+j-v}\frac{\gamma(u+k-g;\,\rho\nu_n r_0^n)}{(k-g)!\Gamma(u)}C^n_{v,u}\cdot\rho\|\Omega\|,$$

in which $g_1 = \min\{k,u\}$, $t_0 = \max\{0, v-j, g-j\}$, and $t_1 = \min\{v+1, u-j, g-1\}$, as before. For $j = 0$ and $k \ge 2$, we have to sum the numbers of all intervals with $g = v+1$:

$$\mathbb{E}[d^{(k,n)}_0(r_0)] = \sum_{u=1}^{n}\sum_{v=1}^{u}\frac{\gamma(u+k-v-1;\,\rho\nu_n r_0^n)}{(k-v-1)!\Gamma(u)}C^n_{v,u}\cdot\rho\|\Omega\|.$$

This completes the proof of Theorem 15.

7. Random inscribed polytopes

In this chapter, we prove Theorem 17. It consists of an integral equation for the expected number of intervals of a Poisson–Delaunay mosaic on $\mathbb{S}^n$ as a function of the maximum geodesic radius, and an asymptotic version of the formula for $\rho \to \infty$.

7.1 Integral equation

We begin with the proof of the first equation in the statement of Theorem 17. The main tools are again the Slivnyak–Mecke formula, and the Blaschke–Petkantschin formula, this time for the sphere (Theorem 21).

The Slivnyak–Mecke approach. To write this integral, we recall that $\mathbf{x} = (x_0, x_1, \dots, x_m)$ is a sequence of $m+1$ points or m-simplex on $\mathbb{S}^n$, that $\mathbb{P}_\emptyset \colon (\mathbb{S}^n)^{m+1} \to \mathbb{R}$ maps $\mathbf{x}$ to the probability that its smallest circumscribed cap is empty, that $\mathbf{1}_{m-\ell} \colon (\mathbb{S}^n)^{m+1} \to \mathbb{R}$ indicates whether or not the number of facets visible from the Euclidean center of the smallest circumscribed cap is $m-\ell$, and that $\mathbf{1}_\eta \colon (\mathbb{S}^n)^{m+1} \to \mathbb{R}$ indicates whether or not $\mathcal{R}_S(\mathbf{x}) \leq \eta$. Choosing points from a Poisson point process with density $\rho > 0$ on $\mathbb{S}^n$, we use Slivnyak–Mecke formula to write the expected number of intervals of type (ℓ, m) and geodesic radius at most η_0 as

$$\mathbb{E}[c^n_{\ell,m}, \eta_0] = \tfrac{\rho^{m+1}}{(m+1)!} \int\limits_{\mathbf{x} \in (\mathbb{S}^n)^{m+1}} \mathbb{P}_\emptyset(\mathbf{x}) \cdot \mathbf{1}_{m-\ell}(\mathbf{x}) \cdot \mathbf{1}_{\eta_0}(\mathbf{x}) \, \mathrm{d}\mathbf{x}, \tag{7.1}$$

in which $0 \leq \ell \leq m \leq n$. The probability that the smallest circumscribed cap of the m-simplex is empty is $\mathbb{P}_\emptyset(\mathbf{x}) = e^{-\rho \mathrm{Area}(\eta)}$, with η the geodesic radius of the cap. To compute the integral in (7.1), we apply the second equation in Theorem 21 with

$$f(\mathbf{x}) = \mathbb{P}_\emptyset(\mathbf{x}) \mathbf{1}_{m-\ell}(\mathbf{x}) \mathbf{1}_{\eta_0}(\mathbf{x}).$$

The corresponding function from the statement of Theorem 21,

$$f_r \colon (\mathbb{S}^{m-1})^{m+1} \subseteq (\mathbb{R}^{n+1})^{m+1} \to \mathbb{R}$$

is defined by

$$f_r(\mathbf{u}) = \mathbb{P}_\emptyset(r) \mathbf{1}_{m-\ell}(\mathbf{u}) \mathbf{1}_{\eta_0}(r),$$

where we write $\mathbb{P}_\emptyset(r) = \mathbb{P}_\emptyset(\mathbf{u})$ and $\mathbf{1}_{\eta_0}(r) = \mathbf{1}_{\eta_0}(\mathbf{u})$ to emphasize that these expressions depend only on the radius. The theorem then gives

$$\int_{\mathbf{x}\in(\mathbb{S}^n)^{m+1}} f(\mathbf{x})\,\mathrm{d}\mathbf{x} = \tfrac{\sigma_{n+1}}{2}\|\mathcal{L}^n_m\| \int_{t=0}^{1} t^{\frac{mn-2}{2}}(1-t)^{\frac{n-m-1}{2}}\mathbb{P}_\emptyset(\sqrt{t})\mathbf{1}_{\eta_0}(\sqrt{t}) \times \int_{\mathbf{u}\in(\mathbb{S}^{m-1})^{m+1}} \mathbf{1}_{m-\ell}(\mathbf{u})[m!\mathrm{Vol}(\mathbf{u})]^{n-m+1}\,\mathrm{d}\mathbf{u}\,\mathrm{d}t. \tag{7.2}$$

Substitution and reformulation. To continue, we recall the notion $E^n_{\ell,m}$ from (4.1). It follows that the second integral on the right-hand side of (7.2) is $m!^{n-m+1}\sigma_m^{m+1}E^n_{\ell,m}$. Rewriting (7.1) using (7.2), we therefore get

$$\mathbb{E}[c^n_{\ell,m},\eta_0] = \tfrac{\rho^{m+1}}{(m+1)!}\tfrac{\sigma_{n+1}}{2}\|\mathcal{L}^n_m\|m!^{n-m+1}\sigma_m^{m+1}E^n_{\ell,m}\int_{t=0}^{s} t^{\frac{mn-2}{2}}(1-t)^{\frac{n-m-1}{2}}\mathbb{P}_\emptyset(\sqrt{t})\,\mathrm{d}t, \tag{7.3}$$

$$= \rho\sigma_{n+1}\cdot\tfrac{\sigma_n^m}{2\Gamma(m)n^{m-1}}\cdot C^n_{\ell,m}\int_{t=0}^{s}\rho^m t^{\frac{mn-2}{2}}(1-t)^{\frac{n-m-1}{2}}\mathbb{P}_\emptyset(\sqrt{t})\,\mathrm{d}t, \tag{7.4}$$

in which we absorb one indicator by limiting the range of integration to the square of the maximum Euclidean radius, $s = \sin^2\eta_0$. To get (7.4) from (7.3), we cancel $m!$, move ρ^m inside the integral, and use (4.1) and (4.3) to substitute $C^n_{\ell,m}$ for $E^n_{\ell,m}$ with appropriate rescaling. This proves the integral equation in Theorem 17.

7.2 Asymptotic result

We continue with the proof of the asymptotic result in Theorem 17. We proceed in two stages, first taking liberties and leaving gaps in the argument, and second filling all the gaps.

Argument with gaps. We are interested in the behavior of the integral in (7.4), when $\rho\to\infty$. We observe that the probability of a cap to be empty vanishes rapidly with increasing geodesic radius: $\mathbb{P}_\emptyset(r) = e^{-\rho\mathrm{Area}(\eta)}$, in which $r = \sin\eta$ is the Euclidean radius. This implies that the integrand is concentrated in the vicinity of 0. To make sense of the radius in the limit, we re-scale by mapping η and ρ to the normalized radius, $\bar\eta = \eta\rho^{1/n}$. To proceed with the informal computations, we assume that η is close to 0 and prepare two approximations and one relation:

A. the squared Euclidean radius is roughly the squared geodesic radius: $s = \sin^2\eta \approx \eta^2$;

B. the square of the height is $1-s\approx 1$, which allows us to simplify the incomplete Beta function:

$$B_s(\tfrac{n}{2},\tfrac{1}{2}) = \int_{t=0}^{s} t^{\frac{n}{2}-1}(1-t)^{-\frac{1}{2}}\,\mathrm{d}t \approx \int_{t=0}^{s} t^{\frac{n}{2}-1}\,\mathrm{d}t = \tfrac{2}{n}s^{n/2}; \tag{7.5}$$

C. the relation $\frac{\sigma_{n+1}}{\sigma_n} = B\left(\frac{n}{2},\frac{1}{2}\right)$ implies $\frac{\sigma_{n+1}}{n}/B\left(\frac{n}{2},\frac{1}{2}\right) = \frac{\sigma_n}{n} = \nu_n$.

Returning to the integral in (7.4), but without the factor ρ^n, we get

$$\int_{t=0}^{\sin^2\eta_0} t^{\frac{mn-2}{2}}(1-t)^{\frac{n-m-1}{2}}\mathbb{P}_\emptyset(\sqrt{t})\,\mathrm{d}t \approx \int_{t=0}^{\bar{\eta}_0^2/\rho^{2/n}} t^{\frac{mn-2}{2}}e^{-\rho\nu_n t^{n/2}}\,\mathrm{d}t, \tag{7.6}$$

in which we approximate the upper limit of the integration using A, and drop the middle factor because it is close to 1 according to B. The probability of having an empty cap is $\mathbb{P}_\emptyset(r) = e^{-\rho\mathrm{Area}(\eta)}$, in which the area of the cap can be written in terms of Beta functions:

$$\mathrm{Area}(\eta) = \tfrac{\sigma_{n+1}B_s(n/2,1/2)}{2B(n/2,1/2)} \approx \tfrac{\sigma_{n+1}(2/n)s^{n/2}}{2B(n/2,1/2)} = \nu_n s^{n/2}, \tag{7.7}$$

using B for the approximation and C to get the final result, which we plug into the left-hand side of (7.6) to get the approximation on its right-hand side. The exponential term motivates us to change variables with $\tau = \rho\nu_n t^{n/2}$. Plugging $t = \tau^{2/n}/(\rho\nu_n)^{2/n}$ and $\mathrm{d}t = [\frac{2}{n}\tau^{2/n-1}/(\rho\nu_n)^{2/n}]\,\mathrm{d}\tau$ into the right-hand side of (7.6), we get

$$\int_{\tau=0}^{v}\tau^{m-1}(\rho\nu_n)^{-m}\left(\tfrac{2}{n}\right)e^{-\tau}\,\mathrm{d}\tau = \tfrac{2n^{m-1}}{\rho^m\sigma_n^m}\cdot\gamma(v;\,m), \tag{7.8}$$

in which the upper bound of the integration range is

$$v = \rho\nu_n(\bar{\eta}_0^2/\rho^{2/n})^{n/2} = \bar{\eta}_0^n\nu_n,$$

the power of τ is

$$\tfrac{2}{n}\tfrac{mn-2}{2} + \tfrac{2}{n} - 1 = m-1,$$

and the power of $\rho\sigma_n$ is

$$-\tfrac{2}{n}\tfrac{mn-2}{2} - \tfrac{2}{n} = -m.$$

We get the right-hand side of (7.8) from the left-hand side using $\frac{\sigma_n}{n} = \nu_n$ and $\gamma(v;\,m) = \int_{\tau=0}^{v}\tau^{m-1}e^{-\tau}\,\mathrm{d}\tau$. Finally plugging the right-hand side into (7.4), we get

$$\mathbb{E}[c_{\ell,m}^n,\eta_0] = \rho\sigma_{n+1}\cdot\tfrac{\sigma_n^m}{2\Gamma(m)n^{m-1}}\cdot C_{\ell,m}^n\int_{t=0}^{\sin^2\eta_0}\rho^m t^{\frac{mn-2}{2}}(1-t)^{\frac{n-m-1}{2}}\mathbb{P}_\emptyset(\sqrt{t})\,\mathrm{d}t \tag{7.9}$$

$$= \rho\sigma_{n+1}\cdot\tfrac{\gamma(v;\,m)}{\Gamma(m)}\cdot C_{\ell,m}^n + o(\rho), \tag{7.10}$$

as claimed in Theorem 17. Making the unjustified substitution $v = \bar{\eta}_0^n\nu_n = \infty$, we get

$$\mathbb{E}[c_{\ell,m}^n] = \rho\sigma_{n+1}\cdot C_{\ell,m}^n + o(\rho), \tag{7.11}$$

as claimed in Remark (4) after Theorem 17.

Formal justifications. We continue with the justification of the asymptotic equivalences claimed above. To recall, there is the approximation in (7.6) and the substitution $\bar{\eta}_0 = \infty$ after (7.10). Fixing a real number $0 \le \delta \le 1$, we introduce some notation to streamline the computations:

$$\alpha = \tfrac{mn-2}{2},\quad \alpha' = \tfrac{n-m-1}{2},\quad \beta = \tfrac{n}{2},\quad \beta' = \tfrac{1}{2},\quad c = \tfrac{\sigma_n}{2}, \tag{7.12}$$

$$g(s) = c\int_{t=0}^{s} t^{\beta-1}(1-t)^{\beta'-1}\,\mathrm{d}t, \tag{7.13}$$

$$J_0 = \rho^m\int_{t=0}^{1} t^\alpha(1-t)^{\alpha'}e^{-\rho g(t)}\,\mathrm{d}t,\quad J_1(\delta) = \rho^m\int_{t=0}^{\delta} t^\alpha(1-t)^{\alpha'}e^{-\rho g(t)}\,\mathrm{d}t, \tag{7.14}$$

$$J_2(\delta) = \rho^m\int_{t=0}^{\delta} t^\alpha e^{-\rho g(t)}\,\mathrm{d}t,\qquad J_3(\delta) = \rho^m\int_{t=0}^{\delta} t^\alpha e^{-\rho\frac{c}{\beta}t^\beta}\,\mathrm{d}t. \tag{7.15}$$

We note that $\alpha, \alpha' \geq -\frac{1}{2}$, $\beta, \beta' \geq \frac{1}{2}$, and $g(s)$ is $c = \frac{\sigma_n}{2}$ times the incomplete Beta function. Recall that $\frac{\sigma_{n+1}}{\sigma_n} = B\left(\frac{n}{2}, \frac{1}{2}\right)$, which implies that $g(s)$ is $\frac{\sigma_{n+1}}{2}$ times the ratio of incomplete over complete Beta functions. Hence $g(s) = \mathrm{Area}(\eta)$, in which $s = \sin^2 \eta$; see (2.1). Note also that J_0 is the integral in (7.4) except that the integration range goes all the way to 1, which corresponds to computing the number of intervals without restricting the radius. For $\delta = 1$, we have $J_1 = J_0$, and for $\delta = \sin^2 \eta_0$, J_1 is ρ^m times the expression on the left-hand side of (7.6). Finally, for $\delta = \bar{\eta}_0^2 \rho^{-1/\beta}$, J_3 is the integral on the right-hand side of (7.6), which we computed in (7.8). Next, we list a sequence of observations:

I. The integral in (7.13) satisfies

$$\tfrac{c}{\beta} s^\beta \leq g(s) = c \int_{t=0}^{s} t^{(n-2)/2} (1-t)^{-1/2} \, \mathrm{d}t \leq \tfrac{c}{\beta} s^\beta + \mathrm{const} \cdot s^{\beta+1},$$

for $0 \leq s \leq 1$ on the left, and for $0 \leq s \leq \frac{1}{2}$ on the right. Indeed, we have $1 \leq 1/\sqrt{1-t}$ for all $0 \leq t \leq 1$ and $1/\sqrt{1-t} \leq 1 + \mathrm{const} \cdot t$ for all $0 \leq t \leq \frac{1}{2}$.

II. The absolute difference between J_0 and $J_1(\delta)$ satisfies

$$|J_0 - J_1(\delta)| = \rho^m \int_{t=\delta}^{1} t^\alpha (1-t)^{\alpha'} e^{-\rho g(t)} \, \mathrm{d}t \leq \rho^m e^{-\rho \frac{c}{\beta} \delta^\beta} B(\alpha+1, \alpha'+1),$$

because $g(t) \geq g(\delta)$ throughout the integration domain, and $g(\delta) \geq \frac{c}{\beta} t^\beta$ by I. The value of the Beta function is a constant independent of ρ.

III. For $\delta \leq \frac{1}{2}$, the absolute difference between J_1 and J_2 satisfies

$$|J_1(\delta) - J_2(\delta)| \leq \rho^m \int_{t=0}^{\delta} [t^\alpha (1-t)^{\alpha'} - t^\alpha] e^{-\rho g(t)} \, \mathrm{d}t \leq \mathrm{const} \cdot \delta J_2(\delta),$$

because $|1 - (1-t)^{\alpha'}| \leq \mathrm{const} \cdot t$ for all $0 \leq t \leq \frac{1}{2}$ and $\alpha' \geq -\frac{1}{2}$.

IV. For $\delta \leq \frac{1}{2}$, the absolute difference between J_2 and J_3 satisfies

$$\begin{aligned} |J_2(\delta) - J_3(\delta)| &= \rho^m \int_{t=0}^{\delta} t^\alpha \left[e^{-\rho \frac{c}{\beta} t^\beta} - e^{-\rho g(t)} \right] \mathrm{d}t && (7.16) \\ &\leq \rho^m \int_{t=0}^{\delta} t^\alpha e^{-\rho \frac{c}{\beta} t^\beta} \left[1 - e^{-\mathrm{const} \cdot \rho t^{\beta+1}} \right] \mathrm{d}t && (7.17) \\ &\leq J_3(\delta) \left[1 - e^{-\mathrm{const} \cdot \rho \delta^{\beta+1}} \right], && (7.18) \end{aligned}$$

in which we use the left inequality in I to get the right signs of the exponential terms in (7.16), and the right inequality in I to get (7.17).

V. For $\eta \leq 1/\sqrt{2}$, the absolute difference between J_1 at the values $\sin^2 \eta$ and η^2 satisfies

$$\begin{aligned} |J_1(\sin^2 \eta) - J_1(\eta^2)| &= \rho^m \int_{t=\sin^2 \eta}^{\eta^2} t^\alpha (1-t)^{\alpha'} e^{-\rho g(t)} \, \mathrm{d}t \leq 2\rho^m \int_{t=\sin^2 \eta}^{\eta^2} t^\alpha \, \mathrm{d}t \\ &\leq \tfrac{2\rho^m}{\alpha+1} [\eta^{2\alpha+2} - (\eta - \eta^2)^{2\alpha+2}] \leq 4\rho^m \eta^{2\alpha+3}, \end{aligned}$$

in which we use $(1-t)^{\alpha'} \leq 2$ for $t \leq \frac{1}{2}$ to get the first inequality. To get the second, we use $\sin \eta > \eta - \eta^2$, which we glean from the Taylor series $\sin \eta = \eta - \frac{1}{6}\eta^3 + \ldots$, and the binomial expansion of $(\eta - \eta^2)^{2\alpha+2}$.

As mentioned earlier, $J_1(\sin^2 \eta_0)$ is ρ^m times the left-hand side of (7.6), and $J_3(\eta_0^2)$ is ρ^m times the right-hand side of (7.6). According to (7.8), ρ^m times this right-hand side is $(2n^{m-1}/\sigma_n^m) \cdot \gamma(v;\, m)$, with $v = \bar{\eta}^n \nu_n$, which is a positive constant; see Remark (3) after Theorem 17 where we first mentioned that this integral is bounded from 0 as well as from ∞. Having established that there is a positive constant $C = J_3(\eta_0^2)$, IV implies that

$$J_2(\eta_0^2) \leq C + (1 - e^{-\rho \frac{c}{\beta} \eta_0^{2(\beta+1)}})C$$

is also bounded by a constant. Using III, IV, V, we get

$$|J_1(\sin^2 \eta_0) - J_3(\eta_0^2)| \leq |J_1(\sin^2 \eta_0) - J_1(\eta_0^2)| + |J_1(\eta_0^2) - J_2(\eta_0^2)| + |J_2(\eta_0^2) - J_3(\eta_0^2)| \tag{7.19}$$

$$\leq 4\rho^m \eta_0^{2\alpha+3} + \text{const} \cdot \eta_0^2 J_2(\eta_0^2) + (1 - e^{-\text{const} \cdot \rho \eta_0^{2(\beta+1)}})C. \tag{7.20}$$

Letting ρ to to infinity, we observe

$$\rho^m \eta_0^{2\alpha+3} = \rho^m \left(\bar{\eta}_0 \rho^{-\frac{1}{n}} \right)^{mn+1} \to 0, \tag{7.21}$$

$$\rho \eta_0^{2(\beta+1)} = \rho \left(\bar{\eta}_0 \rho^{-\frac{1}{n}} \right)^{n+2} \to 0, \tag{7.22}$$

implying the three terms in (7.20) go to 0. This finally justifies the approximation (7.6) and the argument proving Theorem 17.

Justification of (7.11)**.** We finally prove that we can compute J_0 by setting $\bar{\eta}_0$ to infinity in (7.10) or, more formally, by replacing the incomplete gamma function in the expression by the complete gamma function. Such a justification is needed because so far we have treated the geodesic radius as a constant in our computations. We now couple the bound of the integration domain with the density by setting $\delta_0 = \rho^{-1/(\beta+1/2)}$. We reuse Equations (7.6) and (7.10) to compute $J_3(\delta_0) = (2n^{m-1}/\sigma_n^m) \cdot \gamma(v;\, m)$, with $v = \rho \nu_n \delta_0^{n/2} = \nu_n \rho^{1/(n+1)}$. The upper bound for the incomplete Gamma function thus goes to infinity and approaches the complete Gamma function. We still have $J_3(\delta_0)$ bounded by a constant, so the rest of the argument above goes through. We finally use II, which shows $|J_0 - J_1(\delta_0)| \to 0$. This justifies (7.11).

7.3 Uniform distribution

In this section, we sketch the case of the uniform distribution on $\mathbb{S}^n$. The sole difference to the Poisson point process is that the number of points is prescribed rather than a random variable. Setting this number to $N = \rho \sigma_{n+1}$, it makes sense that in the limit, when N and ρ go to infinity, the expected numbers of intervals of the radius function are the same under both probabilistic models. This is indeed what we establish now more formally. By linearity of expectation, the number of intervals of type (ℓ, m) and geodesic radius at most η_0 is

$$\mathbb{E}[c_{\ell,m}^n, \eta_0] = \binom{N}{m+1} \mathbb{E}[\mathbb{P}_\emptyset(\mathbf{x}) \cdot \mathbf{1}_{m-\ell}(\mathbf{x}) \cdot \mathbf{1}_{\eta_0}(\mathbf{x})],$$

in which $\mathbf{x} = (x_0, x_1, \ldots, x_m)$ is a sequence of $m+1$ points on $\mathbb{S}^n$, η is the geodesic radius of the smallest circumscribed cap of $\mathbf{x}$, and $\mathbb{P}_\emptyset(\mathbf{x}) = (1 - \mathrm{Area}(\eta)/\sigma_{n+1})^{N-m+1}$ is the probability that this cap is empty. The analogue of (7.1) is therefore

$$\mathbb{E}[c^n_{\ell,m}, \eta_0] = \binom{N}{m+1} \tfrac{1}{\sigma_{n+1}^{m+1}} \int\limits_{\mathbf{x}\in(\mathbb{S}^n)^{m+1}} \mathbb{P}_\emptyset(\mathbf{x}) \cdot \mathbf{1}_{m-\ell}(\mathbf{x}) \cdot \mathbf{1}_{\eta_0}(\mathbf{x}) \, \mathrm{d}\mathbf{x}.$$

We apply the rotation-invariant Blaschke–Petkantschin formula from Theorem 21. This gives

$$\mathbb{E}[c^n_{\ell,m}, \eta_0] = \tfrac{N!}{(N-m-1)!\sigma_{n+1}^m} \tfrac{\sigma_n^m}{2\Gamma(m)n^{m-1}} \cdot C^n_{\ell,m} \int\limits_{t=0}^{\sin^2\eta_0} t^{\frac{mn-2}{2}} (1-t)^{\frac{n-m-1}{2}} \left(1 - \tfrac{\mathrm{Area}(\eta)}{\sigma_{n+1}}\right)^{N-m+1} \mathrm{d}t,$$

in which $\eta = \eta(t) = \arcsin\sqrt{t}$; compare with (7.4). To prepare the next step, we note that

$$(1 - \tfrac{\mathrm{Area}(\eta(t))}{\sigma_{n+1}})^{N-m+1} \approx e^{-\frac{N}{\sigma_{n+1}}\mathrm{Area}(\eta(t))}$$

as $t \to 0$. From here on, we retrace the steps we took from (7.6) to (7.8). In particular, we change variables with $\tau = \frac{N}{\sigma_{n+1}}\nu_n t^{n/2}$, and we substitute $\bar\eta_0\rho^{-1/n}$ for η_0. Observing $\frac{N!}{(N-m-1)!} \approx N^{m+1}$, we simplify the expression and get

$$\mathbb{E}[c^n_{\ell,m}, \bar\eta_0] = N \cdot \tfrac{\gamma(v;m)}{\Gamma(m)} \cdot C^n_{\ell,m} + o(N)$$

for the expected number of intervals of the radius function of the Delaunay mosaic for N points chosen uniformly at random on $\mathbb{S}^n$, in which $v = \bar\eta_0^n\nu_n$. Comparing with the asymptotic result in Theorem 13, we see the same constants as for the Poisson point process. However, the variance distinguishes the two cases, being smaller for the uniform distribution than for the Poisson point process; see [70].

8. Future directions

The work is the first application of discrete Morse theory in the context of random mosaics. The results we were able to obtain using this approach indicate the power of a simple idea, namely that it might make a difference to characterize the mosaics using their intrinsic properties instead of looking at all random mosaics at a common scale. In particular, changing the general definition of the centroid of a face of a mosaic to take into account the construction of the mosaic, allowed to obtain several new results for the expected number of faces in many important cases. It looks like this approach can give new information when applied to any kind of random mosaics, and this work is the starting point. We finish with a list of open questions.

1. We computed the constants $C_{\ell,m}^{k,n}$ and $D_j^{k,n}$ in many lower-dimensional cases. However, obtaining an explicit formula in all dimensions would be a great achievement. The challenge lies in the spherical expectations, $E_{\ell,m}^n$ and $E_{\ell,m}^{k,n}$, which remain the main obstacle to the ultimate description of Poisson–Delaunay mosaics of all kind. It would be exciting to get explicit values for these constants, but even a good way of computing them numerically is of interest. In any case, the asymptotic behavior as n goes to infinity is another important question.
2. With the description of intervals of radius functions we get some topological information about the complex, which is provided by the discrete Morse inequalities. However, it only sheds some light on the homology, and the question if the results can be extended to the Betti numbers and the framework of persistent homology (see e.g. [12]) remains open. Indeed, the intervals of size larger than 1 correspond to 0-persistent pairs, and it is natural to ask similar questions about the pairs with positive persistence.
3. The slice construction implies a repulsive force among the vertices: the vertices of the weighted Poisson–Delaunay mosaic are more evenly spread than a Poisson point process. For fixed k, the repulsion gets stronger with increasing n. The mosaic can thus model some properties of real objects better than the Poisson–Voronoi mosaic. It would be interesting to study this repulsive force and its consequences analytically.
4. A further interesting question is about the connection between the spherical and the Euclidean case. As proved in this work, the first-order terms of the expected number of intervals of the radius function do not distinguish $\mathbb{S}^n$ from $\mathbb{R}^n$. There are no further terms in the Euclidean case, but what are they for $\mathbb{S}^n$?
5. Projecting the convex hull of a finite $X \subseteq \mathbb{S}^n$ orthogonally onto a $(k+1)$-plane corresponds to slicing the spherical Voronoi tessellation of X with a k-dimensional great-

sphere of $\mathbb{S}^n$. What are the stochastic properties of these slices? Are they different from weighted Poisson–Delaunay mosaics studied in this work?

6. The motivation for the spherical Poisson–Delaunay mosaics came from information theory. The square of the Fisher information metric, studied here, agrees infinitesimally with the Kullback–Leibler divergence [47]. The more general class of Bregman divergences has recently come into focus in [34, 33]. What are the stochastic properties of the Bregman divergences and their corresponding metrics? Is the similarity to the Euclidean metric specific to the Fisher information metric or is it a more general phenomenon?
7. In Chapter 6 we developed the discrete Morse theory for order-k Voronoi diagrams. However, it was a purely combinatorial construction, and its topological implications are to be investigated yet. It can be shown that k-intervals can be obtained by slicing the real intervals, which span over different values of k, and that critical and non-critical cases have similar effect on topology as in the $k = 1$ case; see the follow-up paper [32]. Can similar extensions be also obtained for other complexes?

Bibliography

[1] Akin, E. (1979). *The Geometry of Population Genetics*. Springer, Berlin, Germany.

[2] Amari, S. and Nagaoka, H. (2000). *Methods of Information Geometry*. Amer. Math. Soc., Providence, Rhode Island.

[3] Antonelli, P. L. et al. (1977-80). The geometry of random drift I-VI. *Adv. Appl. Prob.*, 9-12.

[4] Aurenhammer, F. (1987). Power diagrams: properties, algorithms, and applications. *SIAM J. Comput.*, 16:93–105.

[5] Aurenhammer, F. (1990). A new duality result concerning Voronoi diagrams. *Discrete Comput. Geom.*, 5:243–254.

[6] Aurenhammer, F. and Imai, H. (1988). Geometric relations among Voronoi diagrams. *Geometriae Dedicata*, 27:65–75.

[7] Bárány, I., Fodor, F., and Vígh, V. (2010). Intrinsic volumes of inscribed random polytopes in smooth convex bodies. *Adv. Appl. Prob. (SGSA)*, 42:605–619.

[8] Bauer, U. and Edelsbrunner, H. (2017). The Morse theory of Čech and Delaunay complexes. *Trans. Amer. Math. Soc.*, 369:3741–3762.

[9] Baumstark, V. and Last, G. (2009). Gamma distributions for stationary Poisson flat processes. *Adv. Appl. Prob.*, 41:911–939.

[10] Benjamini, I. and Schramm, O. (1998). Conformal invariance of voronoi percolation. *Communications in Mathematical Physics*, 197(1):75–107.

[11] Bobrowski, O. and Adler, R. (2014). Distance functions, critical points, and topology for some random complexes. *Homology, Homotopy and Applications*, 16:311–344.

[12] Bobrowski, O., Kahle, M., and Skraba, P. (2015). Maximally persistent cycles in random geometric complexes. arXiv:1509.04347 [math.PR].

[13] Bobrowski, O. and Weinberger, S. (2016). On the vanishing of homology in random Čech complexes. *Random Struct. Alg*.

[14] Bollobás, B. and Riordan, O. (2006). The critical probability for random voronoi percolation in the plane is 1/2. *Probability Theory and Related Fields*, 136(3):417–468.

[15] Bollobás, B. and Riordan, O. (2006). *Percolation*. Cambridge Univ. Press, England.

[16] Burtseva, L., Werner, F., Valdez, B., Pestriakov, A., Romero, R., and Petranovskii, V. (2015). Tessellation methods for modeling material structure. *Appl. Math. Mech.*, 756:426–435.

[17] Carlsson, G. (2009). Topology and data. *Bull. Amer. Math.*, 46:255–308.

[18] Chenavier, N. (2014). A general study of extremes of stationary tessellations with applications. *Stoch. Process. Appl.*, 124:2917–2953.

[19] Decreusefond, L., Ferraz, E., Randriam, H., and Vergne, A. (2014). Simplicial homology of random configurations. *Adv. Appl. Prob.*, 46:1–23.

[20] Delaunay, B. (1934). Sur la sphère vide. A la mémoire de Georges Voronoï. *Bulletin de l'Académie des Sciences de l'URSS. Classe des sciences mathématiques et na*, pages 793–800.

[21] Dey, T. K. (2011). *Curve and Surface Reconstruction. Algorithms with Mathematical Analysis*. Cambridge Univ. Press, England.

[22] Drton, M., Massam, H., and Olkin, I. (2008). Moments of minors of Wishart matrices. *Ann. Statist.*, 36 no. 5,:2261–2283.

[23] Edelsbrunner, H. (1993). The union of balls and its dual shape. In *Proceedings of the Ninth Annual Symposium on Computational Geometry*, SCG '93, pages 218–231, New York, NY, USA. ACM.

[24] Edelsbrunner, H. (2001). *Geometry and Topology for Mesh Generation*. Cambridge Univ. Press, England.

[25] Edelsbrunner, H. (2003). Surface reconstruction by wrapping finite sets in space. In Aronov, B., Basu, S., Pach, J., and Sharir, M., editors, *Discrete and Computational Geometry: The Goodman-Pollack Festschrift*, pages 379–404. Springer Berlin Heidelberg, Berlin, Heidelberg.

[26] Edelsbrunner, H. and Harer, J. L. (2010). *Computational Topology. An Introduction*. Amer. Math. Soc., Providence, Rhode Island.

[27] Edelsbrunner, H. and Iglesias-Ham, M. (2016). Multiple covers with balls II. weighted averages. *Electr. Notes Discrete Math.*, 54:169–174.

[28] Edelsbrunner, H. and Nikitenko, A. (2017a). Poisson–Delaunay mosaics of order k. arXiv:1709.09380 [math.PR].

[29] Edelsbrunner, H. and Nikitenko, A. (2017b). Random inscribed polytopes have similar radius functions as Poisson-Delaunay mosaics. arXiv:1705.02870 [math.PR].

[30] Edelsbrunner, H. and Nikitenko, A. (2017c). Weighted Poisson–Delaunay mosaics. arXiv:1705.08735 [math.PR].

[31] Edelsbrunner, H., Nikitenko, A., and Reitzner, M. (2017a). Expected sizes of Poisson–Delaunay mosaics and their discrete Morse functions. *Adv. Appl. Prob.*, 49:745–767.

[32] Edelsbrunner, H. and Osang, G. (2017). Persistent homology in depth. Manuscript, IST Austria, Klosterneuburg, Austria.

[33] Edelsbrunner, H., Virk, Ž., and Wagner, H. (2017b). Smallest enclosing spheres in Bregman geometry. Manuscript, IST Austria, Klosterneuburg, Austria.

[34] Edelsbrunner, H. and Wagner, H. (2017). Topological data analysis with Bregman divergences. In *Proc. 33rd Ann. Symp. Comput. Geom.* To appear, arXiv:1607.06274 [cs.CG].

[35] Fejes Toth, G. (1976). Multiple packing and covering of the plane with circles. *Acta Math. Acad. Sci. Hung.*, 27:135–140.

[36] Forman, R. (1998). Morse theory for cell complexes. *Adv. Math.*, 134:90–145.

[37] Freij, R. (2009). Equivariant discrete Morse theory. *Discrete Math.*, 309:3821–3829.

[38] Gelfand, I. M., Kapranov, M., and Zelevinsky, A. (1994). *Discriminants, Resultants, and Multidimensional Determinants*. Birkhäuser, Boston, Massachusetts.

[39] Hadwiger, H. (1957). *Vorlesungen über Inhalt, Oberfläche und Isoperimetrie*, volume 93 of *Die Grundlehren der Mathematischen Wissenschaften*. Springer-Verlag, Berlin.

[40] Hall, P. (1988). *Introduction to the Theory of Coverage Processes*. Wiley, New York.

[41] Hatcher, A. (2002). *Algebraic topology*. Cambridge University Press, Massachusetts, USA.

[42] Hewitt, E. and Stromberg, K. (1965). *Real and Abstract Analysis*. Springer, Berlin, Germany.

[43] Hug, D. (2013). Random polytopes. In Spodarev, E., editor, *Stochastic Geometry, Spatial Statistics and Random Fields*, volume 2068 of *Lecture Notes in Mathematics*, pages 205–238. Springer, Heidelberg, Germany.

[44] Kahle, M. (2011). Random geometric complexes. *Discrete Comput. Geom.*, 45:553–573.

[45] Kahle, M. (2014). Topology of random simplicial complexes: a survey. *AMS Contemp. Math*, 620:201–222.

[46] Kingman, J. F. C. (1993). *Poisson Processes*. Oxford Univ. Press, Oxford, England.

[47] Kullback, S. and Leibler, R. A. (1951). On information and sufficiency. *Amer. Math. Stat.*, 22:79–86.

[48] Lautensack, C. (2007). *Random Laguerre Tessellations*. PhD thesis, Math. Dept., Univ. Karlsruhe, Germany.

[49] Lautensack, C. and Zuyev, S. (2008). Random Laguerre tessellations. *Adv. Appl. Prob. (SGSA)*, 40:630–650.

[50] Lee, D. T. (1982). On k-nearest neighbor Voronoi diagrams in the plane. *IEEE Trans. Comput.*, C-31:478–487.

[51] Leray, J. (1945). Sur la forme des espaces topologiques et sur les points fixes des représentations. *J. Math. Pures Appl.*, 24:95–167.

[52] Li, S. (2011). Concise formulas for the area and volume of a hyperspherical cap. *Asian J. Math. Stat.*, 4:66–70.

[53] Miles, R. E. (1969). Poisson flats in Euclidean spaces. Part I: a finite number of random uniform flats. *Adv. Appl. Prob.*, 1:211–237.

[54] Miles, R. E. (1970). On the homogeneous planar Poisson point process. *Math. Biosci.*, 6:85–127.

[55] Miles, R. E. (1971). Isotropic random simplices. *Adv. Appl. Prob.*, 3:353–382.

[56] Miles, R. E. (1974). A synopsis of 'Poisson flats in Euclidean spaces'. *Stochastic Geometry*, pages 202–227.

[57] Milnor, J. (1963). *Morse Theory*. Annals of mathematics studies. Princeton University Press, Princeton, USA.

[58] Møller, J. (1989). Random tessellations in $\mathbb{R}^d$. *Adv. Appl. Prob.*, 21:37–73.

[59] Okabe, A., Boots, B., Sugihara, K., Chiu, S. N., and Kendall, D. G. (2008). *Spatial Tessellations*. John Wiley & Sons, Inc., second edition.

[60] Olver, F. W., Lozier, D. W., Boisvert, R. F., and Clark, C. W. (2010). *NIST Handbook of Mathematical Functions*. Cambridge University Press, New York.

[61] Olver, F. W. J. (1997). *Asymptotics and Special Functions*. A. K. Peters, Wellesley, Massachusetts.

[62] Prunet, N. and Meyerowitz, E. M. (2016). Genetics and plant development. *C. R. Biologies*, 339:240–246.

[63] Reitzner, M. (2010). Random polytopes. In Kendall, W. S. and Molchanov, I., editors, *New Perspectives in Stochastic Geometry*, pages 45–76. Oxford Univ. Press, UK.

[64] Reitzner, M. and Stemeseder, J. (2016). Expected number of faces of random polytopes with vertices on the boundary of a smooth convex body. Manuscript, Math. Dept., Univ. Osnabrück, Germany.

[65] Renka, R. J. (1997). Algorithm 772: STRIPACK: Delaunay triangulation and Voronoi diagram on the surface of a sphere. *ACM Trans. Math. Software*, 23:416–434.

[66] Schneider, R. (2008). Recent results on random polytopes. *Boll. Unione Mat. Ital.*, 1:17–39.

[67] Schneider, R. and Weil, W. (2008). *Stochastic and Integral Geometry*. Springer, Berlin, Germany.

[68] Shamos, M. I. and Hoey., D. J. (1975). Closest-point problems. In *Proc. 16th Ann. IEEE Sympos. Found. Comput. Sci.*, pages 151–162.

[69] Sibson, R. (1980). A vector identity for the Dirichlet tessellation. *Math. Proc. Camb. Phil. Soc.*, 87:151–155.

[70] Stemeseder, J. (2014). *Random polytopes with vertices on the sphere.* PhD thesis, Math. Dept., Univ. Salzburg, Austria.

[71] Walck, C. (1996). *Handbook on Statistical Distributions for Experimentalists*. Internal Report SUFPFY/9601, Stockholm, Sweden.

[72] Wendel, J. G. (1962). A problem in geometric probability. *Math. Scand.*, 11:109–111.

[73] Whitehead, J. H. C. (1939). Simplicial spaces, nuclei and m-groups. *Proceedings of the London Mathematical Society*, s2-45(1):243–327.

[74] Zähle, M. (1990). A kinematic formula and moment measures of random sets. *Mathematische Nachrichten*, 149:325–340.

Index